AUS DEM INSTITUT
FÜR MEDIZINISCHE MIKROBIOLOGIE UND HYGIENE
MOLEKULARE MIKROBIOLOGIE (VIROLOGIE)
Univ. Prof. Dr. Ralf Wagner
DER FAKULTÄT FÜR MEDIZIN
DER UNIVERSITÄT REGENSBURG

Modifikation von Peptid-Antibiotika mit Hilfe der synthetischen Biologie

Inaugural - Dissertation
zur Erlangung des Doktorgrades
der Medizin

der
Fakultät für Medizin
der Universität Regensburg

vorgelegt von

Malin Zaddach

2020

AUS DEM INSTITUT
FÜR MEDIZINISCHE MIKROBIOLOGIE UND HYGIENE
MOLEKULARE MIKROBIOLOGIE (VIROLOGIE)
Univ. Prof. Dr. Ralf Wagner
DER FAKULTÄT FÜR MEDIZIN
DER UNIVERSITÄT REGENSBURG

Modifikation von Peptid-Antibiotika mit Hilfe der synthetischen Biologie

Inaugural - Dissertation
zur Erlangung des Doktorgrades
der Medizin

der
Fakultät für Medizin
der Universität Regensburg

vorgelegt von

Malin Zaddach

2020

Dekan: Prof. Dr. Dirk Hellwig

1. Berichterstatter: Prof. Dr. Ralf Wagner

2. Berichterstatter: Prof. Dr. Bernd Salzberger

Tag der mündlichen Prüfung: 19.10.2021

Contents

Zusammenfassung

Zu einer der größten Herausforderungen der modernen Medizin gehört die Entwicklung neuer antibiotischer Wirkstoffe, welche gegen eine wachsende Anzahl, zum Teil multiresistenter, pathogener Keime, wirken. Eine in diesem Zusammenhang vielversprechende Substanzklasse ist die der Lantibiotika. Dabei handelt es sich um ribosomal-synthetisierte Peptide, die zur Klasse I der Bacteriocine gehören und eine breite antibiotische Wirksamkeit gegen Gram-positive Bakterien besitzen. Die Kombination aus verschiedenen antimikrobiellen Wirkmechanismen als auch die bisher kaum beobachtete Resistenzbildung macht Lantibiotika zu einem interessanten Forschungsgegenstand. Ihr prominentester Vertreter ist Nisin, ein in seiner maturen Form 34 Aminosäuren umfassendes, natürlicherweise in *Lactococcus lactis* synthetisiertes und posttranslational modifiziertes Polypeptid. Zur Erweiterung des antimikrobiellen Spektrums von Nisin, sowie zur Anpassung seiner pharmakologischen Eigenschaften, ist die ko-translationale Inkorporation von nicht-kanonischen Aminosäuren (nkAS) eine sehr vielversprechende Möglichkeit.

In vorangegangenen Experimente unserer Arbeitsgruppe konnte gezeigt werden, dass diese Inkorporation zwar prinzipiell möglich ist, jedoch abhängig von der ausgewählten Aminosäureposition der Einbau der nkAS lediglich mit einer sehr niedrigen Effizienz erfolgt. Zur relativen Quantifizierung der Einbaueffizienz von nkAS in Nisin wurde ein, in unserer Arbeitsgruppe entwickelter, auf einem Nisin-GFP-Fusionsprotein basierender Assay (im Folgenden „Suppressionseffizienzassay“ genannt) verwendet. Unabhängig von der Anwesenheit der nkAS konnte eine Proteinexpression beobachteten werden, obwohl bei Fehlen der nkAS theoretisch ein Translationsabbruch und somit keine Proteinexpression stattfinden sollte. Dieses Problem galt es, mit dem Ziel die Suppressionseffizienz zu verbessern, zu adressieren. Im Falle einer hohen (verbesserten) Suppressionseffizienz, würde man folglich keine Proteinexpression bei Fehlen der nkAS, beziehungsweise eine starke Expression bei Vorliegen der nkAS im Suppressionseffizienzassay beobachten. Wir postulierten die Entstehung von Nebenprodukten durch interne Ribosomen-Bindungsstellen innerhalb von Nisin als Ursache für die verminderte Supp-

ressionseffizienz, welche zur Verbesserung der Einbaueffizienz von nkAS in Nisin zunächst vermindert bzw. unterdrückt werden sollte. Hierfür wurden zwei Lösungsansätze verfolgt: (i) Änderung der Gensequenz der postulierten internen Ribosomen-Bindungsstelle mit dem Ziel ihre Ribosomen-Bindungsstärke abzuschwächen, (ii) Ersatz der beiden Methionine (ATG) an Position 17 und 21 durch geeignete Codons anderer Aminosäuren, um ihre Funktion als interne Translationsstarter auszuschließen. Lösungsansatz (i) wurde über die Optimierung der natürlich vorkommenden Gensequenz („Codon-Optimierung“) von Nisin A für den Zielorganismus *Escherichia coli* mit Hilfe des GeneOptimzer Algorithmus (1) realisiert. Anschließend konnte mit Hilfe des RBS calculator (2) *in silico* die Verringerung der Bindungsstärke von jeder in der natürlichen Gensequenz existierenden internen ribosomalen Bindungsstellen gegenüber der Codon-optimierten Gensequenz gezeigt werden. Im Suppressionseffizienzassay zeigte sich jedoch keine wesentliche Verbesserung der Suppressionseffizienz im Vergleich zur Variante mit der natürlich Gensequenz. Für Lösungsansatz (ii) wurde auf Basis von publizierten Ergebnissen beschlossen das Methionin an Position 21 durch Lysin zu ersetzen, wodurch die antimikrobielle Aktivität von Nisin nicht vermindert wird. Für das Methionin an Position 17 lagen keine eindeutigen Daten vor, weshalb hier je eine Variante mit jeder der 19 verbleibenden natürlichen Aminosäuren kloniert wurde. Um sicher zu gehen, dass die entstandene Nisin-Varianten mit den zwei ausgetauschten Methioninen mit der besten antimikrobiellen Aktivität für die weiterführenden Suppressionseffizienzexperimente ausgewählt wird, wurden alle 19 Varianten in *Lactococcus lactis* exprimiert und mit Hilfe verschiedener Assays auf ihre Aktivität im Vergleich zum natürlich vorkommenden Nisin A untersucht. Nisin M17WM21K (Methionin an Position 17 zu Tryptophan und Methionin an Position 21 zu Lysin ausgetauscht) zeigte die stärkste antimikrobielle Aktivität und führte im anschließenden Suppressionseffzienzassay zu einer deutlichen Steigerung der Suppressionseffizienz. Durch eine Kombination aus Lösungsansatz (i) und (ii), also ein Codon-optimiertes M17WM21K Nisin, konnte dabei keine zusätzliche Steigerung der Suppressionseffizienz im Vergleich zum nicht-Codon-optimierten M17WM21K Nisin erzielt werden.

Weiterhin wurde im Rahmen der Arbeit ein heterologes Expressionssystem für Nisin in *E. coli* erfolgreich etabliert. Da *E. coli* der am besten studierte und meist genutzte Orga-

nismus für den Einbau von nkAS ist, bietet sich bei dessen Nutzung auch die vielfältigste und Bandbreite an biotechnologischen Werkzeugen. Zur Nisin-Expression wurden zunächst verschiedene *E. coli*-Stämme hinsichtlich ihrer Produktionsrate über Agar-Well-Diffusion-Assays relativ miteinander verglichen und anschließend wurde ein geeignetes Reinigungsprotokoll, bestehend aus einer Kombination von Metall-Affinitätschromatographie, Gelfiltration und Chromatographie durch hydrophobe Wechselwirkungen, für das post-translational modifizierte Nisin ausgearbeitet. Das so gewonnen Nisin konnte mit Hilfe eines antimikrobielle Aktivitätsassay, Massenspektrometrie sowie Peptide Mass Fingerprinting charakterisiert werden und über einen Minimal Inhibitory Dilution Assay die Ausbeute bestimmt werden. Zur zukünftigen Vereinfachungen der Nisin-Produktion in *E. coli* wurde ein erstes Set an orientierenden Experimenten zur Funktionalität des *L. lactis* eigenen Nisin-Transporters NisT in *E. coli* durchgeführt. Die Ergebnisse lassen die Funktionalität des Transporters in *E. coli* vermuten.

Im Zuge dieser Arbeit konnten Methionin-Codons (ATG) innerhalb der Gensequenz von Nisin als alternative Translationsinitiatoren, welche die Einbaueffizienz von nkAS vermindern, identifiziert werden und das Problem durch einen Austausch der Methionin-Codons mit alternativen Aminosäure-Codons weitgehend gelöst werden. Für zukünftige Arbeiten, die sich mit dem Einbau von nkAS in Methionin-haltige Peptide und Proteine beschäftigen, stellt diese Erkenntnis einen wichtigen Hinweis zur Vermeidung der Bildung von verkürzten Translationsprodukten dar. Darüberhinaus konnte die Expression von Nisin in *E. coli* in unserer Arbeitsgruppe erfolgreich etabliert werden, was weiterführenden Experimente zur Modifikation von Nisin mit nkAS den Weg ebnet.

A Introduction

A.1 Antibiotic resistance – an emerging problem

Antibiotics are an indispensable part of modern medicine. Together with vaccination, they have saved millions of lives and formerly lethal diseases, such as bacterial meningitis, can be cured nowadays (3). The history of modern antibiotics began with the discovery of penicillin by Sir Alexander Fleming in 1928, for which he was awarded with the Nobel Prize in Physiology and Medicine in 1945 (4,5). Only 22 years after penicillin's description, resistance of *Streptococcus pneumoniae* was described, threatening the advances which had been made and turning antibiotic resistance into a substantial clinical problem (6).

Easy access, overuse and availability of few new substances prompted bacteria to develop resistance to multiple antimicrobial substances, consequently turning antimicrobial resistance (AMR) into a global concern (7,8). The World Health Organization (WHO) declared AMR to be a 'serious threat [that] is no longer a prediction for the future, it is happening right now in every region of the world and has the potential to affect anyone, of any age, in any country' (9). In the European Economic Area, infections with multidrug resistant bacteria accounted for approximately 33.110 deaths and 874.541 disability-adjusted life-years in 2015 (10). The estimated economic loss of infections with solely six selected antibiotic-resistant bacteria in the European Union (including Iceland and Norway) in 2007 amounted 1.5 billion Euro. In this context, organ transplant patients and oncological patients are particularly vulnerable to acquire multidrug-resistant bacterial infections (11).

Until the 1970s, several new antibacterial drugs were developed, but in the last three decades the number of discovered antibiotics steadily decreased. Compared to 19 antibiotics which have been approved for clinical use between 1980 and 1984, only three new substances could be registered between 2005 and 2009, showing drastically the resulting discovery void (6,12). Reasons for this development are manifold, e.g. low economic benefit, since antibiotics are often curative and only used for short periods, or

economic uncertainty due to eventual and hardly predictable resistance development (6,8).

Without resolute action, medical and economic consequences will be inevitable. Besides globally organized monitoring of resistance development, increasing awareness and supporting antimicrobial stewardship efforts are urgently needed. Other than that, research and discovery of novel antibiotic substance classes or vaccines are the most important building blocks of the wall which needs to be drawn around AMR (8,9,13,14).

A.2 The SYNPEPTIDE project

The EU-funded research collaboration SYNPEPTIDE brings together five academic groups and three enterprises from Austria, the Netherlands, Switzerland and Germany to identify novel antimicrobial peptides (AMP) (15). AMPs are ribosomally synthesized, highly conserved peptides, which can be found in a vast number of organisms, playing an important role in innate immunity (16,17). Over the last decade, peptide research has gained importance as peptide-based drugs offer several interesting features: high target specificity through tight target binding, generally low toxicity due to easy metabolism, and increasing acceptance by physicians and patients (17). Peptide-based drugs represent a rapidly growing sector of the pharmaceutical market: in 2016, more than 50 peptides were already on the global market, about 170 substances were tested in clinical trials and more than 200 others at preclinical stages (18). Within the SYNPEPTIDE project, a naturally occurring class of ribosomally synthesized polypeptides, called lantibiotics, is investigated. By means of synthetic biology and high-throughput screening, naturally occurring lantibiotics shall be expanded by new chimeric, recombinant and modified variants, aiming at the generation and identification of novel antimicrobial active peptides. Rational synthetic peptide design and integration of chemical diversity shall be achieved by pursuing two independent pathways: [1] translational integration of chemically suitable non-canonical amino acids for posttranslational in vivo and in vitro modification; [2] systematic recruitment of selected highly relevant posttranslational modifications (PTM) from natural peptide synthesis routes into the design process (15). This thesis is a contribution to pave the way for implementing approach [1] for the lantibiotic nisin.

A.3 Lantibiotics – a unique class of antibiotics

Lantipeptides are ribosomally synthesized polypeptides, which contain the thioether-cross-linked amino acids (*meso*-)lanthionine and ((2S,3S,6R)-3-)methyllanthionine, that form characteristic ring structures (*Figure 1 A*). Frequently, didehydroalanine (Dha) and/or didehydrobutyrine (Dhb) residues (*Figure 1 B*) can be found (19–21). The atypical amino acid lanthionine consists of two alanine residues that are crosslinked on their β-carbon atoms by a thioether linkage (*Figure 1 A*), thus, forming the typical lanthionine rings and resulting in an increased stability of the lantipeptides towards proteolytic degradation (20,22).

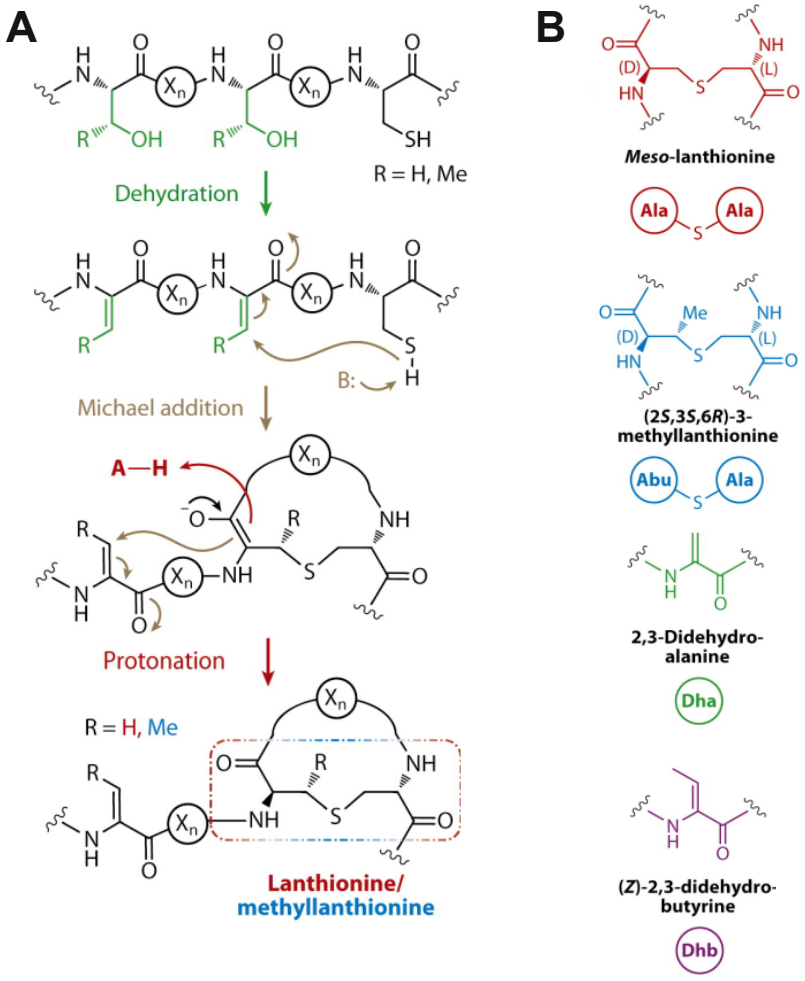

Figure 1. (A) Mechanism of thioether cross-link formation in lantipeptides. First, serine/threonine residues are dehydrated to the α,β-unsaturated didehydroalanine (Dha) and didehydrobutyrine (Dhb), followed by a Michael addition of a thiol side chain from cysteine, creating a thioether bridge. **(B) Typical modified amino acids found in lantipeptides.** (figure adapted from KNERR and VAN DER DONK (20))

Lantipeptides that show antibacterial activity are named lantibiotics and belong to the family of bacteriocins. Bacteriocins are antimicrobial peptides, which are synthesized by gram-positive as well as gram-negative bacteria. The analysis of 238 genomes of lactic acid bacteria revealed the presence of 785 putative bacteriocin gene clusters (23). Lantibiotics represent one of the numerous subclasses of bacteriocins, which are categorized in two main groups. The diverse group of class I bacteriocins is characterized by extend post-translational modifications and includes, besides eleven other subclasses, lantibiotics. In class II bacteriocins, significant modification is absent (24). Lantibiotics possess potent activity against mostly gram-positive bacteria, including clinical relevant and partly drug-resistant strains of *Staphylococcus*, *Streptococcus*, *Enterococcus* and *Clostridium*, as well as against selected gram-negative bacteria, such as *Neisseria gonorrhoeae* and *Helicobacter pylori* (21,24).

A.4 Classification of Lantipeptides

Lantipeptides are subclassified in four different classes (I–IV), depending on the enzymes involved in post-translational modifications (19). Class I lantipeptides are characterized by their modification via two distinct enzymes, the lantibiotic dehydratase (LanB) and the lantibiotic cyclase (LanC). In contrast to class I, the dehydration and cyclization step is carried out by a bifunctional lantipeptide synthetase (LanM) in class II. LanM shows no structural homology to LanB enzymes, however, it has a C-terminal LanC-like domain, which includes three zinc-binding ligands (20,21). Class III lantipeptides are processed by a trifunctional synthetase, which takes the phosphorylation/β-elimination pathway to form Dha and Dhb, bears a N-terminal lyase and a C-terminal cyclase domain that shows limited homology to LanM. Finally, the recently identified class IV synthetase, LanL, contains a N-terminal lyase and a central serine/threonine kinase domain as discovered in class III, but its C-terminal cyclase domain resembles LanC, as well as LanM, including the characteristic zinc-binding motif (20).

In all four classes of lantipeptides the genes encoding the lantibiotic-precursor as well as the PTM enzymes are mostly localized within one single gene cluster. Antimicrobial activity has only been observed for class I and II lantipeptides so far (19).

A.5 The prototype for lantibiotics: Nisin

In 1928, ROGERS and WHITTIER firstly described an antimicrobial substance which shows antibacterial activity against selected strains of *Lactococcus lactis* in fermentation cultures, later on referred to as nisin (25). Nisin is 34 amino acids long, has a molecular weight of 3.35 kDa and a net positive charge (+4) (*Figure 2*). It belongs to class I lantipeptides and is naturally produced by some strains of *L. lactis.* Its antimicrobial activity against various gram-positive bacteria arises from the characteristic five (methyl-)lanthionine rings (referred to as ring A-E) and three dehydrated amino acids (one Dhb and two Dha residues) (26–28). The N-terminal rings A, B and C are connected with the C-terminal rings D and E by a flexible, short hinge region (asparagine-methionine-lysine (N-M-K)), which most probably plays a crucial role in pore formation (29,30). There are nine naturally occurring nisin variants currently known of which nisin A and nisin Z are most frequently found (31,32). Differing only by the 27th amino acid (histidine in nisin A and asparagine in nisin Z), they exhibit similar antimicrobial activity against gram-positive organisms within a nanomolar range (31,33). Nisin has a strong amphiphilic character, having many hydrophilic residues at the C-terminal side and several hydrophobic residues at the N-terminal part, enabling the peptide to interact with phospholipid head-groups of the cellular membrane (29). Interestingly, nisin shows enhanced thermal stability with decreasing pH, which can be explained by the naturally occurring thioether bridges that close the lanthionine rings (34).

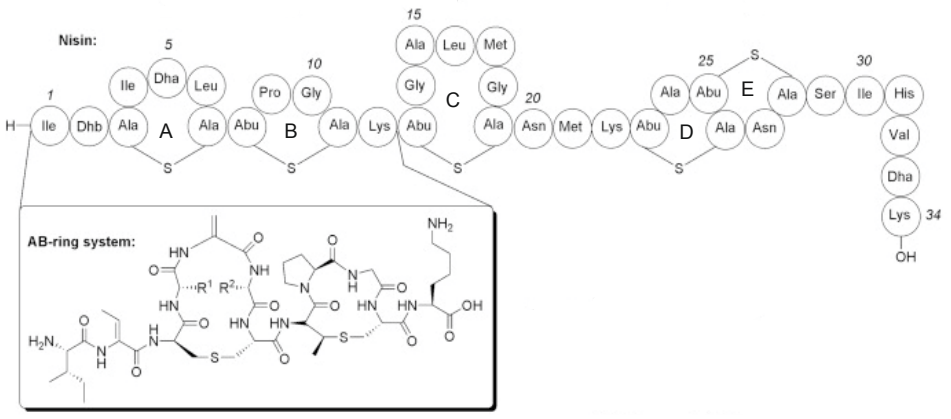

Figure 2. Schematic presentation of fully modified nisin A. Dha: didehydroalanine, Dhb: didehydrobutyrine. Ring structures are denominated consecutively with A to E. Adapted from HARMSEN et al. (35).

Nisin offers numerous advantages over conventional antibiotics, turning it into a highly interesting research subject. The most important benefits are the following:

i. Scarcely reported resistance development
ii. Low toxicity
iii. Amenability for bioengineering

Nisin was approved as a food preservative by the Food and Agriculture Organization of the United Nations (FAO) in 1969 and extensively used ever since (36). It may be added to food in a maximal concentration of 12,5 mg/kg to prevent growth of *Listeria monocytogenes* and *Clostridium botulinum* (34). Despite of being used for more than half a century, development of resistance mechanisms has only been observed once so far. In 2016, KHOSA, FRIEGE et al. firstly described the structure of a nisin resistance protein (NSR) isolated from *Streptococcus agalactiae* (22). NSR is a protease that cleaves nisin between the 28th and 29th residue. The leftover 28 amino acid long fragment showed reduced affinity towards cellular membranes and lower bactericidal activity (22,26,37).

Another grand benefit of many bacteriocins is the low toxicity they show against humans. Due to their polypeptide nature, bacteriocins can naturally be degraded by the body's own proteases. The degree of toxicity of class II bacteriocins has been examined in a few studies, revealing no or only low cytotoxic effects when applied in distinct higher concentrations than needed for antibacterial activity (24).

Owing to the ribosomal synthesis pathway, nisin and other bacteriocins can easily be modified using genetic manipulation strategies as well as manipulation of the natural translation machinery. Being highly promiscuous, lantibiotic modification enzymes allow procession of synthetic analogs, which can then be further investigated upon their activity (38,39). A promising strategy to alter pharmacokinetic and pharmacodynamic properties of nisin is the co-translational introduction of non-canonical amino acids (ncAA). Regarding the whole reservoir of organic chemistry possibilities, introduction of ncAAs would allow addition of diverse supplementary chemical functions to nisin.

A.5.1 Biosynthesis of Nisin

Mature nisin is produced in a five-step process: translation of prenisin, dehydration, formation of (methyl-)lanthionine-crosslinks, secretion and eventually cleaving off the leader peptide (20,40). The genes for prenisin (*nisA*), the PTM machinery (*nisBTC* and *nisP*), as well as immunity mediating (*nisFEG* and *nisI*) and gene regulating enzymes (*nisRK*) are organized in a single gene cluster under the control of four different promotors (19,23). The precursor peptide consists of a 23 amino acid long N-terminal leader and the 34 amino acid long C-terminal core peptide.

The leader peptide contains a highly conserved -FNLD-motif, which is recognized by the N-terminal domain of the lantibiotic dehydratase NisB by hydrophobic interactions, and is essential for the glutamylation activity of NisB, but does not seem to be crucial for glutamate elimination (19,38,41). Attached to its leader, nisin's antimicrobial activity is abolished, concordant with a self-protective mechanism of the producer strain (42). Only when the leader of the prepeptide is cleaved off in the extracellular space, nisin unfolds its antimicrobial activity.

The homodimer NisB catalyzes the dehydration of serine and threonine residues in a tRNA-dependent two-step mechanism. First, nisin gets glutamylated by $tRNA^{Glu}$ bound to NisB, followed by dehydration via the elimination domain in a N- to C-terminal directionality (38).

Dehydrated nisin, including its leader peptide, is then bound to NisC to generate thioether rings, which vary from four to seven amino acids, in an ATP-independent Michael-addition reaction. The proposed mechanism for the cyclization includes the coordination of the sulfur atom of a cysteine residue towards the Zn^{2+} ion. Deprotonation to a thiolate occurs, which is subsequently attacking the β-carbon of Dhb as a nucleophile to generate an enolate intermediate (41). Finally, the intermediate is protonated and the fully processed ring is completed.

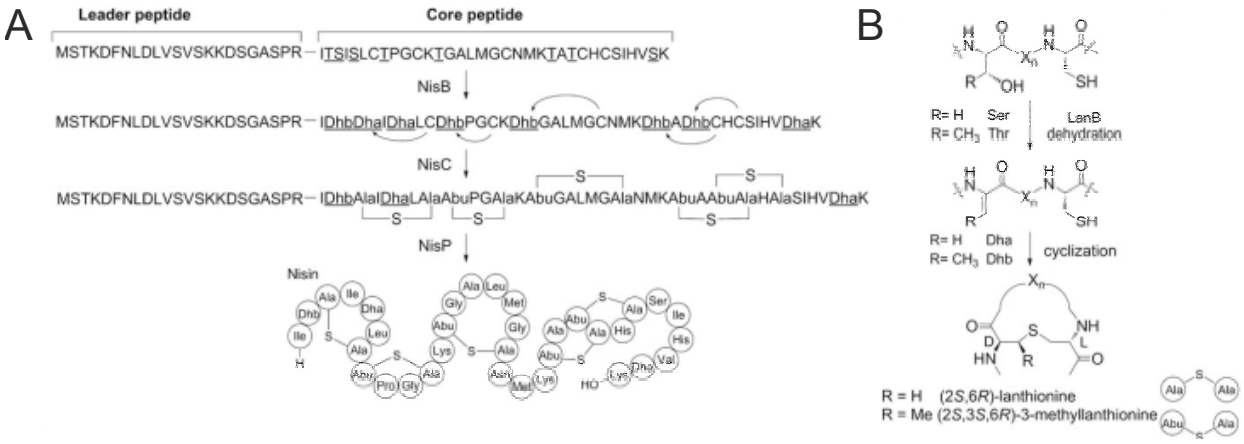

Figure 3. (A) Biosynthesis of nisin. NisB dehydrates Ser/Thr residues in the core peptide of nisin A (NisA). NisC catalyzes the ring formation and NisP removes the leader peptide (43). **(B) Dehydration and cyclization steps.** Ser/Thr residues are dehydrated to Dha and Dhb, respectively. Subsequent intramolecular Michael addition of the thiols of Cys residues to Dha and Dhb results in (methyl-)lanthionines.

NisB and C do not modify prenisin separately, but instead form a quadripartite PTM-complex, consisting of a NisB dimer, one NisC monomer and one prenisin molecule (19). After procession by the membrane-bound PTM-complex, nisin is getting exported by the peptide transporter NisT. NisT is an ATP-binding cassette (ABC) transporter, which is predominantly located at the cellular membrane. It appears to exhibit high substrate promiscuity, as lantibiotics could successfully be exported when bioengineered variants were attached to the leader peptide (20). Other than for modification, export is possible when the -FNLD-motif is not present in the leader (44).

Following export of the modified peptide from the producer cell, the leader peptide is cleaved off by a protease, transforming nisin into its final antimicrobial active form (45). This last step is catalyzed by the serine protease NisP, which is an extracellular, membrane-anchored enzyme with a molecular weight of 75 kDa (26,40).

A.5.2 Nisin possesses diverse antibacterial mechanisms

Only little resistance development against nisin has been reported until today (compare A.5). This uncommon property of an antibiotic is thought to be explainable by nisin's multifaceted mode of action (38,46). First, nisin is able to form a 'cage-like' structure with its A, B and C ring, sequestering the pyrophosphate moiety of the membrane precursor molecule lipid II, which leads to inhibition of cell wall synthesis. Lipid II, which carries a

disaccharide-peptide unit that is integrated into the growing peptidoglycan chain, can be described as the bottleneck of cell wall biosynthesis due to its limited availability. Hence, it represents a highly attractive and accessible target for antibiotics. Lipid II has a strong amphipathic character and consists of a pentapeptide subunit linked to a polyisoprenoid element via a pyrophosphate linker, which integrates the molecule into the bacterial membrane (47). In contrast to the commonly in clinic used antibiotic vancomycin, which interacts with the d-Ala-d-Ala motif of the lipid II-pentapeptide chain, nisin targets the phosphate group on the opposite side of the molecule (48,49). As a second antibacterial mechanism, nisin is able to form pores in the cell membrane in a lipid II-dependent manner, resulting in rapid efflux of ions and small cytoplasmic components (46). MULHOLLAND et al. proposed a mechanism where pore formation is permitted by the assembly of four ternary complexes, each consisting of two nisin and one lipid II molecules (30). Hydrogen bond analysis revealed interaction of the N-termini of both nisin molecules with the pyrophosphate and the pentapeptide chain of lipid II. The analysis also indicates the existence of a second binding site on lipid II for nisin, which is located at the C-terminal region of the first Dha residue (5^{th} position) (30). Moreover, antimicrobial effects such as inhibition of spore outgrowth, activation of autolytic enzymes and lipid II-independent pore formation have been described for nisin (30,46,49–51).

Despite nisin's versatile modes of tackling its opponents it shows only poor activity against gram-negative bacteria. The reason can be found in their differing cell architecture: the outer membrane (OM) of the gram-negative cell wall acts as a natural barrier for the access of peptides to the cytoplasmic membrane (46). Still, some lantibiotics surprisingly show little activity against selected gram-negatives. A hypothesis for this observation is the 'self-promoted uptake pathway' of cationic peptides, where the peptide binds with high affinity to the negatively charged lipopolysaccharide, causing the displacement of divalent cations (Mg^{2+} and Ca^{2+}), which destabilizes the OM and finally leads to cell death (21,52). This phenomenon and the discovery of several synthetic nisin derivatives give hope for future expansion of the activity spectrum of lantibiotics (53).

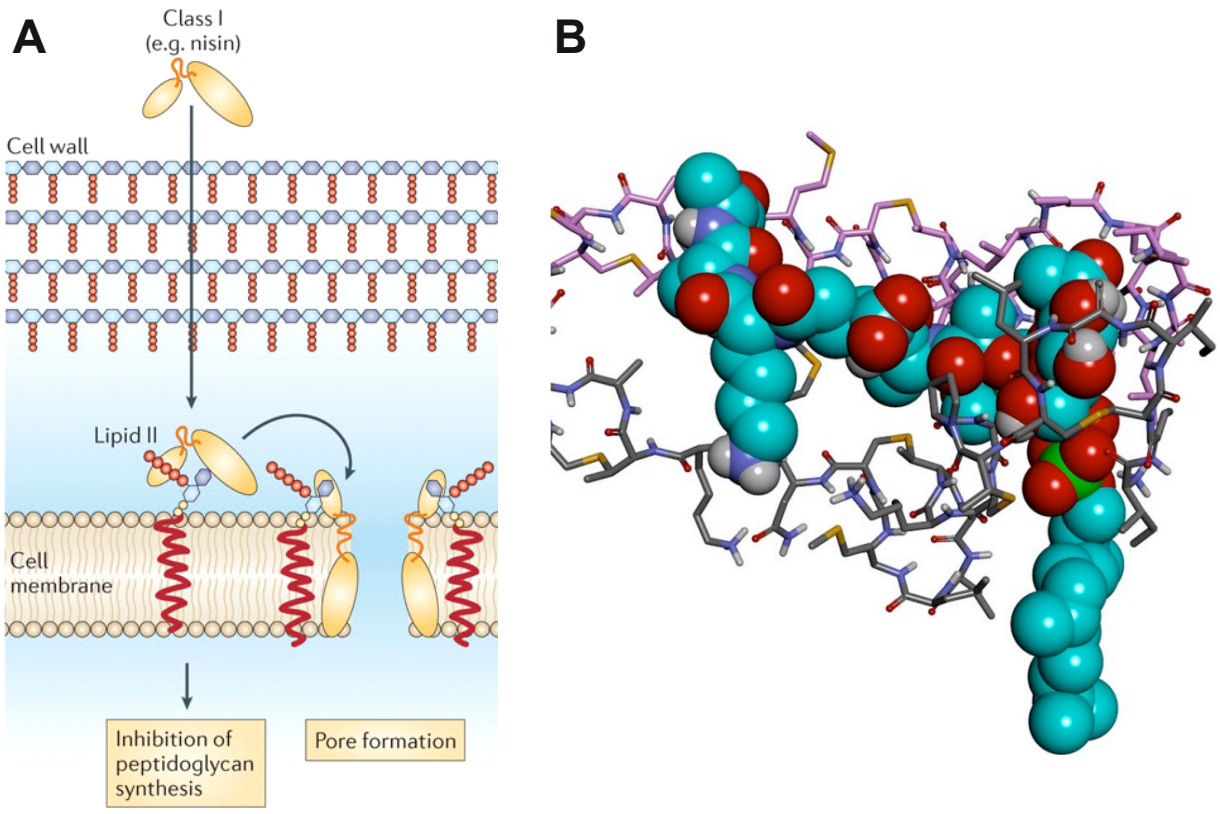

Figure 4. (A) Schematic presentation of the mode of action of a class I lantibiotic. Class I lantibiotics act as antimicrobial substances through two main mechanisms: inhibition of peptidoglycan synthesis and formation of pores. Figure adopted from COTTER et al. (24). **(B) Structure of the ternary nisin$_2$:lipid II complex** formed by docking nisin$_2$ (pink carbon atoms) onto the 3-isoprenyl- lipid II/nisin$_1$ (shown in grey) complex (30).

A.5.3 Biomedical application of nisin

Clinical studies which evaluate the treatment of infections, using solely nisin, are mostly limited to topical applications (31). FERNÁNDEZ et al. showed that nisin is an efficient drug to treat staphylococcal mastitis, leading to the complete eradication of clinical signs in the nisin treated group within one week (54). Furthermore, nisin's potential as oral antibiotic has been investigated *in vitro* and in animal models, confirming its capacity to prevent biofilm formation (31,55). KIM et al. demonstrated in a mice model that the lantibiotic BP$_{SCSK}$, which is similar to nisin A, can reverse antibiotic-induced susceptibility to vancomycin-resistant *Enterococcus faecium* infections (56). To render nisin less sensitive for protease degradation, KOOPMANS et al. created semisynthetic nisin-lipopeptides, which showed potent inhibition of bacterial growth (including VRE and MRSA) (57). An-

other promising applicability is a nisin-eluting nanofiber wound dressing, which significantly reduced *Staph. aureus* colonialization and accelerated wound healing of excisional wounds in mice (58).

Clinical testing of nisin or nisin derivatives has been focused on its anti-gram-positive properties so far. But the current AMR situation calls for both: new drugs against gram-negative germs, which are of rapidly growing concern, as well as novel treatments for increasingly resistant gram-positive pathogens (13,59). Multiple studies examined the synergistic effects of nisin with other antibiotics, whereby the observation of highly synergistic effects of nisin-ceftriaxone and nisin-cefotaxime against clinical isolates of *Salmonella enterica* serovar Typhimurium shall be highlighted (60–62). Bioengineered nisin variants did not only show antibacterial activity against a wide range of gram-positive bacteria, including methicillin-resistant *Staphylococcus aureus* (MRSA) and vancomycin-resistant *enterococci* (VRE): mutation variants of nisin Z (N20K and M21K) also showed antimicrobial activity against pathogenic gram-negative bacteria, such as *Salmonella*, *Shigella* and *Pseudomonas* species (29,63).

In 2012, a completely new chapter was opened: Joo et al. firstly reported an apoptogenic effect of nisin on head and neck squamous cell carcinoma (HNSCC) cells in cell culture, which was further confirmed in subsequent mouse trials. Here, reduction of tumorigenesis *in vivo* was observed and long-term treatments with nisin Z prolonged survival (64,65).

A.6 Expanding the genetic code

Because of its ribosomal synthesis pathway, nisin is easily accessible for genetic engineering during the translation process. Due to the post-translational modification processes that nisin undergoes during its biosynthesis, solid phase peptide synthesis approaches are strictly limited. Co-translational bioengineering would therefore be an elegant and easy to handle method. Moreover, *in vivo* production of modified lantibiotics offers further benefits, such as: less downstream processing steps, high product yields and generation of the correct stereochemistry (66). A particular versatile approach for the introduction of novel chemical functions into proteins is the expansion of the genetic code by introducing non-canonical amino acids (ncAAs) (67,68). This technology has

made remarkable progress in the last decades and has allowed introduction of various functional groups e.g. fluorophores, photo-crosslinkers, isotope-marked amino acids for NMR-studies into proteins and has been used in vaccine design, too (67,69–71). Regarding AMPs, for example, the introduction of unnatural proline-based amino acids into proline-rich peptides increased their antimicrobial activity against *Listeria*, *Brucella* or MRSA and enhanced their stability against proteolytic degradation by trypsin (72).

Two methods are currently used for ncAA incorporation: selective pressure incorporation (SPI) and stop codon suppression (SPS). The former allows installation of isostructural variants of canonical amino acids by replacing a selected natural amino acid in an auxotrophic strain through a ncAA (69). In SPS technology (*Figure 5 A*) the regular function of a specific codon is overwritten and instead used for the incorporation of any desired ncAA, which does not require structural relation to a canonical amino acid. For this purpose one of the three stop codons can be used, as all other codons are reserved for the coding of a natural amino acid. In general, the UAG (amber) stop codon (also: nonsense codon) is preferably reassigned, as it terminates only ~7 % of *E. coli* genes (73). Due to the fact that UAA (ochre) is the most common stop codon, it is rarely used for reassignment (74).

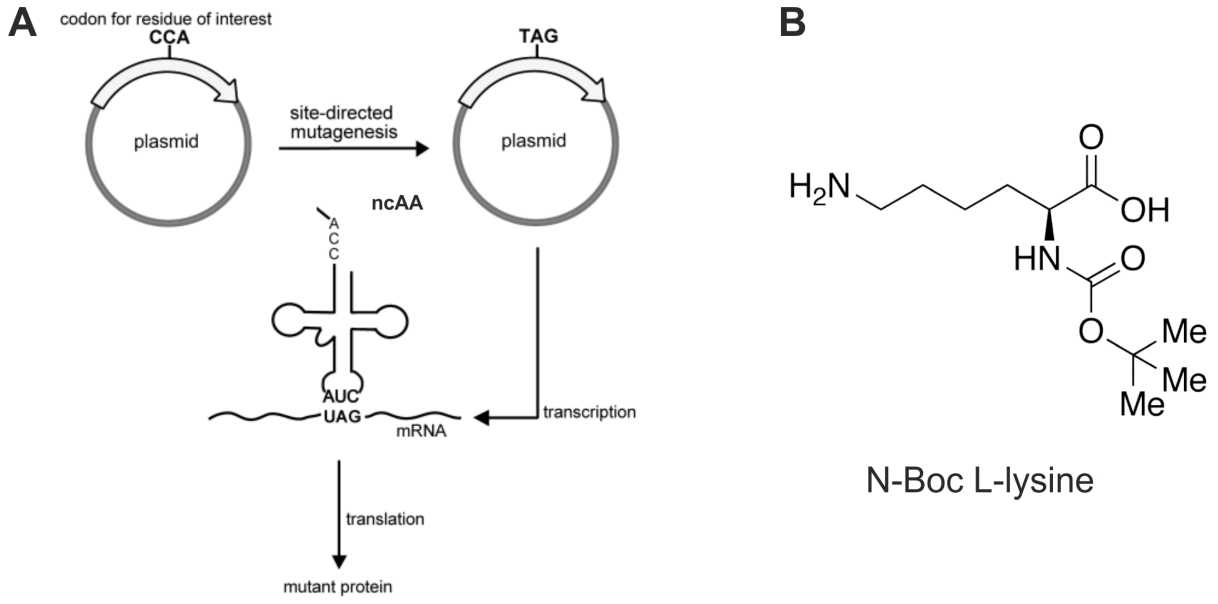

Figure 5. (A) Principle of the site-specific incorporation of a ncAA into the protein of interest. First, side-directed mutagenesis is performed, replacing the codon for the residue of interest by the amber stop codon (TAG), which now codes for the ncAA. Second, the plasmid is transcribed to mRNA and finally translated to the mutant protein by aid of aaRS/tRNAncAA. Adopted and modified from Wang et al. (75). **(B) Structure of N-Boc L-lysine (BocK).**

The following criteria must be met by the modified translation machinery for SPS technology:

i. An orthogonal aminoacyl-tRNA-synthetase (aaRS)/$tRNA^{ncAA}$ pair is needed, meaning that the aaRS specifically charges a cognate tRNA, but may not charge any endogenous tRNA present in the host organism (vice versa $tRNA^{ncAA}$ may not be aminoacylated by any endogenous aaRS) (76,77).

ii. The $tRNA^{ncAA}$ must recognize a unique codon (e.g. UAG), which may not be used by any endogenous tRNA (75).

iii. The ncAA has to be tolerated by the ribosome as well as by EF-Tu, needs to be stable towards metabolism and must be cell-permeable (76).

The most frequently used orthogonal aaRS/tRNA pair is pyrrolysyl-tRNA-synthetase/$tRNA^{Pyl}$ (PylRS/$tRNA^{Pyl}$) from *Methanosarcina* strains (*M. barkeri* and *M. mazei*), which offers two main advantages compared to other aaRS/tRNA pairs. First, ncAAs can be encoded in prokaryotic as well as eukaryotic model organisms and second, destruction of the natural synthetase activity is unnecessary since PylRS is not specific for one of the 20 canonical amino acids (69,76,78). Moreover, $tRNA^{Pyl}$ is a natural amber suppressor and the wildtype PylRS has a deep hydrophobic binding pocket, allowing the incorporation of bulky Nε-carbamate linked lysine derivatives into proteins (76,79). Y384F is a frequently occurring mutation in the flexible loop region of PylRS, which plays an important role in the binding of the substrate to the active site and shows enhanced aminoacylation of N-Boc L-lysine (BocK) (*Figure 5 B*) and pyrrolysine (79,80). Therefore, PylRS(Y384F) was used in this thesis.

A.7 Objective

Incorporation of ncAAs into peptides and proteins is a promising strategy to enhance their diversity, functionality and multiple other parameters (76). To combine advantages of the potent nature of the lantibiotic nisin and expansion of the genetic code, the path for an efficient system which allows ncAA incorporation into nisin needs to be cleared.

Previous experiments indicated that BocK and p-benzoyl-phenylalanine (pBF) as two model ncAAs could successfully be incorporated at every single position of the 34 amino acid long polypeptide nisin using amber SPS technology. To facilitate quantification of the ncAA incorporation efficiency, a so-called amber suppression efficiency screening was set up by linking a GFP gene to nisin, which harbors an amber codon at a selected position (*Figure 6*). By using this fusion assay, rapid scanning of different positions upon their ncAA incorporation strength is realizable through deduction of the amount of successfully ncAA-modified nisin from the measured GFP fluorescence strength.

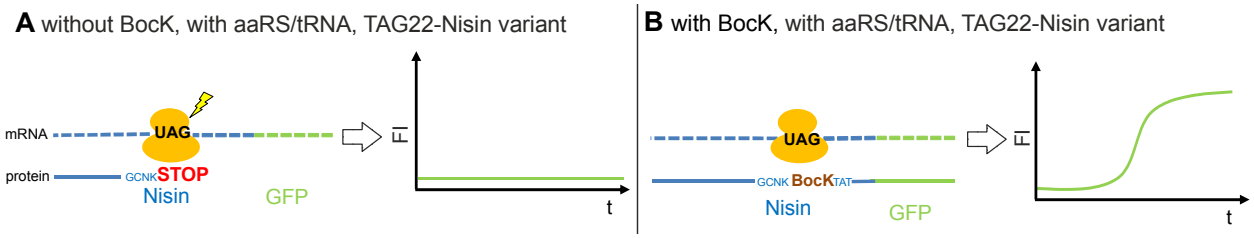

Figure 6. Principle of the nisin-GFP fusion assay. (A) Translation is interrupted in the presence of the suppressor pair (aaRS/tRNA) and in absence of BocK once the ribosome encounters the amber (TAG/UAG) codon (exemplarily position TAG22 is shown). No fluorescence increase is observable (FI is fluorescence intensity). (B) The full-length fusion protein is getting translated upon a successful BocK incorporation event, leading to an increasing FI.

Unexpectedly, GFP fluorescence was also observable in the absence of the ncAA when translation should be interrupted once the ribosome had encountered the internal amber codon. This first set of data suggests the presence of cryptic translation reinitiation sites, which reduces the yield of modified, mature nisin drastically by bypassing the amber stop codon. As a result of this 'leak expression' phenomenon, the hypothesis was proposed that unwanted N-terminally truncated products are getting translated, which compromise the homogeneity of ncAA-modified nisin. Therefore, the project's focus was to investigate and overcome this obstacle, hence, delivering a 'tight' recombinant expres-

sion system, which allows ncAA incorporation into nisin to gain a homogenous ncAA-modified product.

To allow full exploitation of SPS technology, establishment of a recombinant expression strategy of fully processed and active nisin in *Escherichia coli* was expedient. *E.coli* presents the most frequently used host organism for ncAA incorporation and offers the advantage of availability of a genetic toolbox for co-translational bioengineering. Although efforts have been made to allow SPI of ncAAs by ZHOU et al. and BAUMANN et al., only one report of successful stop codon suppression in *L. lactis* exists (66,81,82). Based on a publication of SHI et al., who successfully prepared fully post-translationally modified nisin in *E. coli*, the second goal of this work was the establishment of *E.coli* as nisin expression host in our lab to allow for utilization of SPS technology for the incorporation of ncAA into nisin.

B Methods

B.1 Microbiological techniques

B.1.1 Cultivation and selection of *E. coli* and *L. lactis*

Bacterial strain	Genotype
E. coli BL21(DE3)	*hsdS gal* (λcI*ts*857) *ind*1 *S*am7 *nin*5 *lac*UV5-T7 gene *1*
E. coli DH10B	F^- endA1 $deoR^+$ recA1 galE15 galK16 nupG rpsL Δ(lac)X74 φ80lacZΔM15 araD139 Δ(ara,leu)7697 mcrA Δ(mrr-hsdRMS-mcrBC) Str^R λ^- (83)
E. coli DB3.1	gyrA462 endA1 ∆(sr1-recA) mcrB mrr hsdS20 glnV44 (=supE44) ara14 galK2 lacY1 proA2 rpsL20 xyl5 leuB6 mtl1 (84)
E. coli MC1061	araD139, Δ(ara, leu)7697, ΔlacX74, galU-, galK-, hsr-, hsm+, strA (85)
E. coli T7 Express I^q	F' $proA^+B^*$ $lacI^q$zzf::Tn10(Tet^R)/fhuA2 lacZ::T7 gene1 [lon] ompT gal sulA11 R(mcr-73:: miniTn10--*Tet*^{S})2 [dcm] R(zgb-210::Tn10--*Tet*^{S}) endA1 Δ(mcrC-mrr)114::IS10 (86)
L. lactis NZ9000	Derivative of *L. lactis* subsp. *cremoris* MG1363, pepN::nisRK (87)

Table 1. Genotypes of utilized *E. coli* and *L. lactis* strains.

Cultivation of *E. coli* strains DH10B, DB3.1, MC1061 and T7 Express I^q (T7 Exp) was performed at 37°C, 220 rpm shaking in lysogeny broth (LB) medium (0.5 % (w/v) yeast extract, 1 % (w/v) tryptone, 1 % (w/v) NaCl). For selection of transformed cells antibiotics were added to the medium in the following concentrations: ampicillin 100 µg/ml, kanamycin 50 µg/ml, streptomycin 50 µg/ml, erythromycin 250 µg/ml, chloramphenicol 33 µg/ml.

L. lactis strain NZ9000 was cultivated at 30°C, without shaking in GM17 medium (ascorbic acid, 0.5 g/l lactose, 5 g/l magnesium sulfate, 0.25 g/l meat extract, 5 g/l meat peptone (peptic), 2.5 g/l sodium glycerophosphate, 19 g/l soya peptone (papainic), 5 g/l tryptone, 2.5 g/l yeast extract, 2.5 g/l, 5 g/l glucose). For selection, erythromycin (Ery, 10 µg/ml) and/or chloramphenicol (Cam,10 µg/ml) was added to the medium. GM17 medium with Cam and Ery was stored at +4°C for a maximum of seven days.

Agar plates were prepared by dissolving 15 g/l agarose in GM17 medium, adding the appropriate antibiotic in the same concentrations as in liquid medium, unless otherwise stated, and pouring approximately 16 ml of the 45°C warm solution into sterile petri dishes.

B.1.2 Preparation of chemically competent *Escherichia coli* cells

Chemically competent *E. coli* cells were prepared according to a modified protocol of INOUE et al. (88). First, an overnight culture of a single colony was diluted 100-fold in 100 to 1000 ml of SOB medium (Super Optimal Broth, yeast extract 0,5 % (w/v), tryptone 2 % (w/v), NaCl 10 mM, KCl 2,5 mM, $MgCl_2$ 10mM, $MgSO_4$ 10 mM) supplemented with 20 mM glucose, 10 mM $CaCl_2$ and the appropriate antibiotic. The culture was grown to an OD_{600} of 0,4-0,6 at 37°C, 220 rpm shaking. Cells were harvested in 50 ml falcon tubes by centrifuging at 2500xg, 4°C for 10 min. Each cell pellet was resuspended in 16 ml ice-cold transformation buffer I (RbCl 100 mM, $MnCl_2$*$4H_2O$ 50 mM, CH_3COOK 30 mM, $CaCl_2$*$2H_2O$ 10 mM, 15 % glycerol, adjusted to pH 5,8 with acetic acid) and incubated on ice for 15 min. The cells were again centrifuged at 1000xg, 4°C for 5 min. Next, the cell pellets were resuspended in 4 ml ice-cold transformation buffer II (MOPS (0,5 M, pH 6,8) 10 mM, RbCl 10 mM, $CaCl_2$*$2H_2O$ 75 mM, 15 % glycerol, adjusted to pH 6,8 with NaOH). Aliquots (à 200 µl) were snap-frozen in liquid nitrogen and stored at -80°C for a maximum of six months.

B.1.3 Preparation of electrocompetent *L. lactis* cells

Electrocompetent *L. lactis* cells were prepared according to a modified protocol of HOLO AND NES (89). Initially, an overnight culture of a single colony in GM17 medium was diluted 10-fold in SMGG medium (GM17 medium with 0.5 M sucrose, 1 % glycine), supplemented with the appropriate selection antibiotic. The culture was grown until OD_{600} reached 0,3-0,4 at 30°C, without shaking and was then transferred into 50 ml falcon tubes. Next, cells were harvested at 4500 rpm, 4°C for 25 min. The pellets were then resuspended in 50 ml wash buffer I (sucrose 0,5 M and 10 % glycerin in H_2O) per 50 ml falcon tube and centrifuged (4500 rpm, 4°C, 25 min). In the following step, the supernatant was discarded and cell pellets were resuspended in 25 ml wash buffer II (0.5 M su-

crose, 10 % glycerin, 50mM EDTA in H_2O) per 50 ml falcon tube, kept on ice for 15 min and centrifuged (4500 rpm, 4°C, 25 min). In a final washing step, pellets were washed with 12,5 ml of wash buffer I and centrifuged (4500 rpm, 4°C, 20 min). The cell pellets were then resuspended in 0,5 ml wash buffer I, aliquots à 50 µl were filled in 200 µl PCR tubes, frozen using dry ice and stored at -80°C for a maximum of six months.

B.1.4 Transformation of chemical competent *Escherichia coli* bacteria

For transformation of chemical competent *E. coli* the heat shock method was applied. 200 µl aliquots of bacteria were thawed on ice and either 20 µl of the ligation mixture or 1-100 ng of plasmid DNA were added to the cells. The cells were then incubated on ice for 30 min, followed by a 30 sec heat shock at 42°C and a final 5 min incubation step on ice. The transformation mixture was supplemented with 800 µl LB_0 medium and incubated at 37°C, 220 rpm shaking for 60 min. Finally, 100 µl of the 10 % and 90 % concentrated transformed competent cells were plated on LB-agar containing the selection antibiotics and left grown overnight.

B.1.5 Transformation of electrocompetent *L. lactis* bacteria

For transformation of electrocompetent *L. lactis* (89), 50 µl aliquots of competent bacteria were thawed on ice. 50-200 ng plasmid DNA was added to the cell suspension and immediately transferred to an ice-cooled electroporation cuvette (2 mm electrode gap). The cells were exposed to a single electrical pulse, which was delivered by a Gene-Pulser device (Bio-Rad) that was set to 2,5 kV, 25 µF and 200 Ω (setting option Ec2). Immediately after the pulse, 950 µl of room-temperature warm SMG17MC medium (GM17 with sucrose 0,5 M, MgCl2 20 mM, CaCl2 2 mM) were added to the suspension and incubated for 2 h at 30°C, 200 rpm. The cells were then centrifuged at 4000 rpm, 5 min. 900 µl of the supernatant were discarded and the cell pellet was resuspended in the remaining 100 µl medium. The complete 100 µl were then spread on a M17 agar plate, containing Cam and/or Ery at a concentration of 5 µg/ml. Colony growth was read out after 48 h of incubation at 30°C.

B.2 Molecular biology techniques

B.2.1 General cloning strategy

Inserts for cloning were obtained by reverse transcription polymerase chain reaction (RT-PCR), overlap extension PCR, PCR like reaction or via digestion of the gene of interest containing plasmid. PCR products were purified by agarose gel electrophoresis in 1xTBE buffer (89 mM Tris, 89 mM boric acid, 2 mM EDTA-Na_2, pH 8.0), using ethidium bromide (50 ng/ml gel) as a dsDNA intercalating fluorescence dye to visualize the DNA when observed under a bluescreen tansilluminator, followed by DNA extraction using the QIAquick Gel Extraction Kit (QIAGEN Inc.) according to the manufacturer's guidelines (90). Restriction digestions of vector and insert (500 ng to 5 µg DNA) were conducted at 37°C for 1-3 h, using appropriate restriction enzymes (20 U) and buffers (1 x concentrated) according to the manufacturer's instructions (91). The vector was subsequently treated for 1-2 h with 0.5 U/µl Calf Intestinal Phosphatase (CIP) to minimize recircularization of the vector. Digested products were purified by agarose gel electrophoresis and extracted with the QIAquick Gel Extraction Kit. For ligation, the Quick Ligation Kit (NEB) was used. The reaction was carried out at room temperature for 5-15 min using 1x Quick Ligation Reaction Buffer, Quick Ligase 1 µl/20 µl reaction assay, vector (50 ng) and a triple to fivefold molar excess of insert DNA (molar ratio of vector:insert, 1:3-5). Transformation was performed as described in B.2.1.4.

Analyzation of transformants was done by colony PCR and analytic digestion. For colony PCR, one transformant was inoculated with 50 µl of LB, containing the selection antibiotic, and incubated at 37°C, 220 rpm for 1 h. The reaction (1xGoTaq Green Master Mix, 10 µM of respective forward and reverse primers, 1 µl of the inoculated transformant per 20 µl total reaction volume and nuclease-free water) was prepared and the DNA amplified using the following thermocycler conditions: initial denaturation (94°C, 10 min), 32 amplification cycles (each: 94°C for 30 sec, 55°C for 30 sec, 72°C for 30-60 sec) and final extension (72°C, 10 min). For analytic digestion, 300-500 ng DNA were incubated at 37°C, 1 h, with restriction enzymes (20 U) and buffers (1x concentrated) according to the manufacturer's guidelines (91), followed by DNA length separation via gel electrophoresis and documentation with the AlphaImager HP Transiluminator.

B.2.2 Construction of pScreen_M21K _ *nisA*

The M21K point mutated *nisA* gene (GenBank: HM219853.1) was generated by aligning and elongating oligonucleotide M21K_*nisA*_fw and M21K_*nisA*_rev using the following conditions: denaturation (98°C, 5,5 min), annealing (55°C, 30 sec) and extension (72°C, 60 min). The reaction included 1x Phusion HF buffer, 10 mM dNTPs, Phusion HF DNA polymerase (0,04 U/µl), oligonucleotides M21K_*nisA*_fw and M21K_*nisA*_rev (10 nM) and nuclease-free water. The DNA fragments were run on a 2 % agarose gel and the products were extracted using a QIAquick Gel Extraction Kit. The resulting mutant *nisA* DNA fragment was digested with NheI and HindIII at 37°C for 2 h using 1x CutSmart Buffer. The vector pScreen_*ccdB* was digested with NheI and HindIII at 37°C for 2 h, using 1x CutSmart Buffer and adding CIP (0.5 U/µl) after 60 min. The digests were run on a 1 % agarose gel and the products were purified using a QIAquick Gel Extraction Kit. The resulting digested mutant *nisA* gene was inserted into the respective digested vector pScreen_*ccdB* between the NheI and HindIII restriction sites. Ligation and transformation with chemically competent DB3.1 cells were carried out as described above. The cells were plated on LB_{Amp} agar plates and grown at 37°C for 16 h. Three colonies were picked and incubated in 5 mL LB_{Amp} at 37°C for 16 h, followed by analyzation of the cloned plasmid (analytic digestion) and plasmid isolation using a GeneJET Plasmid Miniprep Kit (Thermofisher). Sequence verification was performed via Sanger DNA sequencing by GATC Biotech (Konstanz, Germany) using the appropriate primers.

B.2.3 Construction of pScreen_M17XM21K_final_*nisA*(co-LI)

Plasmid DNA pSEVA_M21K_*nisA*(co-LI) (cloned with the same protocol as pScreen_M21K_*nisA*(co-LI), but with pSEVA_silent as vector) was used as a template for introducing the site specific M17X randomized mutation by overlap extension using PCR (92). In a first step, two PCR reactions were prepared. PCR 1 contained forward primer M17X_*nisA*_fw, binding in the *nisA* gene of pSEVA_M21K_*nisA(*co-LI), harboring the desired NNK-mutation at amino acid position 17 and a 3' overhang complementary to the sequence of *nisA,* and reverse primer PS2, binding outside of the gene. PCR 2 included forward primer PS1 and M17X_*nisA*_rev, binding directly in front of the mutation site and creating a 20 bp overlap with the product of PCR1. The conditions for

PCR1 and 2 were the following: initial denaturation (94°C, 5 min), 30 amplification cycles (each: 94°C for 30 sec, 55°C for 30 sec, 72°C for 1 min) and final extension (72°C, 10 min). The reaction included 1x Phusion HF buffer, 10 mM dNTPs, Phusion HF DNA polymerase (0,04 U/µl), 160 ng plasmid DNA, 10 µM forward and reverse primer, and nuclease-free water. Amplified products were purified on a 2 % agarose gel and extracted using a QIAquick Gel Extraction Kit, yielding 2,9 µg of DNA fragment from PCR1 (198 bp) and 1,5 µg DNA from PCR2 (250 bp). Both PCR products were combined as templates in a third PCR amplification step (PCR1+2) with primers PS1 and PS2. Here, the same PCR cycler conditions as described above were applied. The reaction included 1x Phusion HF buffer, 10 mM dNTPs, Phusion HF DNA polymerase (0,04 U/µl), 100 ng DNA of PCR1 and 2, and nuclease-free water. The final PCR product, encompassing the mutated *nisA*, was again purified by gel electrophoresis, giving 4,5 µg of DNA (428 bp), followed by digestion with NheI, HindIII and SpeI to obtain the 118 bp long mutated *nisA* gene. The digested vector pSEVA (NheI, HindIII) and the insert were ligated and transformed into DB3.1 cells (see B.2.2.1 and B.2.1.4). A colony PCR was performed and all positive transformants were inoculated in 5 mL LB_{Amp} at 37°C for 16 h, followed by isolation of the plasmids using a GeneJET Plasmid Miniprep Kit. The integrity of the plasmid and the identity of the different mutants were verified via Sanger DNA sequencing by GATC Biotech using the appropriate primers. The pSEVA_M17XM21K_*nisA*(co-LI) plasmid was then again digested with NheI and HindIII, as well as pScreen_*ccdB*. Complete cutting of the insert was ensured by doing so. Finally, ligation and transformation into DB3.1 cells was conducted and the plasmid pScreen_M17XM21K_*nisA*(co-LI) was sequenced.

B.2.4 Site-directed mutagenesis to obtain variants M17H, W, Y, C, E, T and M17IM21K

For construction of the seven missing variants site-directed mutagenesis was performed using the corresponding primers M17H_*nisA*_fw to M17I_*nisA*_fw and pNZ_rev (compare table in section E.1.3.1) for part 1 of the overlap extension PCR and pNZ_fw and M17X_*nisA*_rev (X is H, W, Y, C, E, T, I) for part 2 of the PCR. The reaction mixture included the same components and PCR conditions were consistently applied as de-

scribed in B.2.3, whereas pScreen_M21K_*nisA* was used as template DNA. A third PCR (PCR 1+2) combined the obtained DNA pieces from PCR 1 and 2, using primers pNZ_fw and pNZ_rev. The final products were subsequently digested with NheI and HindIII, ligated into pScreen_*ccdB* and transformed into *E. coli* MC1061 (compare B.2.3).

B.2.5 Confirm presence and integrity of plasmid in *L. lactis*

To confirm the presence of the respective plasmid (pScreen, containing the NisA derivative) in *L. lactis*, plasmid DNA was isolated using the GeneJET Plasmid Miniprep Kit from a 10 ml overnight culture. Prior treatment with 30 mg/ml lysozyme (disruption of the gram positive cell membrane) did not improve yields significantly. Therefore, the manufacturer's protocol for DNA preparation from *E.coli* was followed. The obtained DNA was subsequently used as template DNA for PCR, aiming at the amplification of the sequence section of interest. The conditions for PCR were as follows: 1xGoTaq Green Master Mix, 10 µM of forward (pNZ forward) and reverse (pNZ reverse) primers, 1 µl plasmid DNA and nuclease-free water (ad. 20 µl). Components were mixed and the respective DNA sequences were amplified (95°C 5 min, 35x (95°C 30 sec, 55°C 30 sec, 72°C 1 min), 72°C 10 min, 4°C infinite hold). Subsequently, the PCR products were sequenced at GATC Biotech (Konstanz) or Seqlab (Göttingen).

B.3 Protein biochemistry techniques

B.3.1 Nisin expression and purification from *Escherichia coli*

BL21(D3) or T7 Exp cells were transformed with the respective plasmids (pRSFDuet_*nisBC* (codon optimized for *E. coli* (co-Ec) sequences) and pET21a_His6_leader_*nisA*(wt or co-Ec DNA sequence)), containing the gene sequences for the proteins of interest. A single clone was picked to inoculate LB medium with selection antibiotics (Kana, Amp) for 16 h at 220 rpm shaking. The overnight culture was diluted 1:100 in Terrific Broth (TB) medium (1,2 % tryptone, 2,4 % yeast extract, 0,5 % glycerol, 89 mM phosphate buffer, H_2O) containing the respective selection antibiotics. Protein expression was induced with 0,5 mM IPTG when OD_{600} 0,3-0,5 was reached. The cells were

then incubated for 16-18 h at 18°C and harvested by centrifugation at 4500 rpm, 4°C, for 15 min.

Protein purification was carried out in a modified procedure according to SHI et al. (93). Cell pellets were thoroughly resuspended in 5 ml start buffer (20 mM Tris, pH 8,0, 500 mM NaCl, 10 % glycerol, containing a protease inhibitor cocktail from Roche Applied Science) per gramm cell pellet and homogenized by sonication for approximately 15 min using a Branson sonifier 450 device (0,5 ms pulse, 0,5 ms pause, level 5). The samples were centrifuged at 21.000-24.000×g for 30 min at 4°C. Purification of the peptide using a His Gravi/SpinTrap TALON column (GE Healthcare) was done according to the producer's manual. First, the supernatant was loaded onto the His-trap column, which was pre-equilibrated with start buffer. Following loading, the column was washed with wash buffer (start buffer+30 mM imidazole). The peptide was eluted from the column using elution buffer (start buffer+1 M imidazole). Further concentration of the sample was performed by applying the solution on an Amicon Ultra 3K centrifugal filter (Merck). Prior to further purification via high-performance liquid chromatography, buffer exchange was achieved by gel filtration using 10 ml NAP columns (GE Healthcare) to 100 mM acetic acid/ammoniumacetat (pH 3,9) according to the manufacturer's protocol.

B.3.2 Reverse phase high-performance liquid chromatography (RP-HPLC)

An Agilent 1100 series HPLC system connected to an Agilent Zorbax Eclipse XDB C8 column (4.6 x 150 mm, 5 µm) was used to further purify protein samples. The column was pre-equilibrated with 100 % H_2O + 0,1 % (v/v) TFA (solvent A). The run started with 100 % solvent A for 5 min. Afterwards a gradient of 0-100 % acetonitrile + 0,1 % (v/v) TFA (solvent B) was steadily built up in a 30 min time period to elute the different sample compounds. Finally, 100 % solvent B (5 min) was used to elute all remaining protein from the column. Protein or peptide elution was monitored at 210, 220 and 280 nm. Modified prenisin began to elute at 60 % solvent B. Fractions were analyzed by agar well diffusion assay and 16,5 % Tricin-SDS-PAGE.

B.3.3 Mass spectrometry

Mass spectrometric analysis of samples was kindly provided by Eduard Hochmuth (AG Meister, University of Regensburg). Potential contaminations of HPLC-purified proteins were excluded by low flow liquid chromatography, using the Ultimate 3000 RSLC nano system (Thermo Scientific), prior to matrix-assisted laser desorption/ionization time-of-flight mass spectrometry (MALDI-TOF MS) with a 4800 Plus MALDI TOF/TOF Analyzer and a connected Maxis 4G electron spray device (Bruker).

B.3.4 SDS-PAGE

Proteins were separated according to their size via sodium dodecyl sulfate polyacrylamide gel electrophoresis (SDS-PAGE). Protein samples were mixed with 2x boiling mix (10 % (v/v) mercaptoethanol, 2 % (v/v) SDS, 0,5 mM EDTA, 10 % (v/v) glycerol, 0,005 % (w/v) bromphenol blue, 62,5 mM Tris/HCl pH 6,8), boiled at 95°C for 10 min and centrifuged (1 min, 4000 rpm). The stacking gel was prepared by mixing 0,33 ml 30 % acrylamide, 0,4 ml stacking gel buffer (0,625 M Tris, pH 6,5), 0,4 ml 0,5 % SDS, 0,86 ml H_2O, 1,7 µl TEMED and 10 µl 10 % APS. A prestained protein ladder (Precision Plus Protein Dual Xtra Standards) as reference and protein samples were loaded on a 15 % SDS gel (30 % acrylamide 3,1 ml, separation gel buffer (1,88 M Tris/HCl, pH8,8) 1,2 ml, SDS 0,5 % (w/v) 1,2 ml, H_2O 0,55 ml, TEMED 4,6 µl, APS 10 % (w/v) 31 µl → giving a total volume of 6 ml) and electrophoresis was performed at 90 V for ca. 20 min until the samples reached the separation gel (migration could be observed by addition of bromphenol blue). Proteins were separated at 130 V for ca. 60 min using the Mighty Small II system (8x7cm; Serva Electrophoresis).

B.3.5 Tricin-SDS-PAGE

By using a Tris-Tricin-buffer system, proteins/polypeptides in the range of 1-100 kDa can be separated in superior quality to glycine-SDS-PAGE systems. According to an adapted protocol from SCHÄGGER AND JAGOW, the anode buffer (0,2 M Tris/HCl, pH 8,9) and cathode buffer (12,11 g Tris, 17,92 g Tricin, 10 ml 10 % (w/v) SDS ad 1 l H_2O; can be stored for a maximum of one month at 4°C) were prepared (94,95). Protein samples were prepared by mixing the sample with 2x sample buffer (1 ml 1 M Tris/HCl, pH6,8,

0,8 g SDS, 3 g glycerol, 0,31 g dithiothreitol (DTT), 2 mg Coomassie blue R-250 ad 10 ml H_2O) and boiled at 100°C for 5 min. The samples were loaded onto a stacking gel (for one gel: 0,33 ml 30 % acrylamide, 0,4 ml stacking gel buffer (0,625 M Tris, pH 6,5), 0,4 ml 0,5 % SDS, 0,86 ml H_2O, 1,7 µl TEMED, 10 µl 10 % APS) and a 16,5 % separation gel (for one gel: 4,04 ml 30 % acrylamide, 2,5 ml separation gel buffer (3 M Tris/HCl, pH 8,45), 75 µl 10 % SDS, 90 µl H_2O, 25 µl 10 % APS, 5 µl TEMED). The cathode buffer was filled into the upper chamber and the anode buffer into the lower chamber of the Mighty small II electrophoresis system (Serva Electrophoresis). Stacking of the protein samples was performed at 90 V for 20 min and separation was accomplished by increasing the tension to 130 V for 60 min.

B.3.6 Coomassie staining

Proteins were visualized by incubation of the SDS gels with Coomassie staining solution (1.25 % (w/v) Coomassie Brilliant Blue R-250, 50 % (v/v) ethanol, 7 % (v/v) acetic acid) for 15 min. Gels were destained by incubation with H_2O at room temperature for several hours (up to 48 h).

B.3.7 Silver staining

Silver staining of SDS gels was performed according to an adapted procedure from SWITZER et al. (96). Gels were first incubated for 60 min in 25 ml fixation solution (50 % methanol, 12 % acetic acid, 12,5 µl 37 % formaldehyde). The gel was then washed in 50 % (v/v) ethanol for 10 min, followed by another washing step in 30 % (v/v) ethanol for another 10 min. To reduce unspecific background binding of silver ions, the gel was incubated for 1 min in 25 ml sodium thiosulfate (0,2 g/l) and washed three times with 25 ml H_2O, each time for 20 sec. In the next step, the gel was incubated for 20 min in 25 ml staining solution (0,1 % (w/w) $AgNO_3$, 18,75 µl 37 % formaldehyde) and afterwards washed three times with 25 ml H_2O, each time for 20 sec. Protein bands were visualized by reduction of Ag^+ to Ag using 25 ml developing solution (6 % (w/w) Na_2CO_3, 12,5 µl 37 % formaldehyde, 50 µl sodium thiosulfate (0,2 g/l)). The reaction was stopped by incubation with 25 ml 5 % (v/v) acetic acid for 5 min once protein bands reached the de-

sired intensity (maximum 10 min incubation in developing solution). Finally, gels were washed twice with H_2O, each time for 10 min.

B.3.8 TCA precipitation

One volume 100 % trichloroacetic acid (TCA) (prepared by dissolving 10 g TCA in 7 ml H_2O, stored at room temperature) was added to four volumes of protein sample, incubated for 120 min at -20°C and centrifuged at 14.000 rpm, 5 min, 4°C. The supernatant was removed and the pellet was washed with 200 µl ice-cold acetone/ml sample and once more centrifuged at 14.000 rpm, 5 min, 4°C. Finally, the pellet was completely dried by incubation at 50°C for 10 min and dissolved in 0,05 % acetic acid (if the protein was nisin).

B.3.9 Amber suppression reporter assay/ amber suppression efficiency screening

Nisin and nisin variant expression was relatively quantified by measuring the fluorescence of the reporter protein eGFP (enhanced green fluorescent protein). For this purpose, NisA variants were cloned into the pET21a_His6_leader_*nisA*_PLrigid_*egfp* (= pET_*nisA*_*egfp*) vector from Miriam Thewes' project using standard cloning techniques (compare B.2.1) and the XhoI and NdeI restriction sites. Fluorescence measurements were performed using an Infinite 200 Pro microplate reader (Tecan) and the corresponding Magellan software (Tecan) in a 24-well plate format (Greiner Bio-one, Austria). The excitation wavelength was 480 nm (bandwidth: 9 nm) and the emission wavelength 510 nm (bandwidth: 20 nm, 5 flashes, top mode, 20 µs integration time and 0 µs lag time, 3x3 reads per well in a square file type). The optical density was measured at the same time by determining the absorbance at 600 nm (3x3 reads per well in a square file type, 2 flashes). The device's (bottom and lid) temperature was kept between 36,5 and 37,5°C and the lid was sealed with parafilm to prevent loss of fluid due to evaporation (weight loss before to after measurement was less than 0,25 %). The first measurements were performed after 20 sec of shaking (amplitude 3 mm). Subsequently, 40 kinetic cycles were measured. Each cycle started with 600 sec of shaking (amplitude

3 mm) and was continued by absorbance and fluorescence intensity measurements as described in detail above.

Bacterial cultures were prepared by diluting an overnight culture ($LB_{Cam/Amp}$ supplemented with 1 % glucose to suppress any kind of leak expression) of T7 Exp cells containing pTB290 (encoding the PylRS(Y384F)/$tRNA^{Pyl}$ orthogonal suppressor pair) and the respective pET21a plasmid, by 1:100 in $LB_{Cam/Amp}$ supplemented with 1 % glucose (addition of 200 µl 25 % glucose stock solution to 5 ml LB medium). Overnight cultures were inoculated from glycerol stocks. Each biological replicate was inoculated from a different glycerol stock (except for wt TAG variants, as these were taken over from Miriam Thewes' project and here only one glycerol stock per variant was available). Cultures were then left grown to a steady state (ca. 5-9 h) and again diluted 1:25 in $LB_{Cam/Amp}$ without glucose in a screw cap tube to reach an OD_{600} of ~0,1 (here: 200 µl bacterial culture in 5 ml $LB_{Cam/Amp}$). When OD_{600} reached 0,5-1,0, samples were transported to the Tecan plate reader (transportation time approximately 10 min) and normalized to an OD_{600} of 0,25. 0,02 % (w/w) Arabinose (1,5 µl from a 20 % stock solution per 1,5 ml total volume), 1 mM IPTG (1,5 µl from a 1 M stock solution), and 1 mM BocK (30 µl from a 50 mM BocK in 50 mM NaOH stock solution) were added, giving a total volume of 1,5 ml per well (24-well-plates were used). Addition of water instead of BocK served as negative control. In case of measurement of controls, where bacteria did not possess an ampicillin and/or chloramphenicol resistance gene, the respective antibiotic was abolished from the medium and LB_{Amp}, LB_{Cam} or LB_0 was used.

B.4 Antimicrobial activity assays

B.4.1 Production of prenisin by *L. lactis*

Variants of *nisA* (on plasmid pScreen_*nisA*) were transformed into the producer strain *L. lactis* harboring a pScreen plasmid, which carried the DNA sequence of the NisA variant and pIL_BTC for the PTM machinery (compare B 1.5). A culture was inoculated for 48 h from 20 picked clones and glycerol stocks were prepared by centrifuging the cells at 4000 rpm, 10 min, diluting the cell pellet in GM17 medium with 50 % (v/v) glycerol and storage at -80°C until further utilization. The glycerol stocks were used to inoculate overnight cultures of the producer strain and diluted 1:20 on the next morning. Cells

were left grown to an OD_{600} of 0,4-0,6 at 30°C without shaking, normalized to an OD_{600} of 0,4 and induced by adding 1 mM IPTG (binds to lac repressor, which consequently releases the lacO site) and 5 ng/ml nisin (prepared from a 1 mg/ml nisin (Sigma Aldrich) in 0,05 % acetic acid stock solution). Cultures were then incubated for another 3 h at 30°C, normalized to an OD_{600} of 1,5 and harvested by centrifugation at 4500 rpm for 10 min. The supernatant was sterile-filtered and stored at -20°C for a maximum of six weeks.

B.4.2 Agar well diffusion assay

Agar plates were prepared by heating sterile GM17 supplemented with 15 g/l agarose in a microwave until the medium was completely fluid. The solution was then held at 45°C in a water bath for a minimum of 30 min. Next, 10 µg/ml Cam and 10 µg/ml Ery and 1 % (v/v) of a *L. lactis* (containing pIL253, harboring the Cam^R, and pNZ*_nisP*, which encodes the NisP protease) (*L. lactis* [pIL,pNZ]) overnight culture were added and gently mixed. The warm, fluid agar was poured in 9 cm petri dishes until the bottom was completely covered and left to dry (takes about 3-5 min). In the next step, four wells with 7 mm diameter were made in each quarter of the plate using the bottom of a 200 µl pipette tip. 25-30 µl of the prenisin containing supernatant (compare B.4.1) were pipetted in each well and plates were incubated overnight at 30°C. Documentation was done with the AlphaImager HP Transiluminator (Proteinsimple, United States).

B.4.3 Minimal inhibitory concentration and dilution assay

For comparative estimation of the antimicrobial activity of the different NisA variants, the minimal inhibitory concentration or dilution assay (MID/MIC) was applied. Principally, this assay tests the antimicrobial activity of the supernatant of nisin producing bacteria or commercial nisin against a specific sensor strain (*L. lactis* [pIL,pNZ]).

Prenisin containing supernatant (compare B.4.1) or freshly prepared nisin stock solutions (each 1 mg/ml in H_2O, sterile-filtered) were diluted as required with GM17 medium (containing Cam and Ery) in a 96-well plate (total volume of each dilution step: 100 µl). An overnight culture of the sensor strain was diluted 1:20 and left grown to an OD_{600} of 0,5-0,8 (logarithmic growth phase, takes approximately three to four hours). Next, the

sensor was diluted to an OD_{600} of 0,1 and thoroughly mixed in equal parts (100 µl) with the diluted supernatant or the commercial nisin, resulting in an overall OD_{600} of 0,05. Bacterial growth was monitored using the Tecan Infinite 200 Pro by applying the following conditions: temperature 30°C, each cycle: 120 sec shaking, 6 mm amplitude (corresponds to 142 rpm, orbital mode), followed by immediate absorbance measurement at 600 nm (bandwidth: 9 nm, three flashes) and 18 min waiting time (no shaking). 72 repetitions were measured and the MIC/MID values were read out after ten hours.

B.4.4 Growth curve analysis

To further analyze and reveal the subtle differences between the different variants, the prenisin containing supernatants of *L. lactis* (B.4.1) were subjected to a growth curve analysis. Different dilutions of the supernatant were prepared by mixing the supernatant with GM17 medium and 100 µl were pipetted into a 96-well plate (flat bottom with lid, Sarstedt, Germany). An overnight culture of the sensor strain (*L. lactis* [pIL,pNZ]) was diluted 1:20. Once an OD_{600} of 0,5 was reached, it was normalized to an OD_{600} of 0,1 and 100 µl were added to the dilutions of the supernatant. Same measurement conditions as described in B.4.3 were applied, using the Tecan Infinite 200 Pro. Depending on the time period of interest, cycles were repeated 42-72 times.

B.5 Statistical analyses

Statistical analyses were performed using Microsoft Excel 2010 and GraphPad Prism. If statistical significance of the comparison of two values was calculated, the Shapiro-Wilk test of normality was performed prior to further analyses (97). In case of a Gaussian distribution, a paired Student's t-test was applied. For samples with non-Gaussian distribution, the Mann-Whitney U-test was applied. Significance levels of $p<0,05$, $p<0,01$ and $p<0,001$ were marked with (*), (**) and (***), respectively. The standard error of the mean (SEM) is indicated as parameter for sampling distribution. In case of growth curve analysis, FI measurements and protein expression, measurement differences which could occur because of clonal variations were assumed to be negligible. Data fitting was performed using GraphPad Prism version 5.01 (GraphPad Software, 2007). All experiments were performed in technical and biological triplicates unless otherwise stated.

C Results

Two major goals were pursued:

[1] Investigation of the reasons for the occurrence of GFP-harboring products in the absence of BocK ('Leak expression') (C.1).

[2] Establishment of a stable expression system for nisin in *E. coli* (C.2).

C.1 Translation reinitiation leads to leak expression of the reporter when incorporating ncAAs into nisin

C.1.1 Leak expression can be observed in the amber suppression efficiency screening of NisA(wt)

To investigate the position-dependency of the efficiency of ncAA incorporation into nisin, a nisin-GFP fusion assay for relative protein quantification was established in the group of Prof. Dr. Ralf Wagner by Maximilian Fischer (98) and Miriam Thewes.

The principle of the amber suppression reporter assay is shown in *Figure 7* with nisin A (NisA), harboring a TAG codon at position 22, as an example of a nisin TAG variant. Basically, *nisA* is linked to an enhanced green fluorescence protein (eGFP) gene, which allows indirect monitoring of successful protein expression via measurement of the fluorescence intensity (FI). Without addition of the ncAA, the TAG codon works as a stop signal, terminating translation ahead of the eGFP gene and consequently no increase of fluorescence is measurable (*Figure 7 A*). In case of presence of: [1] the orthogonal suppressor pair, [2] the plasmid which carries *nisA*, with an amber codon at a selected position, linked to *egfp* and [3] the ncAA, the full length fusion protein NisA-eGFP is translated and one can observe an increasing fluorescence over the time that has passed since induction of protein expression (*Figure 7 B*). Depending on the selected TAG position within nisin, different strong amber suppression is expected. The expression 'amber suppression efficiency' means the efficiency by which the amber stop codon's (TAG) function is successfully replaced by not interrupting translation but instead coding for a ncAA. The amber suppression reporter assay is therefore used to perform the 'amber suppression efficiency screening'. As suppression rate was the focus of this experiment,

it was decided to use the extensively studied, commercially available BocK as model for a ncAA.

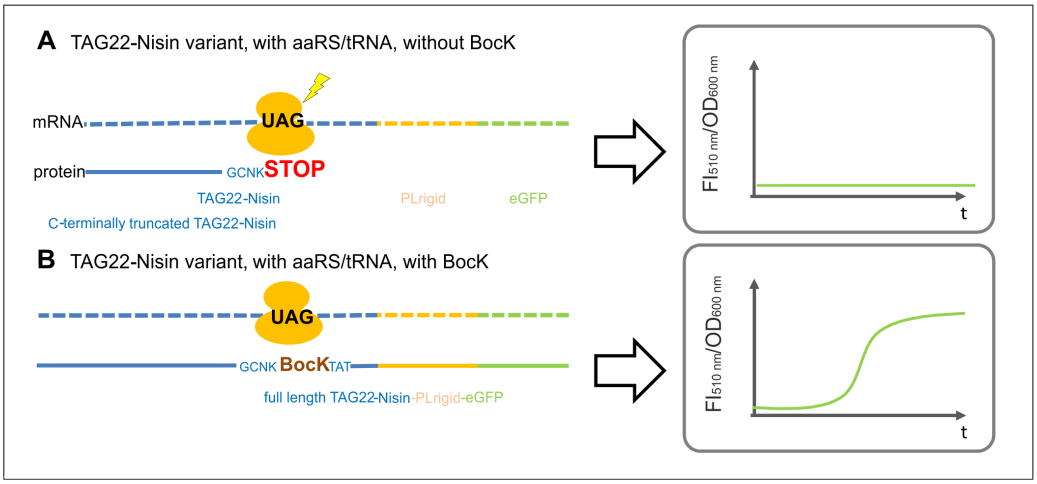

Figure 7. Principle of the amber suppression reporter assay. (A) When BocK is not present, the TAG codon functions as a stop signal for translation and no fluorescence can be observed, as no fused eGFP is expressed. Exemplarily, the mRNA of *nisA* with the TAG codon at position 22 is schematically shown as a dashed blue line, connected via the linker (yellow) to *egfp* (green). **(B) When BocK is present,** the full length fusion protein is translated and increasing fluorescence can be observed after induction of expression.

To introduce the required genetic information into bacteria, plasmids pET_*nisA*_*egfp* (*Figure 8 A*), which was constructed within Miriam Thewes and Maximilian Fischer's projects, and pTB290 (*Figure 8 B*), harboring the elements for the modified translation machinery, were utilized.

pET21a is a commercial vector (Merck), carrying an Amp^R, a pBR322 ori, a T7 promoter, followed by a lacO site and the lac repressor LacI that allows induction of protein expression with IPTG (99). For our purposes, the *nisA* (GenBank: HM219853.1), including its leader peptide, was N-terminally fused to a 6xHis-Tag by a small linker (complete encoded amino acid sequence: MGSSHHHHHHSQDP) and linked to *egfp* via the PLrigid sequence (based on a previously characterized α-helix motif published by YAN et al. (92)). PLrigid consists of a repetitive EAAAR-motif forming an inflexible 20 amino acid long $((EAAAR)_4)$ α-helix, which is expected to separate nisin and eGFP to minimize sterical hindrances that could otherwise affect protein translation and folding (100). The TAG codon was then integrated into nisin at the position of interest by common cloning strategies (B.2.1). To introduce the necessary elements for the modified translation machinery, the pTB290 plasmid (kindly provided by Dr. Tobias Baumann and Prof. Dr. Nedeljko Budisa, TU Berlin) was used. pTB290 contains an *E. coli* codon optimized (co-

Ec) version of pyrrolysyl-aaRS from *M. mazei* with an Y384F point mutation (compare A.6), *glnS*, which encodes the glutamine tRNA ligase, and $tRNA^{Pyl}$ under the control of the tryptophan promoter (Trp promoter). Replication is enabled by a p15a ori and Cam^R allows bacterial selection.

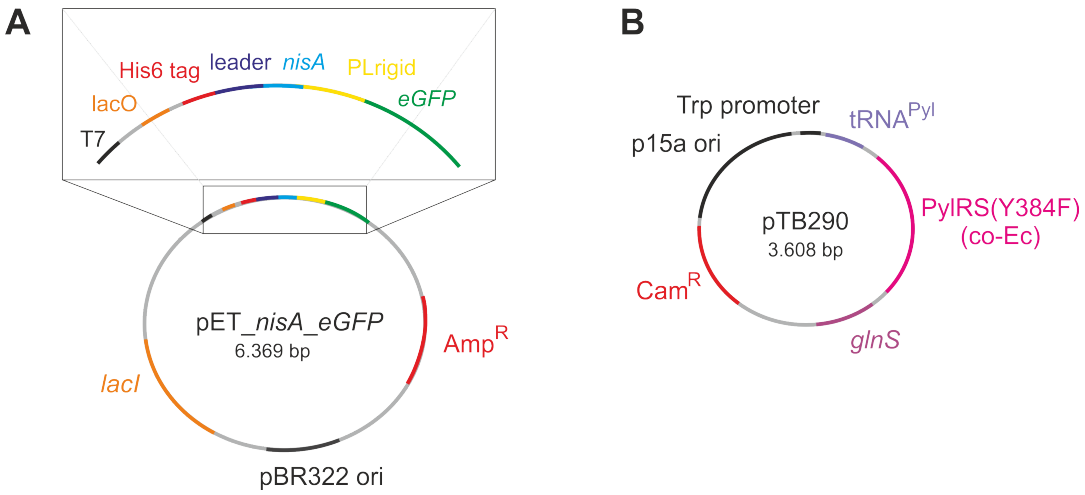

Figure 8. Schematic vector map of (A) pET_*nisA*_*eGFP* and (B) pTB290. For abbreviations of components compare E.4.

A set of eight pET_*nisA*_*egfp* variants (TAG codon at position 5, 8, 12, 13, 17, 22, 29 and 32) was used to measure the amber suppression efficiency at selected positions covering different segments of the nisin molecule. Besides their distribution which spans nearly the complete polypeptide chain, TAG positions were selected based on first results from an activity screening, which was conducted by the group of Prof. Dr. Budisa ((82) and unpublished data). Here, nisin modified with BocK at position 12, 17 and 22 maintained its antimicrobial activity. T7 Exp cells, harboring pTB290, were individually transformed with the eight TAG variants of pET_*nisA*_*egfp* and subjected to the amber suppression reporter assay (compare B.3.9). Addition of arabinose induced expression of the suppressor pair while addition of IPTG was used to regulate induction of NisA-eGFP protein expression. IPTG is a molecular mimic of the lac repressor binding substance allolactose that, in turn, controls the lac promoter in front of the T7 RNA polymerase gene (101). T7 Exp cells steadily overexpress the lac repressor (LacI), leading to a tightly controlled expression system (86).

Prior to screening, controls were made to verify that the gathered data and its evaluation are valid. These controls included: check if [1] inoculation of overnight cultures from

glycerol stocks stored at -80°C instead of freshly transformed cells, [2] glucose addition to medium of the overnight culture, [3] taking single clones or a pool of 20 clones for inoculation has an impact on protein expression (see *Supplementary Figure S2*). Moreover, growth rates of the different variants were compared at the time when FI and OD values were taken for analysis to make sure that they were all in a similar stage.

Repetition of the same experiment on different days and with different bacterial clones showed a high reliability of the measurements (*Figure 9 A*). No difference between the mean of OD measurements of the control with (OD [+BocK]) and without BocK (OD [-BocK]) and a difference of less than 5 % of the mean of FI with and without BocK indicated that the presence of BocK does not influence the unmodified NisA-eGFP expression. As an example for the obtained raw data, TAG variant 29 of NisA(wt) is shown in *Figure 9 B*. All growth and FI curves can be found in *Supplementary Figure S1*. Six hours post induction was determined as time for data analysis, because steady bacterial growth was reached and differences in fluorescence intensities were well observable by then. For data evaluation FI values of the TAG variant were normalized to the respective OD values, which were measured concurrently. The obtained FI/OD of every biological replicate was then divided by the FI/OD of the control construct (wildtype NisA without amber codon), which was in each case measured simultaneously, to yield the relative increase or decrease of FI compared to the control. This allowed reduction of growth and FI variations of replicates and gave a valid entity for the comparison of different constructs to each other (important in C.1.6 and C.1.7). The obtained unit is defined as effective FI ($FI_{effective}$) (*Formula 1*).

$$FI_{effective} = \frac{FI_{510nm}(TAG\ variant\ X, +/-ncAA)/OD_{600nm}(TAG\ X, +/-ncAA)}{FI_{510nm}(without\ TAG, +/-ncAA)/OD_{600nm}(without\ TAG, +/-ncAA)}$$

Formula 1. Calculation of $FI_{effective}$. The FI_{510nm} is normalized to the respective OD_{600nm} and divided by the normalized FI of the control (without TAG) to yield the relative increase or decrease of FI compared to the control. X stands for 5,8,12,13,17,22,29 or 32. Depending on the investigated measurement, the FI and OD values either with (+ncAA), or without ncAA (-ncAA) are used.

Results of the amber suppression efficiency screening are shown in *Figure 9 C* (please note that these measurements have been commenced by Miriam Thewes and can therefore also be found in parts in her thesis). For TAG position 5, 8 and 12 the effective FI [+BocK] lay between 83 % and 125 % of the FI of the control. Whereas position 17

showed a similar $FI_{effective}$ [+BocK] to position 13 (120 % and 137 %, respectively), the $FI_{effective}$ [+BocK] dramatically dropped to values smaller than 53 % for position 22, 29 and 32. Contrary to expectations, the $FI_{effective}$ [-BocK] does not show a consistent level for all variants, but instead varies largely in the range of 14-138 %, suggesting the expression of eGFP even when the reassigned TAG codon should theoretically have served as a stop signal.

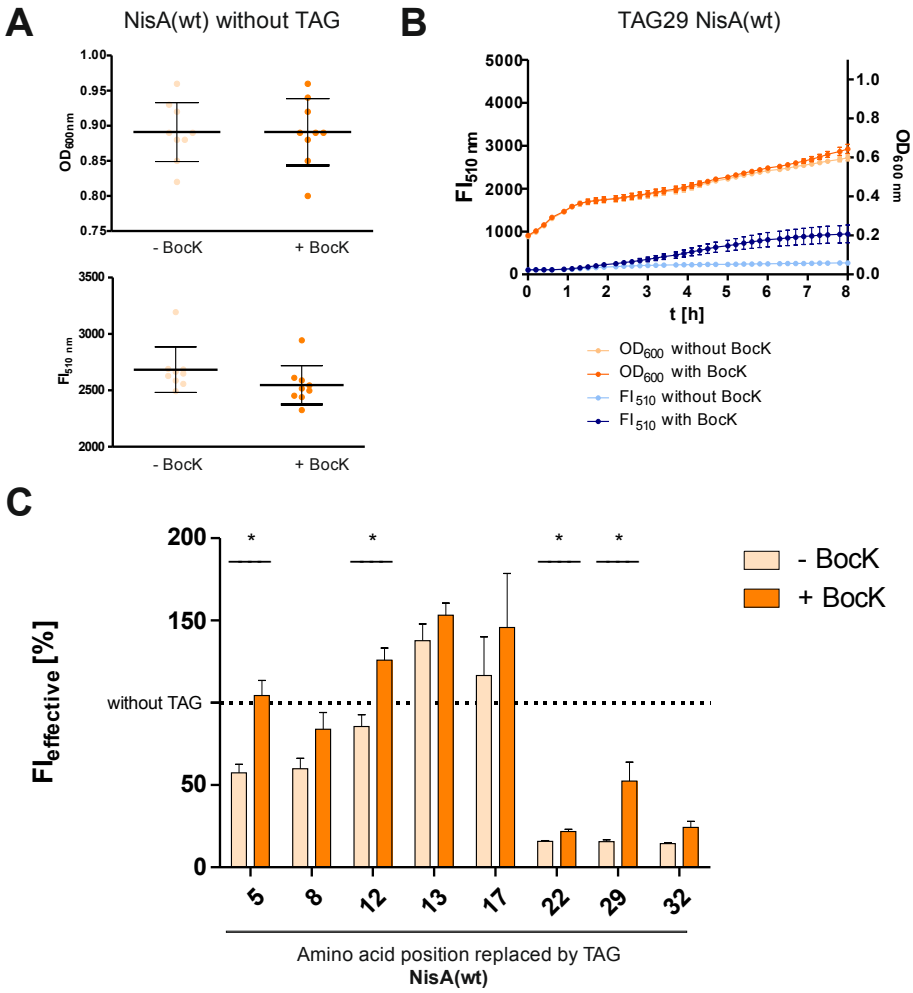

Figure 9. (A) Retest reliability of the experimental setup using the example of the control construct NisA(wt) without amber codon. The mean of OD_{600} and FI_{510} as 6 h post induction [+/-BocK] of nine independent experiments is shown. Error bars indicate the standard deviation of three independent experiments. **(B) Growth and FI curves of TAG29 NisA(wt)** as an example of the obtained raw data. Error bars indicate the SEM. **(C) Amber suppression efficiency screening of eight selected TAG positions of NisA(wt).** $FI_{effective}$ was calculated according to *Formula 1.* Eight TAG variants of NisA(wt) were measured (+/-BocK). Error bars indicate the SEM. Significance of difference of measurements +/-BocK was calculated in a two-sided t-test with equal variance (Student's t-test).

In summary, a clear trend was visible: the two front and three middle positions (5, 8, 12, 13, 17) showed generally higher $FI_{effective}$ [+BocK] values, which varied between 84-

153 %, whereas the three rear positions (22, 29, 32) showed lower $FI_{effective}$ [+BocK] values of 22-52 %. Remarkably, $FI_{effective}$ [-BocK] values vary widely from 57-138 % for the just named five anterior positions, but reached a consistently low level of 15 % for all three rear positions. The fact that the $FI_{effective}$ [-BocK] of variant TAG13 and 17 even exceeds the FI of the control construct without amber codon particularly indicates that unexpected translation mechanisms beyond the theoretical considerations affect the experiment's outcome. Due to this incongruence of expected and observed results in regard to $FI_{effective}$ [-BocK] we aimed for uncovering the underlying mechanisms of this observation. To assess the amber suppression efficiency, which had been the original interest of the assay, the relative suppression efficiency $SE_{relative}$ was specified for every TAG variant. It can be obtained by calculating the difference between the $FI_{effective}$ with ncAA and without ncAA (ΔncAA), which is in turn divided by the $FI_{effective}$ without ncAA (*Formula 2*). Accordingly, $SE_{relative}$ describes the rise of $FI_{effective}$ in percent, which stems solely from the ncAA-modified NisA-eGFP protein.

$$SE_{relative}\,[\,\%] = \frac{FI_{effective}\,(TAG\ variant\ X, + ncAA) - FI_{effective}\,(TAG\ X, - ncAA)}{FI_{effective}\,(TAG\ X, - ncAA)} \times 100$$

$$= \frac{FI_{effective}\ (\Delta \mathrm{ncAA})}{FI_{effective}\,(TAG\ X, - ncAA)} \times 100$$

Formula 2. Calculation of $SE_{relative}$ [%] from the $FI_{effective}$ values in the presence and absence of the ncAA (*here*: BocK).

Comparing the $SE_{relative}$ among the different variants can consequently give information about the relative protein yields, which stem from a successful amber suppression and incorporation event of BocK.

All eight variants of *nisA*(wt) were analyzed upon their $SE_{relative}$ (*Figure 10*). The highest increase of the normalized FI by addition of BocK was observed for variant 29, where the $SE_{relative}$ is on average 230 %. All other variants showed very low ($SE_{relative}$ <17 %) (variant 13, 17) or low ($SE_{relative}$ >17 % and <82 %) (variant 5, 8, 12, 22, 29, 32) relative suppression efficiencies. Obviously, the $SE_{relative}$ was not as high as desired for an efficient amber suppression based incorporation system for ncAA. Hence, re-evaluation of the reliable functioning of the ncAA incorporation system was necessary.

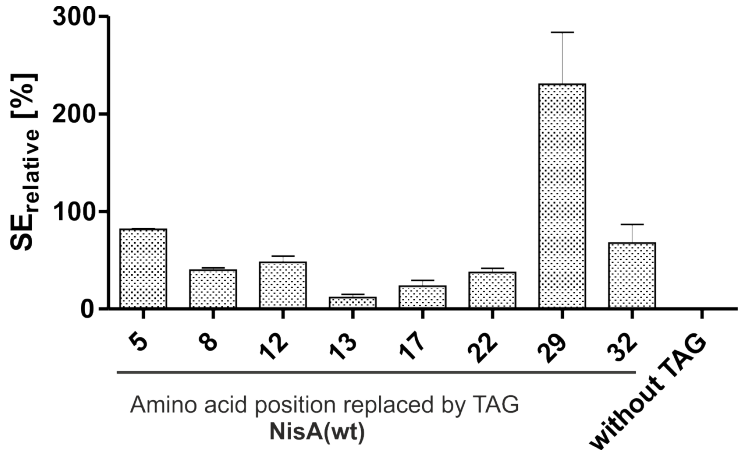

Figure 10. Relative suppression efficiency as a measure for the rise of $FI_{effective}$ [%], which stems solely from the ncAA-modified NisA-eGFP protein calculated (*Formula 2*) for the eight TAG variants of NisA(wt). Wildtype *nisA* (without a TAG codon) served as control (zero-height bar, due to no difference of FI/OD values with or without addition of BocK). Error bars indicate SEM.

The widely varying values for the measurements without BocK suggest the presence of translation products, which are created without the ncAA, contain the eGFP part of the protein and are formed more or less likely dependent on which position in nisin is replaced by TAG. One explanation could be the presence of unexpected cryptic internal translation starts, which lead to truncated translation products. Thus, limiting the incorporation of ncAA into nisin by bypassing the suppressed amber codon which leads to an additional undesired 'background fluorescence' and an inhomogeneous product mix.

C.1.2 Deletion of enigmatic internal translation starts

Two different explanations for the internal translation start were assumed: [i] enigmatic ribosome binding sites (RBS), also called Shine-Dalgarno sequence in prokaryotes, or [ii] methionines (M) at position 17 and 21 in the nisin sequence that serve as alternative translation (re)initiation sites.

In order to test both hypotheses, the following experiment was designed (*Figure 11*). To address hypotheses [i], an *E. coli* codon optimized (co-Ec) NisA variant was created, which aimed at general reduction of internal RBSs' binding strength. Based on the NisA(co-Ec) basic construct, eight NisA(co-Ec) TAG variants (again 5, 8, 12, 13, 17, 22, 29, 32) were cloned into the vector pET_*nisA_egfp*. Originating from the hypothesis that M17 and M21 are responsible for the occurrence of leak expression products, methionine amino acid substitution (M-aaS) variants of NisA were designed by replacing

M17/21 with other selected amino acids. As we were interested in maintaining NisA's antimicrobial activity, we subjected all designed M-aaS NisA variants to antimicrobial activity tests to isolate the M-aaS NisA variant with the highest activity. Once this goal was fulfilled, the amber codon at the above-mentioned eight positions was introduced into M-aaS NisA(wt) and cloned into the vector pET_*nisA*_*egfp*. Last, both approaches were combined in a M-aaS NisA(co-Ec) construct. Here again, eight TAG variants were created, leading to eight TAG pET_M17XM21X_*nisA*(co-Ec)_*egfp* constructs and one control construct without amber codon.

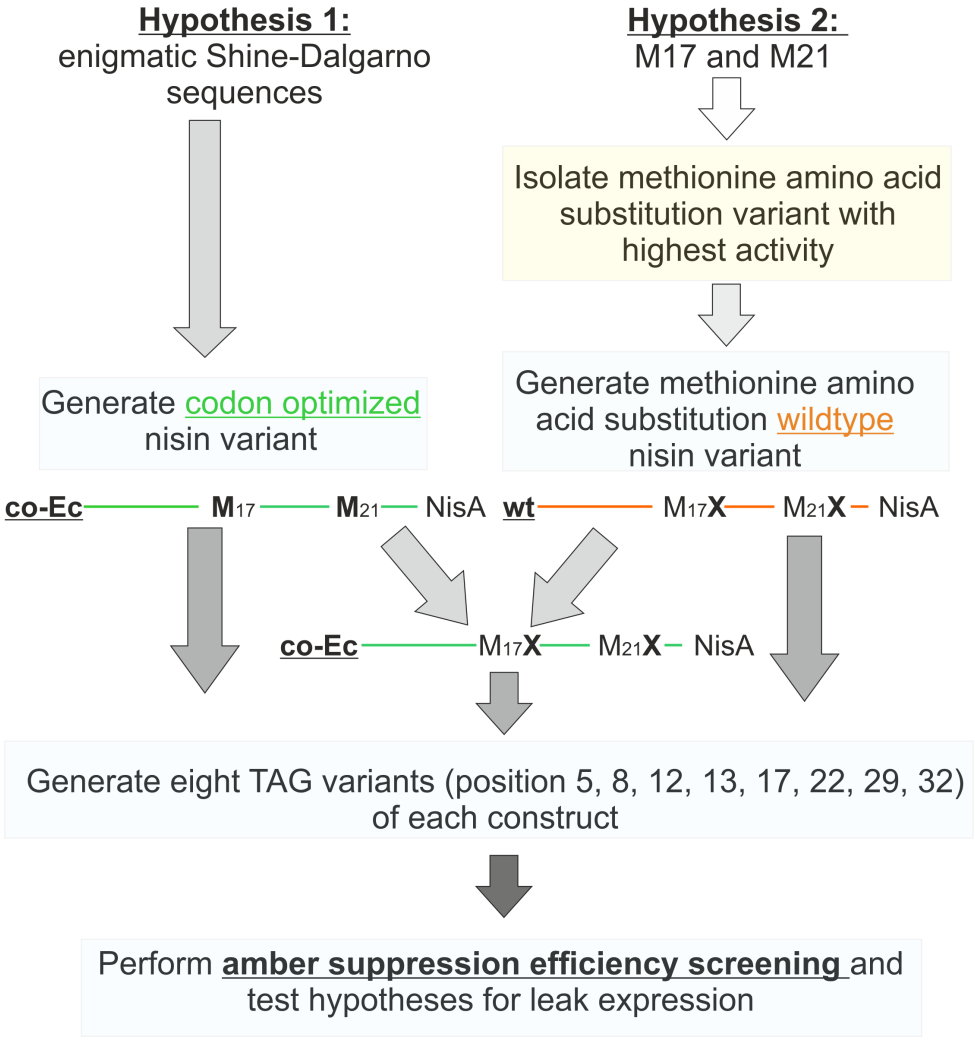

Figure 11. Design of experiment to test the hypotheses for the putative internal translation starts. The workflow for the investigation of the reasons for leak expression when incorporating ncAAs into nisin in *E. coli* is shown. The background color indicates the host organism for the respective experimental step: blue – *E. coli*, yellow – *L. lactis*. Orange indicates that wildtype (wt) DNA has been used for the respective construct. Green visualizes the use of the on *E. coli* codon optimized (co-Ec) DNA.

The total of 24 variants (eight TAG variants of pET_*nisA*(co-Ec)_*egfp*, pET_M17XM21X_ *nisA*(wt)_*egfp* and pET_M17XM21X_*nisA(*co-Ec)_*egfp*, respectively) were then used for the same amber suppression efficiency screening as performed with NisA(wt) (C.1.1) and described in B.3.9.

C.1.3 Generation of a codon-optimized NisA variant

To reduce the presence of enigmatic Shine-Dalgarno (SD) sequence motifs within the *nisA* sequence, a codon optimized variant for *E. coli* was designed. Owing to the redundancy of the genetic code, it is possible to alter the gene's sequence while maintaining the corresponding amino acid sequence. Although most amino acids are encoded by more than one codon, not all of them are used with equal frequency (102). The term 'codon usage' describes the frequency of occurrence of a certain codon in a large set of analyzed genes from the organism of interest. One possibility to reduce the occurrence of internal RBSs is the use of statistical optimization methods which exchange synonymous codons to avoid those (103). In our case, it was decided to apply the GeneOptimizer algorithm (1). The most relevant optimization parameters are listed in *Table 2.* The GeneOptimizer tool does not solely take into account ribosomal entry sites, but also optimizes, among others, the codon usage to increase the total protein yield. Depending on the organism's codon usage, tRNA levels differ which comes along with the possibility of influencing the protein expression yield through varying the DNA composition.

Transcriptional level	mRNA level	Translational level
• GC content • Consensus splice sites • Cryptic splice sites • SD sequences • TATA boxes • Termination signals • Artificial recombination sites	• RNA instability motifs • Ribosomal entry sites • Repetitive sequences	• Codon usage • Premature poly(A) sites • Ribosomal entry sites • Secondary structures

Table 2. Selected parameters optimized by the GeneOptimizer algorithm (1,103)**.**

C.1.4 Generation and cloning of NisA M17XM21K derivatives

To tackle the second possibility (hypothesis [ii]), M-aaS derivatives of nisin were designed.

M21 is the second residue in the three amino acids long hinge region (N-M-K) of nisin. The hinge region is a flexible region within the polypeptide, which enables the molecule to form pores via conformational changes (104). Studies showed that mutations within this segment do not lead to a dramatic decrease of antimicrobial activity *in vivo*. N20/M21 mutated nisin derivatives could still bind to lipid II, thus, inhibiting the bacterial cell wall synthesis, but lacked the ability to form pores in the cellular membrane (40). Previous studies revealed that nisin A M21K showed enhanced anti-gram-negative activity and FIELD et al. demonstrated that nisin A M21K has equal activity to the wildtype nisin against *L. lactis* HP and *Staph. aureus* RF122 (29,53). Therefore, we decided to replace M21 by lysine (K). Amino acid M17, has only rarely been a target in mutagenesis studies (33,105). M17 is located in the C ring of nisin, suggesting less variability, due to its position within the delicate lanthionine ring system. Thus, it was decided to randomize M17, replacing it by every other canonical amino acid to prevent exclusion of a potent M17X mutant.

pScreen was used as host vector for cloning for M-aaS NisA variants for activity tests. pScreen is a shuttle vector replicating in *E. coli* and *L. lactis*, which was designed by Dr. Manuel Montalban-Lopez (Kuipers lab, University of Groningen) and further improved by Anh Le (Wagner lab). Based on the pSH71 vector, pScreen replicates by a rolling circle replication mechanism and offers a broad range of potential host organisms (106). A lacO site in between the PnisA promoter and the beginning of the leader peptide allows improved expression control. Furthermore, a multiple cloning site (MCS) offers the possibility to introduce additional gene sequences.

By codon optimizing *nisA* for *L. lactis* (co-LI) we intended to improve peptide yields and thereby reveal subtle activity differences between the M-aaS NisA variants. Therefore, all 19 variants were cloned into pScreen_*nisA*(co-LI) (compare B.2.3 and B.2.4). All 19 plasmids were then quality controlled upon their purity and integrity by analytic digestion and sequencing of the section of interest (B.2.5).

C.1.5 Antibacterial efficacy analysis of NisA(co-LI), M21K NisA and M17XM21K NisA derivatives

The designed NisA M17XM21K derivatives were subjected to an assay for investigation of antimicrobial activity in order to identify the most potent variant which could subsequently be used for the amber suppression efficiency screening.

For the comparative analysis of nisin variants, bacterial susceptibility to the respective antibiotic needed to be determined. Various techniques can be used for the specification of the antibiotic's potency, including agar diffusion methods, broth dilution assays and Etests (107). Variations of the agar diffusion and broth dilution assay were carried out to acquire information about the different candidates. As antibacterial activity was not the only parameter which was of interest for the identification of the most promising NisA M17XM21K candidate, but also parameters like production, modification and secretion rate, it was decided to carry out the same expression protocol for all variants (B.4.1) and test the cell-free supernatants against a selected sensor strain. Hence, it was not only possible to study the combined effect on the antimicrobial activity of all factors mentioned above (summarized under the term antibacterial 'efficacy'), but also to perform a rapid screening of the variants, enabling us to proceed with the best one.

It is important to note that cell-free supernatants of expression cultures for the antimicrobial activity tests were gained from *L. lactis* cultures. At this point, nisin expression in *E. coli* was not established, which was achieved later on (C.2), leaving *L. lactis* as the only and commonly used host organism for nisin production.

C.1.5.1 Agar well diffusion assay

The agar well diffusion assay is based on the principle that a sensor strain, which is assumed to be susceptible to the antibiotic to be tested, is equally seeded onto an agar plate at a certain concentration. Small cavities, wells, are punched out of the agar allowing the application of a small volume of a solution which contains the antibiotic. The agar plates are then incubated, enabling the growth of the sensor strain and the diffusion of the antibiotic into the surrounding agar. Afterwards growth inhibition can be read out by measuring halo diameters or areas around the wells (according to (108)).

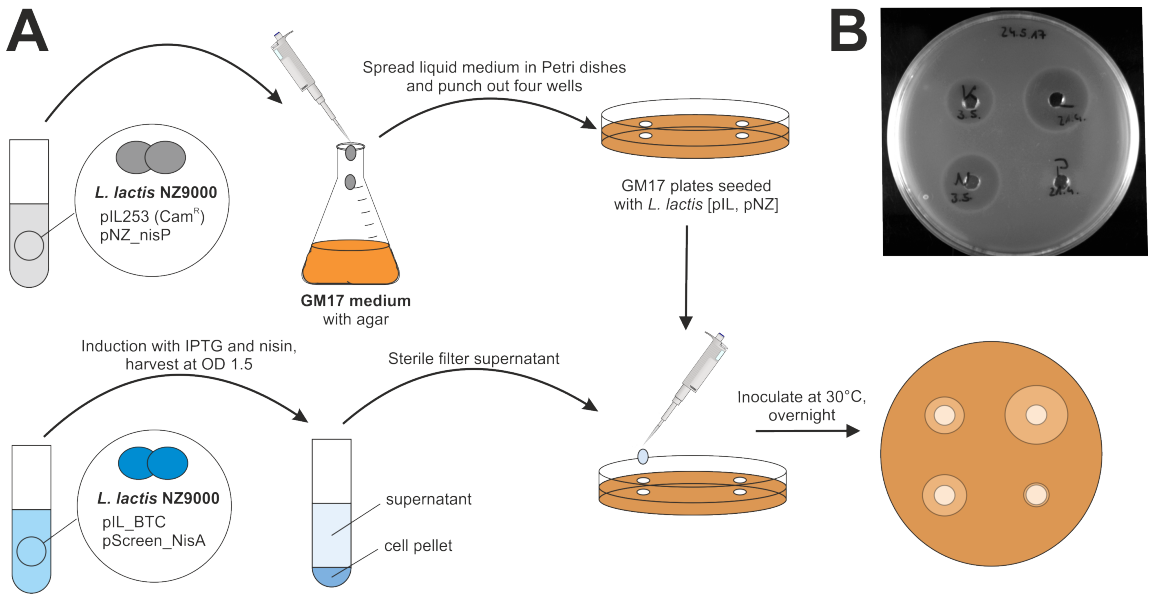

Figure 12. (A) Schematic workflow of the agar well diffusion assay. The sensor strain L. lactis was co-transformed with pIL253 (containing the Cam^R) and pNZ_nisP, cultivated and diluted in GM17 agar. The medium was poured in Petri dishes and four wells were punched out. Sterile filtered supernatant of L. lactis [pIL_BTC, pScreen_NisA] cultures producing nisin A variants was given into the wells. Plates were then inoculated at 30°C, overnight and halos were read out. **(B) Agar well diffusion assay of nisin A variant M17XM21K (X stands for K, L, N or P).**

Here, we utilized *L. lactis* (containing pIL253, which harbors a Cam^R, and pNZ_*nisP*, encoding NisP) (*L. lactis* [pIL,pNZ]) as sensor strain. Since all nisin variants were expressed in their inactive, leader-containing form, the sensor was required to express the leader-cleaving protease NisP. Co-transformation with pIL253 was necessary to facilitate selection of bacteria to erythromycin and chloramphenicol, which was especially useful for the growth curve assay (C.1.5.2) Cell-free supernatants of the 19 M17XM21K nisin A variants, NisA (co-LI) and NisA (wt), each with and without M21K mutation, and pScreen_without _*nisA* were applied to the wells. Halo radii were measured with ImageJ and normalized to the radius of NisA(co-LI).

Figure 13 A shows the size of the halo radius measured around the respective well (A.U.). It can be seen that codon optimization of NisA for *L. lactis* or/and introduction of mutation M21K did not show an effect on the halo size compared to NisA(wt). In *Figure 13 B* the two controls (M21K NisA(co-LI) and NisA(co-LI)) and the sizes of the halo radii of all 19 M17XM21K variants NisA(co-LI) normalized to the control NisA(co-LI), which was set to 100 %, are shown. This facilitates comparison of their antibacterial efficacy to the control's one. For 15 out of the 19 M17XM21K variants no significant difference to NisA(co-LI)'s halo size could be found, while at first glance drastically downturned anti-

bacterial efficacy of variants M17D, and M17EM21K can be seen. No halo at all could be observed for these two variants. M17PM21K NisA(co-LI) also performed worse than the control, while showing strongly variations between the independently performed experiments. However, three variants with larger halo radii could be identified: M17FM21K (137 %), M17VM21K (118 %) and M17WM21K (131 %). Other than expected a small halo (33 %) could also be observed when the supernatant of *L. lactis* (containing pIL3BTC and pScreen_without _*nisA*) was applied.

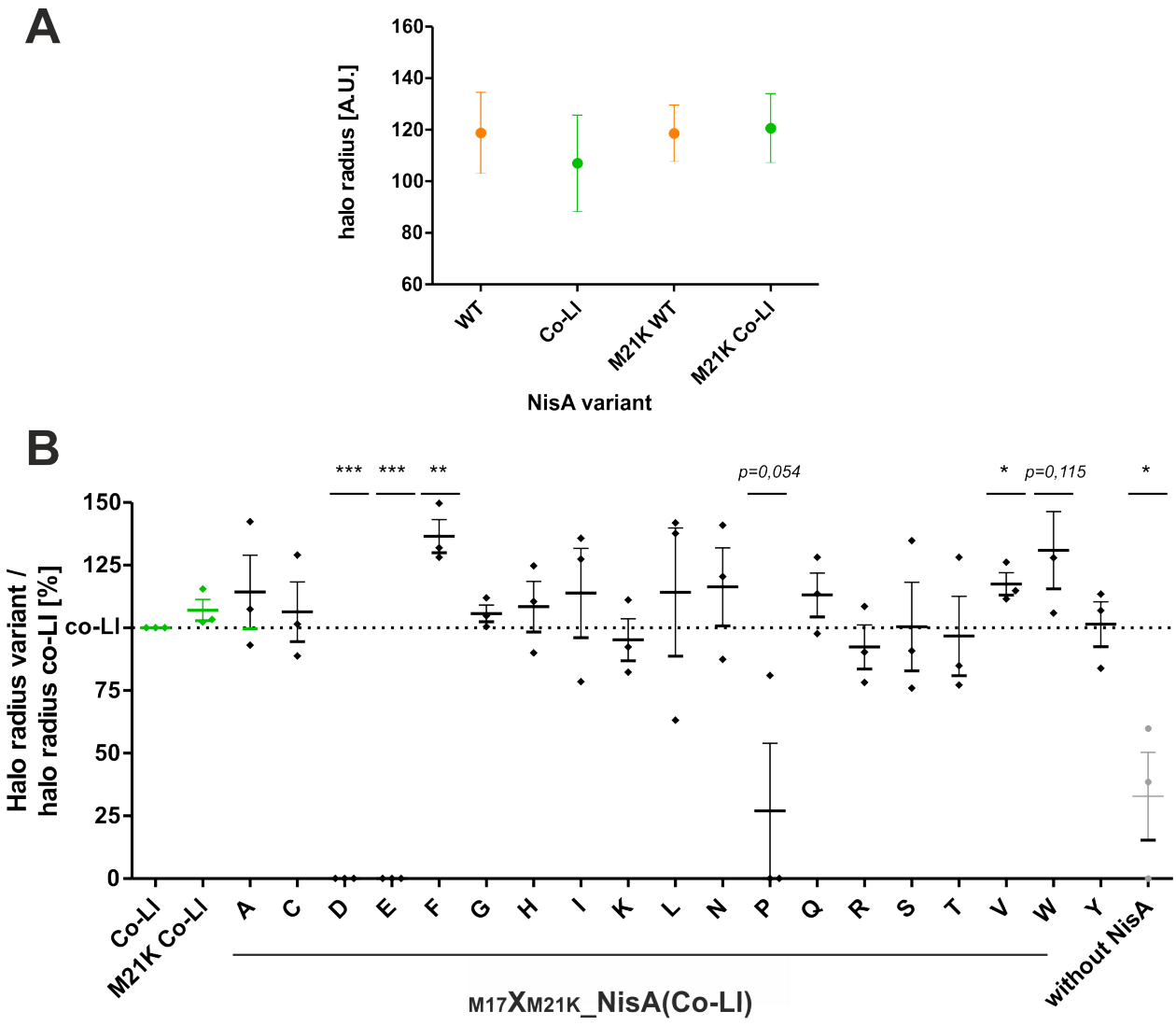

Figure 13. Agar well diffussion assay with *L. lactis* [pIL, pNZ] as sensor and cell-free supernatants of *L. lactis* (containing pIL3BTC and different variants of pScreen_*nisA*). (A) Comparison of mean halo radii around wells loaded with cell-free supernatants of (M21K) NisA(wt) and (M21K) NisA(co-LI), measured after a 24 h growth period with ImageJ. Expression was carried out for all variants with an identical protocol. Error bars indicate the SEM. (B) Scattered dot blot of halo radii of the variants normalized to the value of the halo radii of NisA(co-LI) (109). Statistical significance was calculated by comparison of the respective values to NisA(co-LI). Error bars indicate the SEM.

Although agar-based diffusion assays are the most commonly used tests for determination of the antibacterial activity and facilitate the study of surface-active compounds, they are accompanied by several drawbacks, which are mainly linked to the differing diffusion properties of particularly hydrophobic or amphiphilic molecules, such as nisin (compare A.5) (53,107). To ensure the correctness of the findings and exclude deviations due to altered diffusion rates, a second broth-dilution based efficacy test was implemented.

C.1.5.2 Broth-dilution based growth curve tests

Compared to agar-based activity assays, broth-dilution based growth curve tests circumvent a diffusion-related bias and reveal subtle differences in bacterial growth under the influence of the antibiotic of interest. Again, cell-free supernatants of standardized expression experiments (compare C.1.5.1) were tested against *L. lactis* [pIL,pNZ]. Growth was monitored for 24 h in a 20-minutes interval using a Tecan Infinite 200 Pro device. All growth curves can be found in *Supplementary Figure S3*.

To reduce the collected data to its quintessence, a threshold was set to 50 % of the maximum sensor growth (OD_{600}(t=24.13 h)) under the influence of the cell-free supernatant of an *L. lactis* (containing pIL3BTC and pScreen_without_*nisA*) expression culture. Subsequently, all variants were analyzed upon the last point in time at which the sensor growth under the influence of the respective nisin candidate underwent this threshold. The later the threshold was reached, the longer the cell-free supernatant of the variant was able to suppress the sensor's growth. The combined data of three independent experiments is shown in *Figure 14 A and B*.

No significant difference between growth inhibition properties of Nis(co-Ll), NisA(wt) and the respective M21K variants could be found (*Figure 14 A*). Regarding the 19 M17XM21K variants, only four candidates could be identified, which showed different growth inhibition properties than NisA(co-Ll). Replacing M17 by aspartic acid (D) or proline (P) lead to virtually uninhibited sensor growth, so that both variants reached the threshold at the same time at which the growth control (sensor supplemented with cell-free supernatant of *L. lactis* (containing pIL3BTC and pScreen_without*nisA*)) reached it. Corresponding to the agar well diffusion assay, variant M17WM21K (21,98 h) prolonged growth inhibition significantly compared to NisA(co-Ll) (14,72 h). Furthermore, cell-free supernatant of an

expression culture of M17QM21K NisA(co-LI) inhibited sensor growth to 50 % for an average of 20,96 h from the start of the measurement.

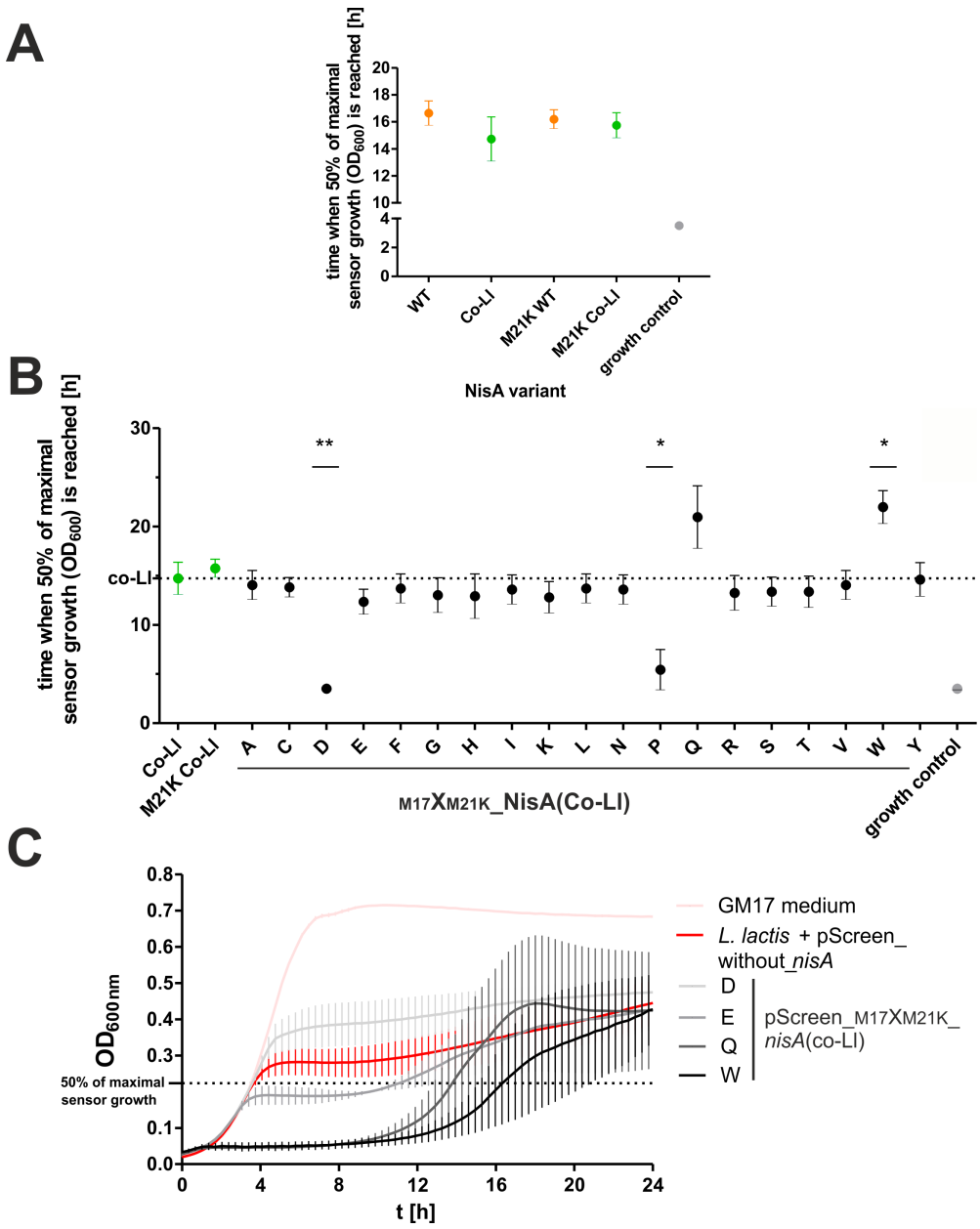

Figure 14. Broth-dilution based growth curve tests with *L. lactis* [pIL,pNZ] as sensor and cell-free supernatants of *L. lactis* (containing pIL3BTC and different variants of pScreen_*nisA*). (A) Growth curve analysis of (M21K) NisA(wt) and (M21K) NisA(co-LI). The time when sensor growth supplemented with the respective supernatants reaches 50 % of the OD_{600} of the 24,13 h value of *L. lactis* [pIL,pNZ], supplemented with the cell-free supernatant of *L. lactis* (containing pIL3BTC and pScreen_without*nisA*), was determined. Corresponding growth curves which were taken for data evaluation can be found in the supplements. Error bars indicate SEM. If sensor growth of 50 % of the growth control was not reached until the end of the measurement, the last time point (24,13 h) was taken for analysis. **(B) Growth curve analysis of all 19 M17XM21K NisA(co-LI) candidates** and controls (NisA(co-LI) and M21K NisA(co-LI)). **(C) Selected growth curves of controls and pScreen_M17XM21K_*nisA*(co-LI) variants.** The sensor was equally mixed with either GM17 medium or cell-free supernatants of *L. lactis* (containing pIL3BTC and pScreen_without _*nisA* or pScreen_M17D/E/Q/WM21K_*nisA*(co-LI) as indicated in the legend. Error bars represent the SEM.

Although not significantly different to NisA(co-LI), two other variants shall be highlighted. Examining the sensor's growth properties under the influence of M17EM21K, one can see that in the first three hours of measurement no inhibition at all is observed (*Figure 14 C*). Afterwards growth is steadily inhibited, but not to full extent, leading to a flattened growth curve, comparable to the one of M17DM21K, which reaches the same OD_{600} value as the growth control after 17,33 h. Moreover, variant M17Q and M17WM21K were able to inhibit 50 % of sensor growth for on average 20,96 h and 21,98 h, but values of the individual experiments varied strongly.

Furthermore, an inhibition effect on sensor growth could be observed when the sensor is supplemented with supernatant from *L. lactis* producing cells, harboring pIL3BTC and pScreen_without_*nisA*. As shown in *Figure 14 C*, the growth rate is unexpectedly lower when compared to the one of sensor supplemented with plain GM17 medium.

Therefore, a control experiment was set up to investigate the effect of the presence of none, one (pIL3BTC, pIL253, pScreen_*nisA*(co-LI), pScreen_without_*nisA*) or two (pIL253 + pNZ_*nisP*, pIL3BTC + pScreen_without_*nisA*) plasmids in the producer strain on the sensor growth (*Figure 15*).

When GM17 medium was added, *L. lactis* [pIL,pNZ] maintained the same growth rate as under the influence of cell-free supernatants of *L. lactis*, independent of transformation with none or one plasmid. Only when the producer strain was transformed with two plasmids, an inhibition of growth was monitored, commencing after four hours. After 24 hours this effect lead to a 36 % smaller OD_{600} value for *L. lactis* (containing pIL3BTC and pScreen_without_*nisA*) compared to addition of GM17 medium and to 20 % inhibition for *L. lactis* [pIL,pNZ]. A possible explanation of this phenomenon could be an enhanced metabolism in the two plasmid containing bacterium, which reduces the nutrients in the growth medium. This lack of essential compounds for bacterial growth can then be recognized by reaching the stationary phase at an earlier stage. Moreover, residues of the selection antibiotic(s) used for growth of *L. lactis* harboring one or two plasmid(s) still remained in the cell-free supernatants, leading to different concentrations of the antibiotic in the growth medium, which could affect bacterial growth.

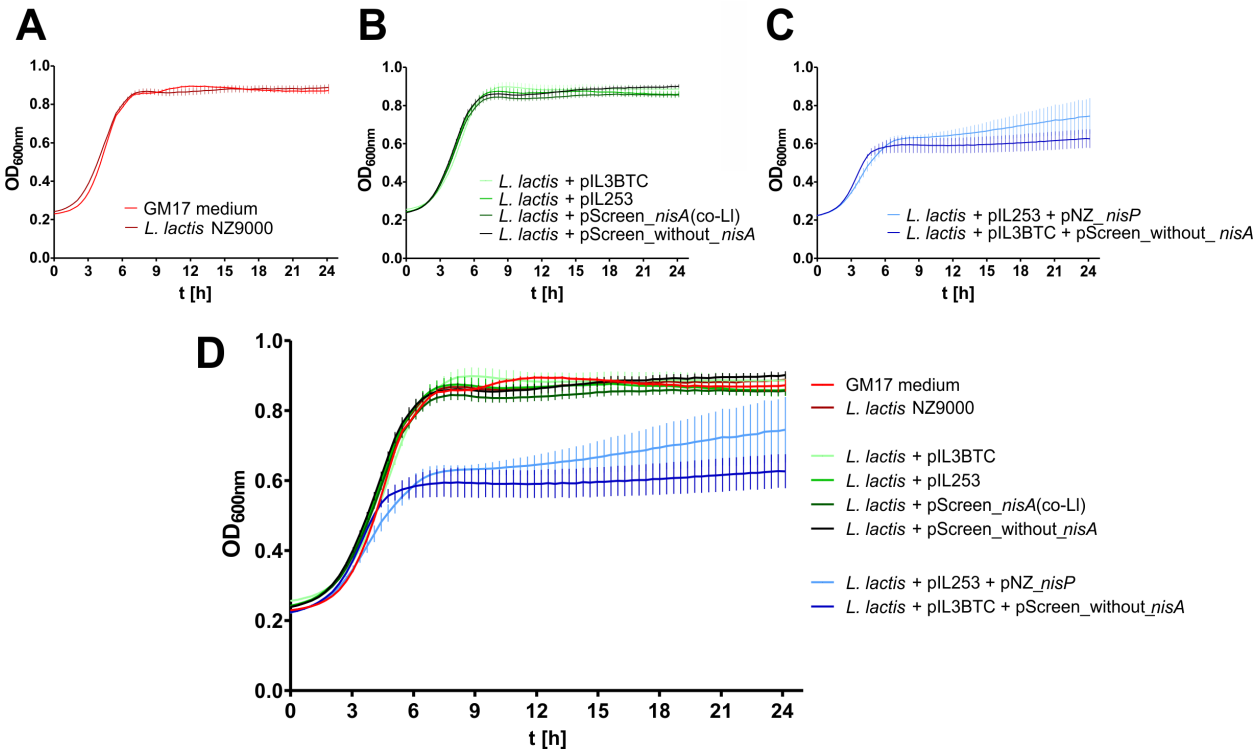

Figure 15. Control experiment for the investigation of the effect of the presence of none (A), one (B) (pIL3BTC, pIL253, pScreen_*nisA*(co-LI), pScreen_without_*nisA*) or two (B) (pIL253 + pNZ_nisP, pIL3BTC + pScreen_without_*nisA*) plasmids in the producer on sensor growth (*L. lactis* [pIL,pNZ]). Growth curves are mean values of technical triplicates with errors bars indicating the SEM. (D) Combined data.

C.1.6 Amber suppression efficiency screening of *nisA*(co-Ec)

Aiming at the reduction of leak expression, hypothesis [i]: translation (re)initiation through internal RBSs, was tested by performing a relative amber suppression reporter assay with the *E. coli* codon optimized nisin A sequence. Eight TAG variants were constructed on the basis of pET_*nisA*(co-Ec)_*egfp* and the screening was carried out according to B.3.9. All experimental conditions, except for the DNA sequence of NisA, were kept consistent to the suppression efficiency screening in C.1.1. Results are shown in *Figure 16*.

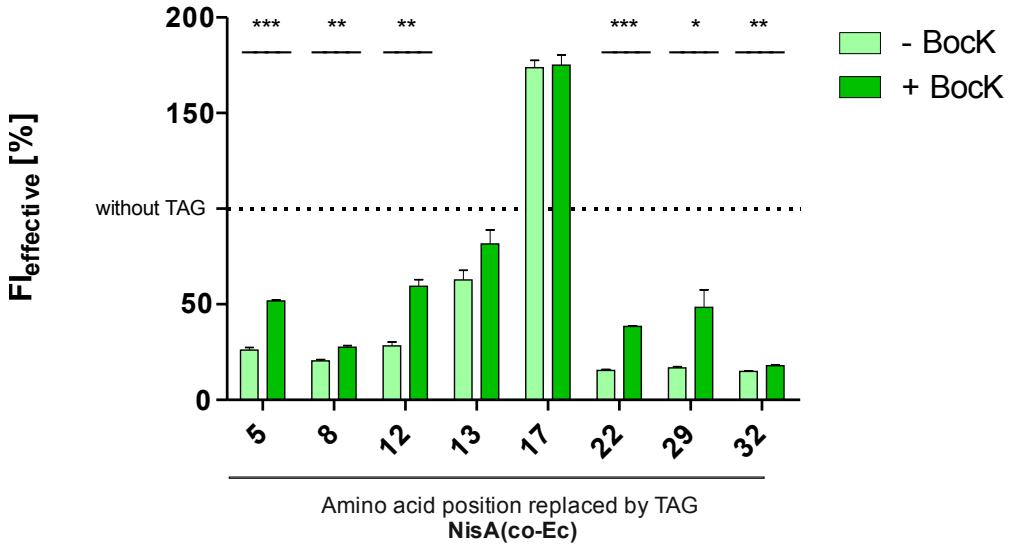

Figure 16. Amber suppression efficiency screening of eight selected TAG positions of NisA(co-Ec). $FI_{effective}$ was calculated according to *Formula 1.* Eight TAG variants of NisA(co-Ec) were measured (+/-BocK). Error bars indicate the SEM. Significance of difference of measurements +/-BocK was calculated with Student's t-test.

Contrary to an expected rise of the control's FI due to an expected higher protein yield through codon optimization, similar values as for NisA(wt) were measured (compare *Supplementary Figure S3*). Similar to the pattern of the amber suppression efficiency screening of NisA(wt) shown in *Figure 9*, the $FI_{effective}$ [-BocK] varied strongly from values of 20-174 % between front and middle positions (5, 8, 12, 13, 17), and less (15-17 %) for the three rear TAG codons (22, 29, 32). Compared to NisA(wt), the $FI_{effective}$ was generally lower for amber codons lying in the anterior part (5, 8, 12, 13) and equally high in the rear part (22, 29, 32). Noticeably, $FI_{effective}$ values [+BocK] and [-BocK] for variant TAG17 were outstandingly high (174 % and 175 %) and no influence of ncAA addition at all could be observed for this specific variant. However, stronger differences between measurements with and without BocK could be observed in several cases (TAG 5, 8,12, 22, 32) when compared to the amber suppression screening of NisA(wt).

Nevertheless, codon optimization did not reduce leak expression.

C.1.7 Amber suppression efficiency screening of M17WM21K NisA(wt) and M17WM21K NisA(co-Ec)

According to the results of the agar well diffusion assay (*Figure 13*) and the growth curve analysis (*Figure 14*), nisin variant M17WM21K was identified as the most active M-aaS

NisA variant and cloned into pET_*nisA*(wt)_*egfp* and pET_*nisA*(co-Ec)_*egfp*. Eight TAG variants of each construct were generated and subjected to an amber suppression efficiency screening.

First, the isolated effect of the M-aaS on basis of NisA(wt) was studied (*Figure 17 A*). Compared to NisA(wt), very similar FI values were reached for the control construct (M17WM21K NisA(wt)) which does not carry any TAG mutation and is therefore equally expressed independent of BocK addition (compare *Supplementary Figure S4*). In contrast to NisA(wt) with M17/M21 (*Figure 17 B*), a dramatic decline of $FI_{effective}$ [-BocK] to a constant level of on average 16,5 %, with little variation (13,6-18,9 %), for every single TAG variant of M17WM21K NisA(wt) could be observed. Now, all variants showed significant differences between measurements [+BocK] and [-BocK], indicating an improved tightness of the amber suppression system and improved fidelity of ncAA incorporation. Generally, a lower $FI_{effective}$ [+BocK] was now observed for the front and middle positions (5, 8, 12, 13, 17), suggesting the omission of fluorescence from side products which originated from 'leak expression'. Moreover, strong variations between the effective FI of the eight variants were no longer visible. Except for variant TAG8 (75 %) and TAG32 (23 %), the $SE_{relative}$ lay in a small range of 145-206 % (*Figure 17 C*).

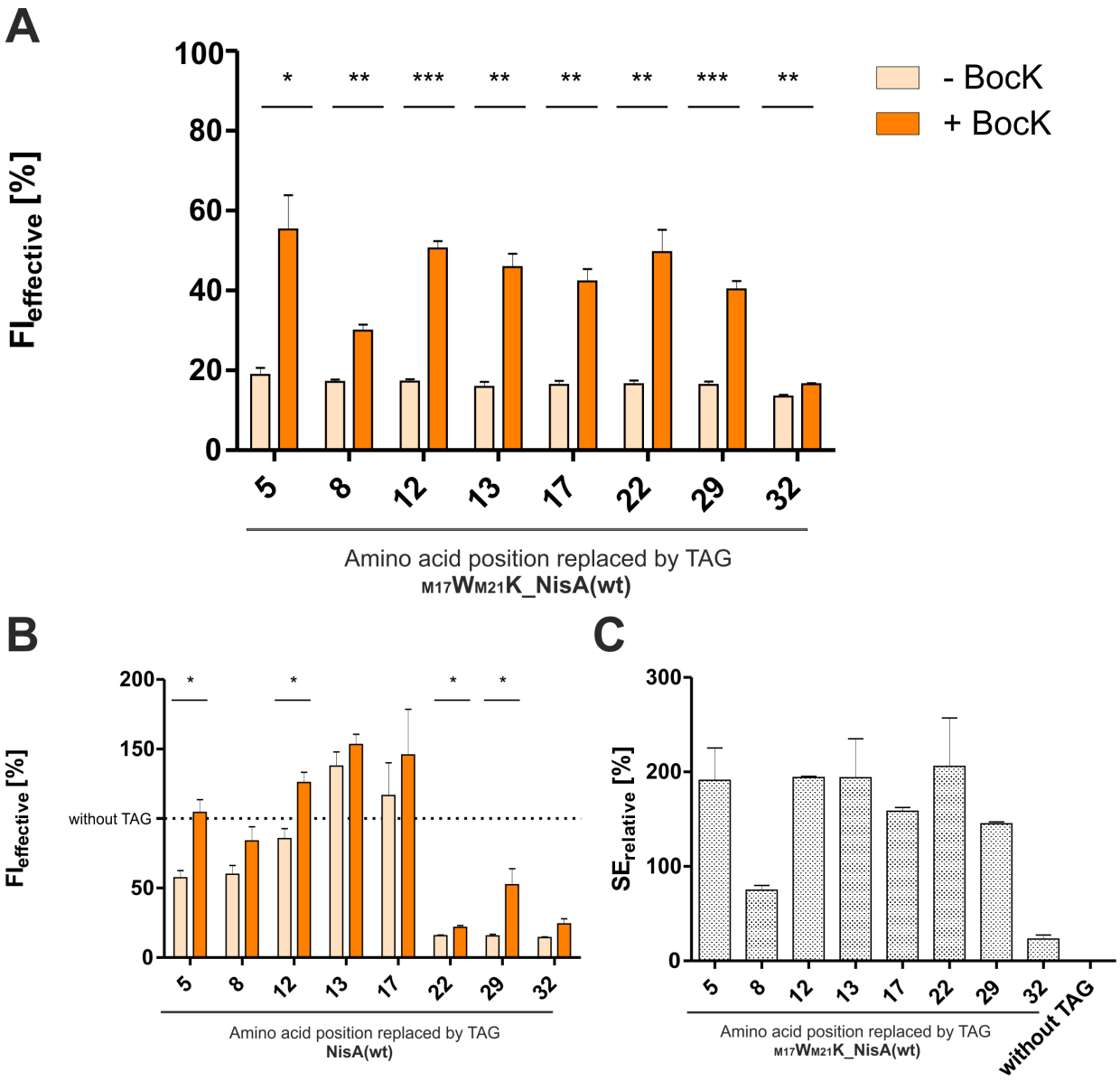

Figure 17. (A) Amber suppression efficiency screening of eight selected TAG positions of M17WM21K NisA(wt). $FI_{effective}$ was calculated according to *Formula 1.* Eight TAG variants of M17WM21K NisA(wt) were measured (+/-BocK). Error bars indicate the SEM. Significance of difference of measurements +/-BocK was calculated with Student's t-test. **(B) Amber suppression efficiency screening of eight TAG positions of NisA(wt). (C) Relative suppression efficiency calculated (*Formula 2*) for the eight TAG variants of M17WM21K_*nisA*(wt).**

Second, a combination of hypothesis [i] and [ii] was tested by replacing M17/21 through tryptophan and lysine in NisA (co-Ec) (*Figure 18*). The overall picture of the measurements widely resembled the one for M17WM21K NisA(wt) (*Figure 17 A*). However, two differences were remarkable: first, $FI_{effective}$ [-BocK] of TAG17 was 12 % higher than the $FI_{effective}$ [-BocK] of the other seven constructs and second, $FI_{effective}$ [+BocK] of TAG22 was 19 % lower for NisA(co-Ec) than for NisA(wt).

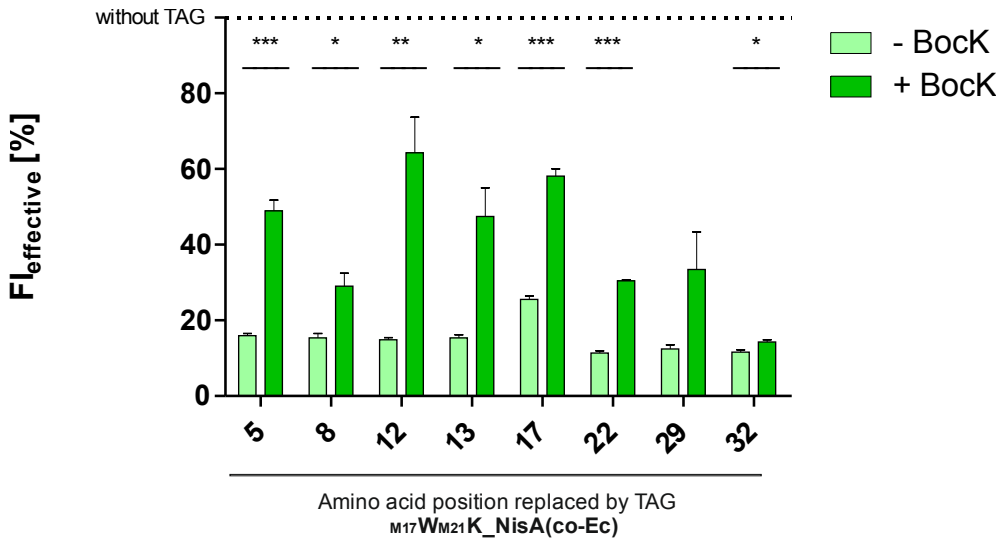

Figure 18. Amber suppression efficiency screening of eight selected TAG positions of M17WM21K **NisA(co-Ec).** Same experimental conditions and statistical evaluation as designated in *Figure 17* were applied.

C.1.8 Investigating the cause of fluorescence in the absence of the non-canonical amino acid

Three questions remained after performance of all amber suppression efficiency screenings: [1] Where does the constant $FI_{effective}$ [-BocK] ('background fluorescence') in the screening of M17WM21K NisA(wt) and M17WM21K NisA(co-Ec) come from, [2] how high is this background for NisA(wt) and NisA(co-Ec), which does not stem from translation reinitiation at M17/21, and [3] where does the comparably high background of TAG17 M17WM21K NisA(co-Ec) come from?

First, a contribution of LB medium, BocK and pTB290 to the measured FI was investigated with a set of control experiments (*Figure 19 B.1-B.4*). A basal level of fluorescence was traced back to the growth medium (102 A.U.) with little increase (48 A.U.), originating from addition of T7 Exp cells (*Figure 19 B.1 and B.2*). By subtracting the FI of T7 Exp cells, every $FI_{effective}$ value is consistently getting reduced by ~6 % (+/-1 %, depending on the individual variant). No FI change was observed when pTB290 was transformed into cells, when BocK was added or with higher cell density (*B.2 and B.3*). The growth rate was very similar for all constructs and their variants independent of BocK addition (*Supplementary Figure S6*). However, the increasing FI over the time of T7 Exp with pET_M17WM21K_*nisA*(wt)_*egfp* harboring TAG5, but missing pTB290, was not explainable by these findings (*B.4*). In contrast to M17WM21K NisA(wt), the same experimental

constellation with pET_*nisA*(wt)_*egfp* did not show such an FI increase while having the same growth properties (*B.5*), and consequently, the deduced $FI_{effective}$ [-BocK] was lower, too (*A.1 and A.2*).

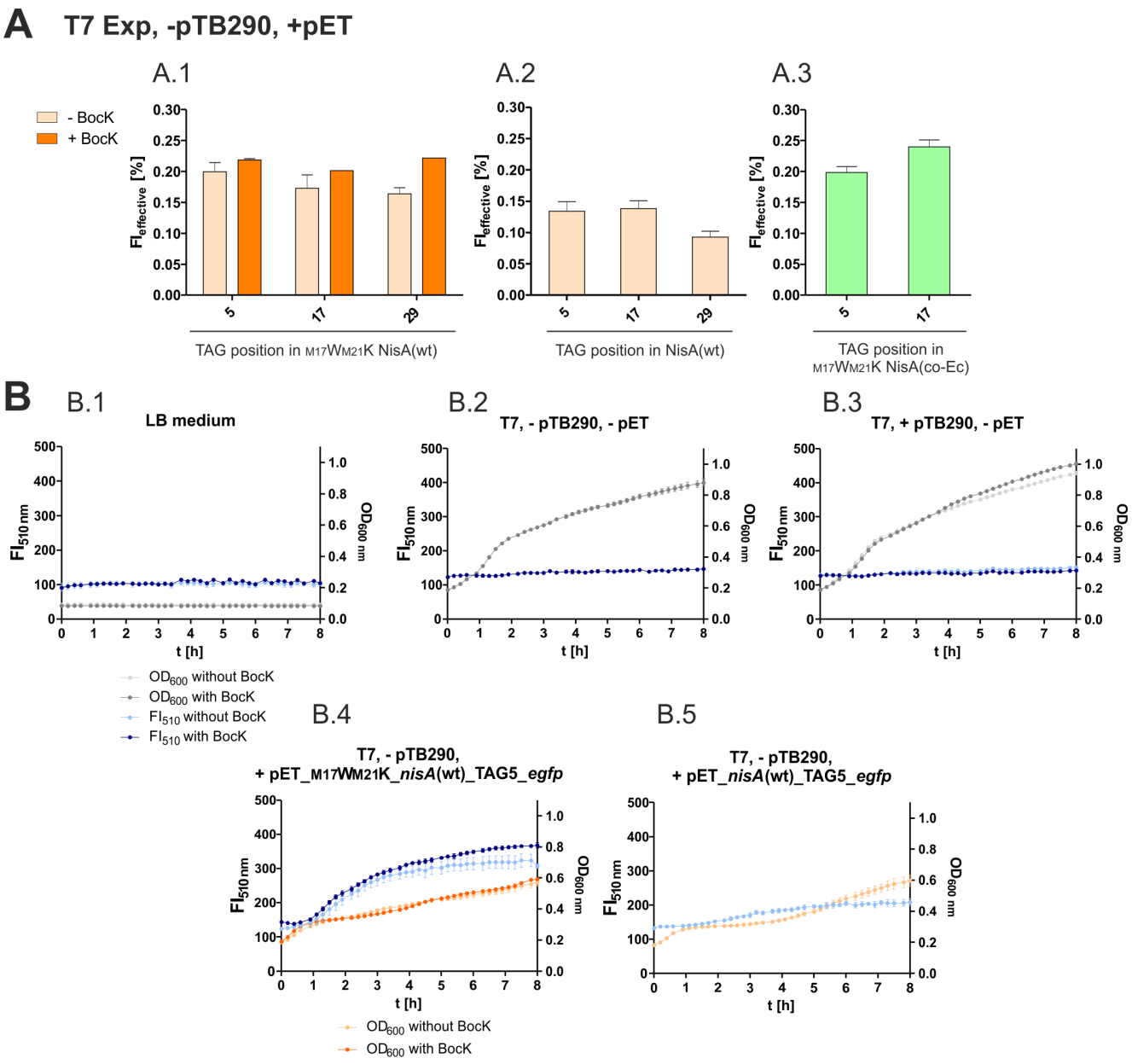

Figure 19. Control experiments for investigating the background fluorescence. (A) $FI_{effective}$ of selected TAG variants of the four different constructs (A.1-A.4). Except for a missing pTB290 plasmid, same experimental and evaluation conditions as designated in *Figure 17* for the amber suppression efficiency screening were applied. (B) Selected FI and OD curves of controls. Individual constellations are indicated above the respective diagram. All experiments were performed in technical and biological triplicates, except for LB medium [-BocK], M17WM21K NisA(wt) TAG17 and 29, which were only measured in technical triplicates.

The mean $FI_{effective}$ [-BocK] of T7 Exp with pET_M17WM21K_*nisA*(wt)_*egfp* harboring TAG5, 17 or 29, but missing pTB290 (*Figure 19 A.1*), was 17,9 % with little variation

(<3,6 %) between the TAG variants. This value corresponded to the background fluorescence of the same TAG variants in the amber suppression efficiency screening of M17WM21K NisA(wt), which was on average 17,2 % (compare *Figure 17 A*), indicating high fidelity of the orthogonal suppressor pair PylRS(Y384F)/tRNA^{Pyl}. If PylRS(Y384F)/tRNA^{Pyl} worked nonspecifically, meaning it bound also canonical amino acids, a gap between the measurement with and without pTB290 would be expected.

For M17WM21K NisA(co-Ec) TAG5, a gap of 12,3 % was found between the $FI_{effective}$ [-BocK] with and without pTB290 (*A.3 and Figure 18*). Surprisingly, the higher $FI_{effective}$ [-BocK] was found without pTB290, which excluded an explanation of a nonspecific synthetase and left the question open if this is explained by experimental variability or other unidentified reasons. For the higher $FI_{effective}$ [-BocK] of TAG variant 17, the same question remained open.

C.1.9 Conclusion

The aim of solving the problem of ‘leak expression’, which was first observed in the amber suppression efficiency screening of NisA(wt), could successfully be reached by replacing M17/21 in the NisA sequence. Codon optimization did not show a beneficial effect in this context. The remaining ‘background fluorescence’ was not caused by a nonspecific orthogonal suppressor pair.

Concerning the substitution of M17/21, a replacement by tryptophan at position 17 and lysine at position 21 showed the best results in two different antimicrobial activity tests. Next, the establishment of *E. coli* as recombinant expression host for post-translationally modified and active nisin was the subject of interest.

C.2 Heterologous expression, purification and characterization of mature nisin from *E. coli*

For decades, *L. lactis* has been the only producing organism for nisin and is still used in industrial production nowadays. The first full-length mature nisin production in *E. coli* has not been reported earlier than 2011 by SHI et al. (93). *In vitro* reconstitution of an active LanB dehydratase, which is crucial for the biosynthesis of fully modified nisin, has not been successful so far (110). Thus, *in vivo* approaches represent the only possibility for the production of nisin to date. Using *E. coli* as nisin expression host would allow the full exploitation of *in vivo* introduction of ncAAs as SPS technology is not available for most lantibiotic expression hosts (93).

In this work, an expression system for nisin in *E. coli* was established in the lab, based on the work of SHI et al. and by using an *E.coli* codon optimized version of *nisB* and *nisC* and the wildtype or *E.coli* codon optimized sequence of *nisA*.

C.2.1 Choice of *E. coli* expression host strain

First, BL21 (D3) and T7 Exp expression cell strains containing pET21a_*nisA*(wt) (including the leader sequence) and pRSFDuet_*nisBC*(co-Ec) (*Figure 20*) were compared upon their nisin production rate by carrying out the same expression protocol concurrently and performing an antimicrobial activity test (agar well diffusion assay).

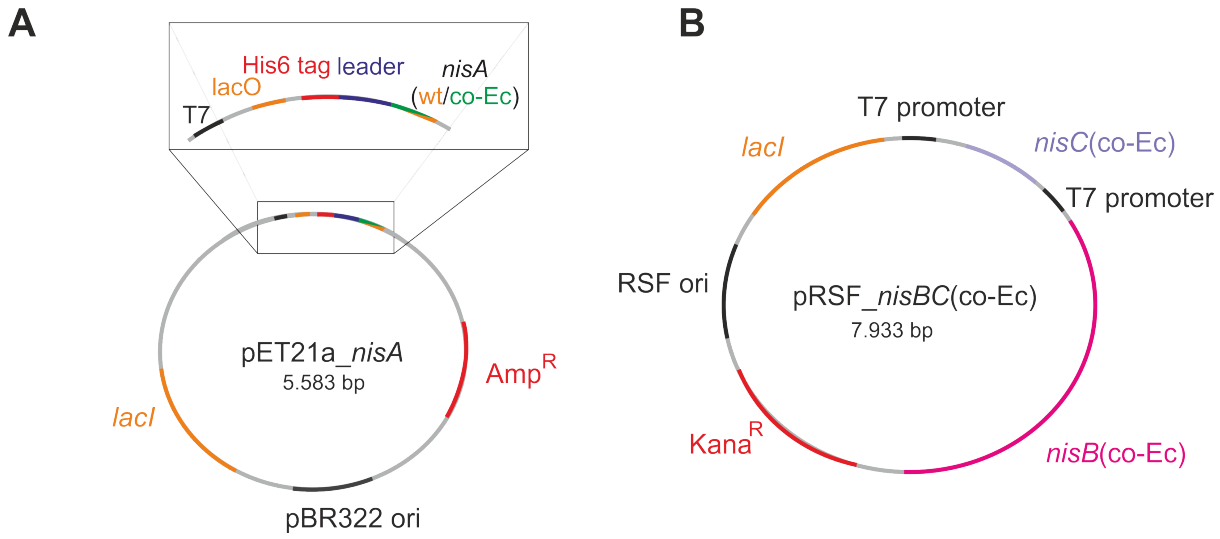

Figure 20. (A) Schematic vector map of pET21a_*nisA* and (B) pRSF_*nisBC*(co-Ec). For abbreviations of components compare E.4.

pET21a and pRSFDuet are both commercially available vectors from Merck. pET21a_*nisA*(wt) was similar to the one described in C.1.1, except for the lack of the PLrigid and eGFP fusion part. Instead, translation of His6-tagged *nisA* was terminated by a stop codon directly adjacent to the NisA sequence. pRSFDuet was designed for coexpression of two target ORFs, which allow insertion of the desired genes (here: *nisB* and *nisC*) through two MCS sites. Both MCS are preceded by a T7*lac* promoter and a ribosome binding site (RBS). Moreover, the vector carries a RSF1030-derived RSF replicon, which is compatible with pET21a's origin of replication, *lacI* and a kanamycin resistance gene (99,111).

Peptide expression was carried out simultaneously after a simplified protocol of SHI et al. in a 50 ml scale (93). The schematic workflow is shown in *Figure 21* A. The cell-free lysate was first applied to affinity chromatography columns (HisTrap) and subsequently used for the performance of an agar well diffusion assay, allowing comparative estimation of the amount of antimicrobial active compounds in the purified cell-lysate (see B.4.2) and facilitating the choice of the potentially more productive host strain for future expression experiments.

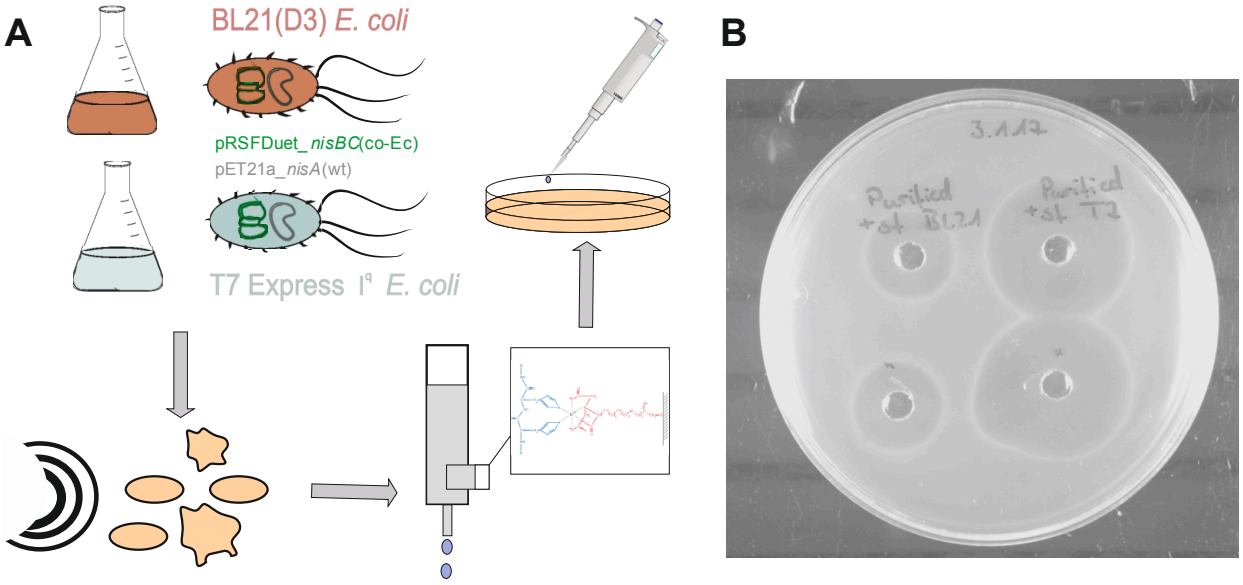

Figure 21. (A) Workflow of the expression experiment for the choice of nisin expression host strain. Both, BL21(D3) (colored in brown) and T7 Exp (blue-green) were co-transformed with pRSFDuet_*nisBC*(co-Ec) and pET21a_*nisA*(wt). Cell lysis was achieved via sonication. Peptides were purified by affinity chromatography (HisTrap) and subsequently used for activity tests. **(B) Comparative agar well diffusion assay of purified T7 Exp and BL21 (D3) cell lysates.** 30 µl purified and cell-free eluate was applied in each well. Technical duplicates were performed. *L. lactis* [pIL, pNZ] was used as sensor strain.

Here, the size of the halo diameter around the well which contained the purified cell extract of T7 Exp cells was twice as large as the one around the well with BL21(D3) cell lysate (*Figure 21 B*). Consequently, T7 Exp cells were used for further experiments and pET21a_*nisA*(co-Ec) was cloned, aiming at the optimization of product yields in successive experiments by codon optimizing the *nisA* sequence for *E. coli.*

C.2.2 Establishment and optimization of the purification protocol

Next, nisin expression in T7 Exp cells was carried out accordingly in a 250-ml scale, yielding 2,09 g wet biomass for NisA(wt) and 1,01 g for NisA(co-Ec). SDS-PAGE of the purified cell extracts showed a thick band in the low molecular weight range (expected size: 7,6 kDa) for NisA(wt) and NisA(co-Ec), each including the leader sequence and the His6-tag, which was accompanied by several larger compounds (*Figure 22 A*). The same band was not visible in the negative control, which contained the cell extract of T7 Exp cells, including the pRSF_*nisBC*(co-Ec) plasmid, but missing *nisA* in pET21a. Estimation of the amount of His6-tagged prenisin by comparison of the band intensity with a BSA dilution series via ImageJ gave an amount of 237 µg His6-prenisin/g wet cell pellet for NisA(wt) and 306 µg/g for NisA(co-Ec) (109). In a second large-scale expression, 17,4 g wet biomass could be obtained from a two-liter culture for T7 Exp, containing pRSFDuet_*nisBC*(co-Ec) and pET21a_*nisA*(wt), and 11,9 g cell pellet from the two-liter expression with pET21a_*nisA*(co-Ec). Further purification was achieved by reverse phase high performance liquid chromatography (RP-HPLC) connected to metal affinity chromatography and buffer exchange via gel filtration (NAP column) (*Figure 22 B and C*). Due to the high resolution of tricine-SDS electrophoresis in the low molecular range, a clear shift to ~12 kDa from the expected 7,6 kDa was now visible, demanding further confirmation via protein analytic tools (e.g. mass spectrometry).

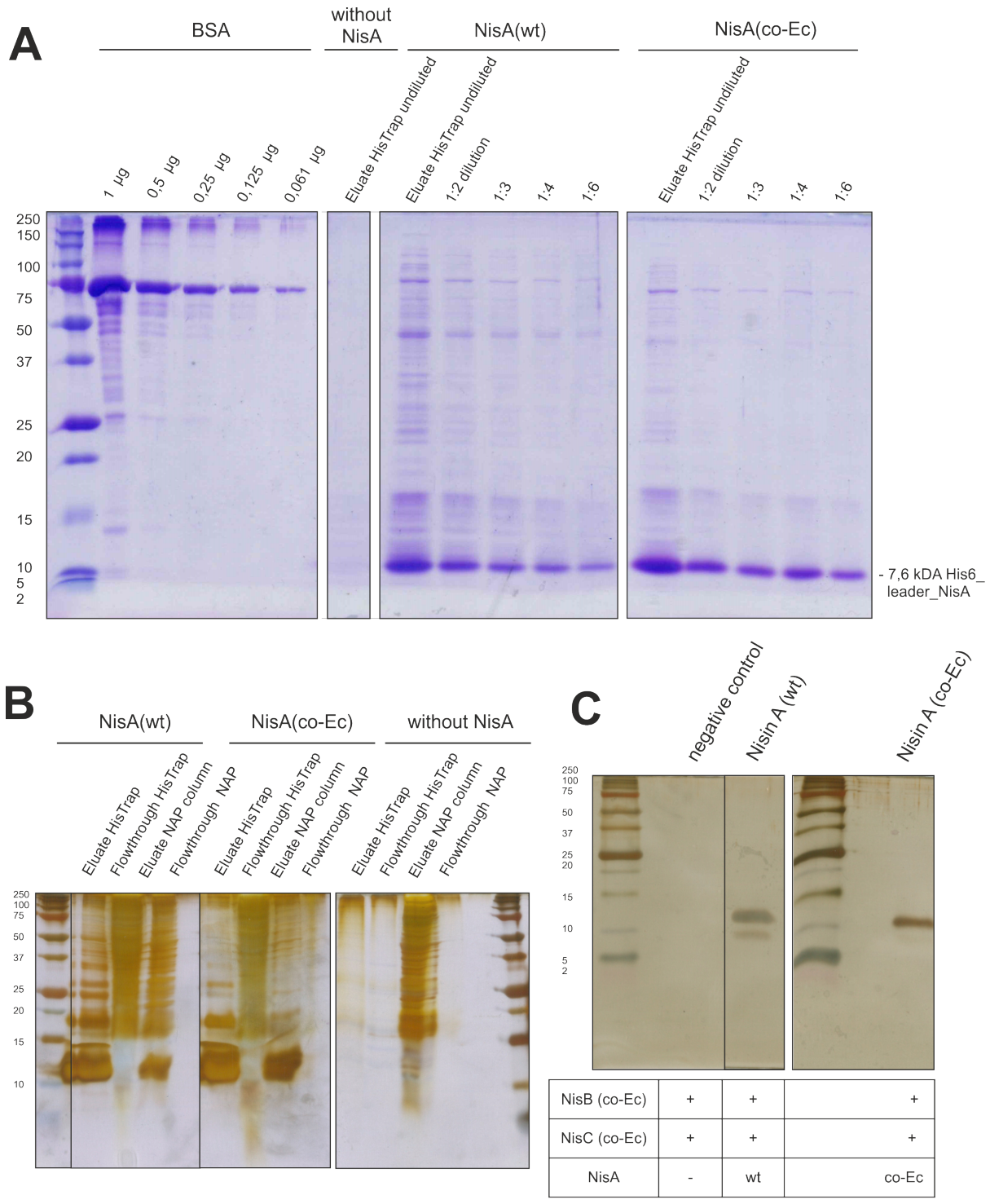

Figure 22. Purification steps of nisin A overexpressed in *E. coli*. (A) Coomassie stained SDS-PAGE (15 %) of a BSA dilution series as reference for the quantification via densitometry. Five dilution steps of the HisTrap purified NisA(wt) and NisA(co-Ec), obtained from a 250 ml expression are shown. Each undiluted lane was loaded with the equal amount of purified cell extract from 3,33 µg wet cell mass. (B) Silverstained tricine-SDS-PAGE (16,5 %) of the eluate and flowthrough of the HisTrap and NAP column. NisA(wt) and NisA(co-Ec) were obtained from a 2 l expression. (C) Silverstained tricine-SDS-PAGE (16,5 %) of further HPLC purified samples of NisA(wt), NisA(co-Ec) and negative control (without *nisA*).

Attempts to purify nisin by size exclusion chromatography failed, but hydrophobic interaction chromatography proved to be an efficient method for purification. Elution profiles are shown in *Figure 23*. Purified NisA(wt) showed an asymmetric peak with a maximum of 1390 mAU at a retention time of 17,5 min, with peak fronting beginning at 17 min and an additional front shoulder. For NisA(co-Ec) the picture seemed more inhomogeneous. A total of four peaks in the intensity range of 619 to 741 mAU appeared at a retention time of 17,2 to 17,6 min, suggesting the presence of several similar components.

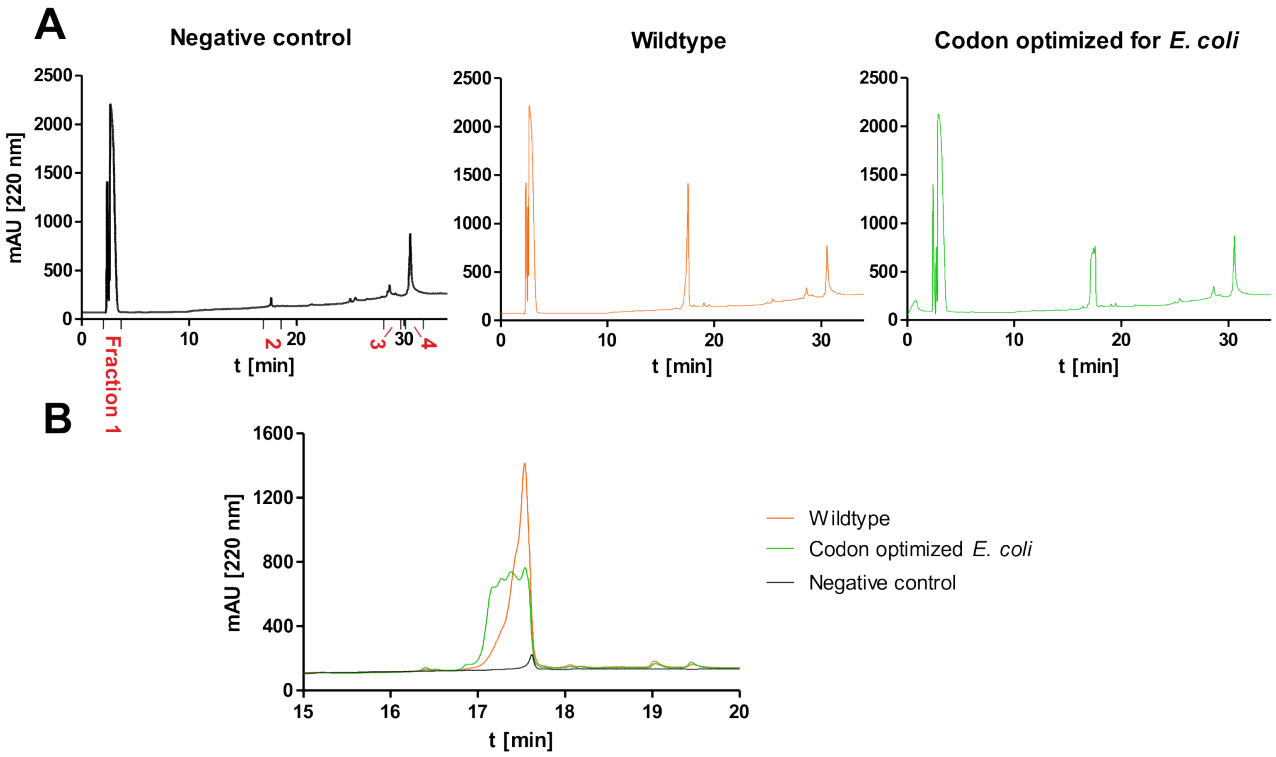

Figure 23. HPLC elution profile of modified and prepurified nisin A, expressed in *E. coli*. T7 Exp co-transformed with pET21a_ *nisA*(co-Ec and wt) and pRSFDuet_*nisBC*(co-Ec) were used for expression of nisin A. pET21a (without *nisA*) served as negative control. Cell lysates were prepurified by metal affinity chromatography. Buffer exchange was achieved using gel filtration prior to purification on an C8 column (Agilent Zorbax Eclipse XDB C8 (4.6 x 150 mm, 5 µm)) operated on an Agilent HPLC system. Pre-equilibration with 100% H_2O + 0,1% (v/v) TFA (solvent A). Minute 0-5: 100% solvent A. Minute 5-35: Constant gradient of 0-100 % acetonitrile + 0,1 % (v/v) TFA (solvent B). Minute 35-40: 100% solvent B. **(A) Complete elution profiles** of the negative control, NisA(wt) and NisA(co-Ec). **(B) Detail of the elution profile** (15 to 20 min). The three curves (negative control, wt and co-Ec) are overlayed.

C.2.3 Characterization and quantification of nisin A from *E. coli*

To confirm the identity of the purified peptides, mass spectrometric and antimicrobial activity analysis was used. An easy to handle and rapid method for the determination of

the presumably nisin-containing HPLC-fraction is the qualitative agar well diffusion assay. Solely fraction number two (retention time: 16,5 to 18,5 min) showed a halo in the activity test of NisA(wt) and NisA(co-Ec), corresponding to the peak observation in the HPL elution profiles (*Figure 24*).

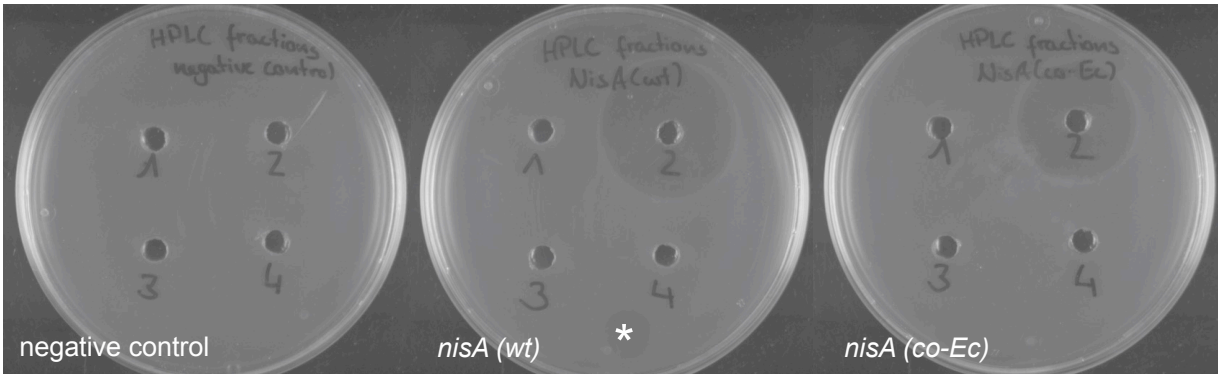

Figure 24. Agar well diffusion activity test of HPLC fractions of prepurified T7 Exp cell lysate. *L. lactis* [pIL, pNZ] was used as sensor strain. Retention times were: 1,5 to 3,5 min, 16,5 to 18,5 min, 28,0 to 29,7 min and 30,0 to 32,0 min for fraction one, two, three and four, respectively (compare *Figure 23*). A small halo, caused by an unintentionally spilled drop of fraction 2 of NisA(wt) is marked with an asterisk.

Since the antimicrobial activity test substantiated the supposition that fraction number two contained nisin, mass spectrometric analysis of HPLC fraction two of NisA(wt) and NisA(co-Ec) samples was conducted next. Peptide Mass Fingerprinting (PMF) after digestion of our samples with trypsin and comparison of peptide fragment masses to the Swiss-Prot database confirmed that peptide fragments belonged to the His6-tagged (leader including) prepeptide nisin A (data not shown). However, several differently modified species of the molecule could be detected. Further confirming the identity of nisin and nisin subspecies, a total mass of 7366,6 g/mol for NisA(co-Ec) and 7331,1 g/mol for NisA(wt) was detected with tandem mass spectrometry (*Figure 25*). Again, more subspecies and modifications of nisin were found, when the codon optimized sequence was used for expression (*Figure 25 C and D*).

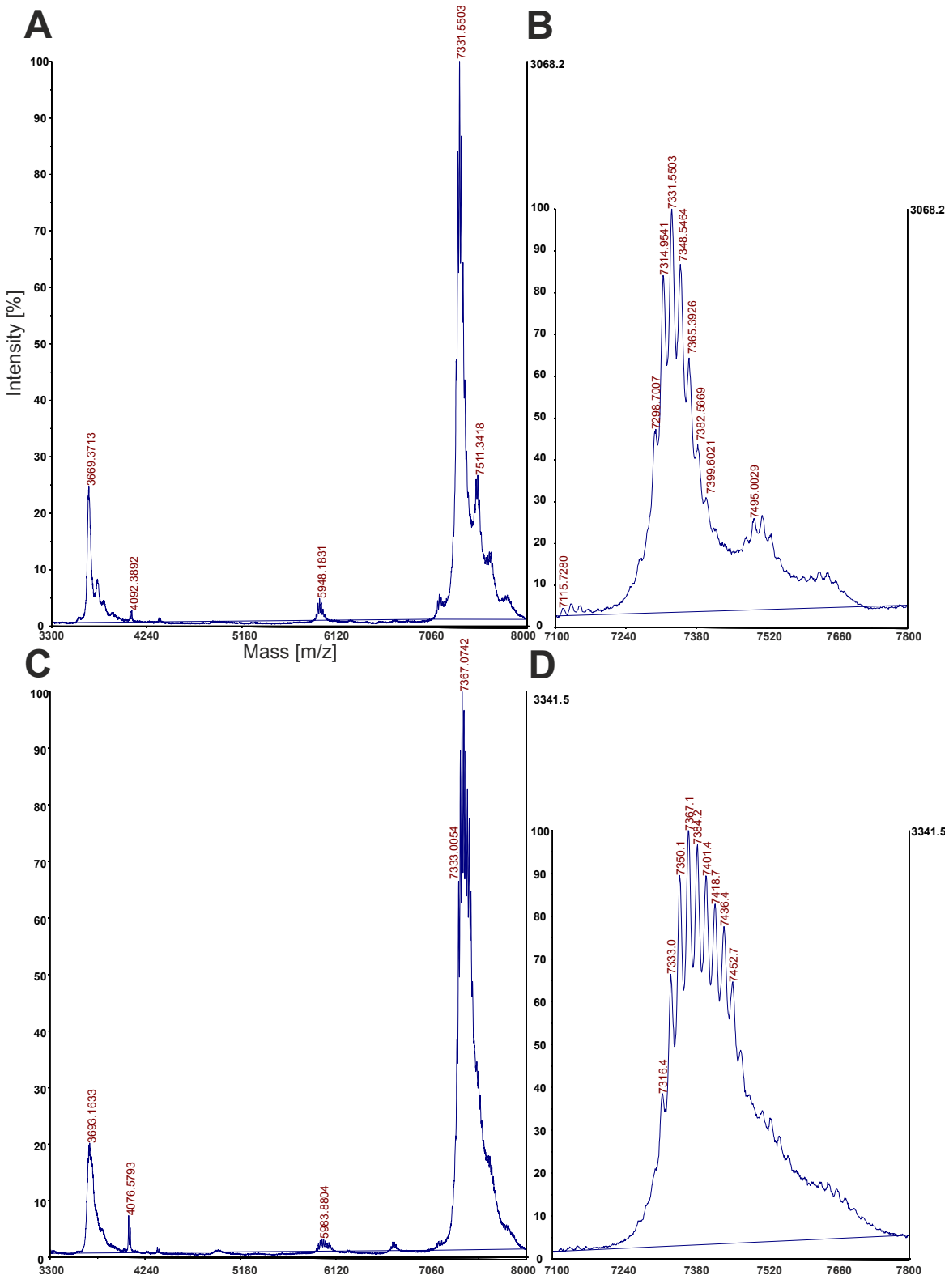

Figure 25. TOF/TOF linear mass spectrum of nisin A from *E. coli*. (A) Full spectrum of nisin A, expressed using the wildtype DNA sequence. (B) Detail of the spectrum of NisA(wt) from 7100 to 7800 [m/z]. (C) Full spectrum of NisA, expressed using the *E. coli* codon optimized DNA sequence. (D) Detail of the spectrum of NisA(co-Ec).

Deviations of observed and calculated masses were in the range of 1,63 to 9,96 kDa and mapping of dehydration status to the species found in the spectrum was therefore difficult. An overview of dominant subspecies and distribution of the amount of modification variants can still be given (*Table 3*).

Dehydrations	**Calculated [Da]**	**Observed [Da] for NisA (wt)** (relative intensity [%])	**Observed [Da] for NisA (co-Ec)** (relative intensity [%])
8	7300,33	7298,7 (47 %)	-
7	7318,35	7315,0 (84 %)	7316,4 (39 %)
6	7336,37	7331,5 (100 %)	7333,0 (67 %)
5	7354,38	7348,5 (87 %)	7350,1 (89 %)
4	7372,40	7365,4 (65 %)	7367,1 (100 %)
3	7390,41	7382,6 (43 %)	7384,2 (96 %)
2	7408,43	7399,6 (31 %)	7401,1 (82 %)
1	7426,44	7417,0 (23 %)	7436,4 (77 %)
0	7444,46	-	7452,7 (65 %)

Table 3. Analysis of masses and relative intensities of NisA(wt) and NisA(co-Ec) obtained with tandem TOF/TOF mass spectrometry.

Quantification of nisin represented an immense challenge, because common protein quantification assays, such as Bradford, Pierce 660 mm or DC protein assay (Biorad), are biased by the extremely low molecular weight and the uncommon ring structure of nisin.

As nisin does not possess any tryptophan residue, quantification via the molar extinction coefficient at 280 nm is no reliable method. Instead, calculation of the molar extinction coefficient at 205 and 214 nm according to published formulas was done (112,113). Here again, quantification was not reliably possible which is why this option was eventually rejected. Another possibility would be comparison of the area under the curve at 226 nm measured via HPLC of samples and a nisin standard series (114). As nisin standard including the leader peptide was unavailable, this method was non applicable for our purposes, too.

Another option for the estimation of the nisin concentration in *E. coli* expressed purified cell lysates was the inference from its antimicrobial activity compared to a known

amount of nisin. For the determination of the amount of active nisin A in the cell extract, a MID assay (B.4.3) was performed and the observed minimal inhibition dilution step was compared to a MIC assay, which was done with commercial nisin (*Figure 26*). The same sensor as before, *L. lactis* [pIL, pNZ], was used. The growth control, which monitored the uninhibited bacterial growth showed the typical logarithmic curve (see *Supplementary Figure S7*). The $MIC_{50\,\%}$ (meaning that 50 % of the normal cell growth, without added antibiotic, is inhibited) of commercial nisin A and nisin ZP were determined to 125 ng/ml and 1 µg/ml, respectively (compare *Figure 26 A*). Both commercial substances were of >95 % purity according to the manufacturer's specifications. Compared to literature, which reports same MICs for nisin A against *L. lactis* subsp. *cremoris* BA3 of 50 ng/ml or against *L. lactis* HP of 108 ng/ml, the $MIC_{50\,\%}$ of nisin A from Cayman Chemicals found in our setting was more congruent with literature values and was therefore used for calculation of concentrations (115,116).

The last dilution step of the MID assay, where growth was inhibited to 50 %, was determined to 1/800 for NisA(co-Ec) and 1/3200 for NisA(wt). These dilutions were then taken to determine the amount of active nisin to 0,33 mg/g (co-Ec) and 1,79 mg/g (wt) crude wet cell pellet, by comparison with the $MIC_{50\,\%}$ value for nisin A (Cayman Chemicals) (compare *Figure 26 B*).

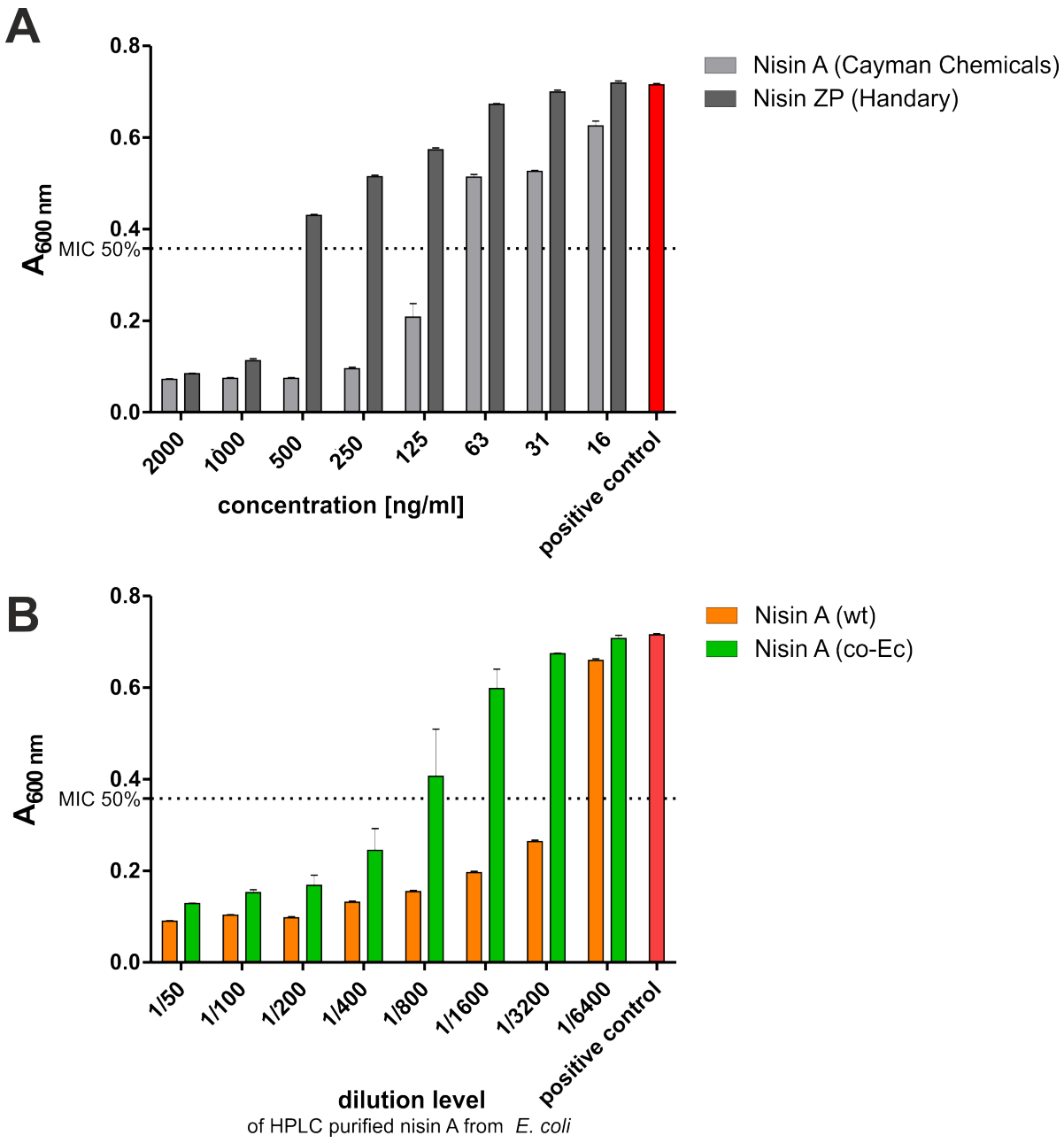

Figure 26. Minimal inhibitory concentration/dilution assay for the concentration determination of nisin A from *E. coli*. (A) MIC assay testing the potency of commercial nisin A and nisin Z. (B) MID assay for the quantification of NisA (wt) and NisA (co-Ec). The dilution level of the HPLC purified NisA obtained from expression in *E. coli* is indicated on the x-axis. The horizontal black dashed line indicates the inhibition of 50 % of the positive control (sensor without any nisin added). Error bars indicate the standard deviation of three technical replicates.

C.2.4 NisT – functionality of a gram-positive transporter in a gram-negative organism

To further facilitate nisin testing systems and nisin production in *E. coli*, a huge benefit could be drawn from the establishment of a fully functioning nisin-export machinery in *E. coli*. Cell lysis and separation from intracellular proteins, which both leads to losses in nisin purification would then be unneeded. No attempts to encode the *L. lactis* specific transporter NisT in a gram-negative organism have been reported to date. To provide a first glimpse into the operating mode of NisT encoded in *E. coli*, different combinations of Nisin A, B/C and T were tested upon the amount of antimicrobial active nisin in the cell-free supernatants of the respective *E. coli* expression cultures (compare *Figure 27 A*).

Different hypothesis were tested with these constructs. Those were:

[1] No antimicrobial acitivity in the cell-free supernatant is visible when *nisA* is not present on the plasmid (compare red couloured data in *Figure 27*).

[2] Addition of a His6-tag to *nisA* for simplified purification hampers the transportation of prenisin by NisT. Thus, lower antimicrobial acitivity is visible when a His6-tag is attached to *nisA* (compare greenish data in *Figure 27*).

[3] A stronger antimicrobial activity is observed in case NisT is encoded. The opposite is true if *nisT* is not present on the plasmid (compare bluish data in *Figure* **27**).

[4] In the event of a NisT transport function over the inner but not outer membrane of *E. coli*, addition of PMBN as an outer-membrane disorganizing agent leads to higher levels of nisin in the medium (117–119). As shown by DES FIELD et al., addition of PMBN increases the sensitivity of gram-negative targets to nisin by abolishing the impenetrable barrier function of the outer membrane (53). Therefore, a *vice versa* effect of PMBN was postulated and examined in the experiment (experimental groups marked on the bottom of *Figure 27 B*).

Figure 27 A provides an overview of the different characteristics of the pETDuet vector: presence or absence of either His6-tagged or untagged *nisA* and *nisT*. Moreover, the genes for the posttranslational modification enzymes *nisB* and *nisC* were needed to obtain fully-modified and antimicrobial active nisin A. Therefore, *nisB* and *nisC* were cloned

into a second commercial vector system (pRSFDuet). Both vector systems, pETDuet and pRSFDuet, include a dual expression cassette under T7 promoter control. Hence, unbalanced, equally strong gene expression of all genes is induced by addition of IPTG. All genes (*nisABCT*) were codon optimized for *E. coli*, aiming at maximizing the peptide yield. T7 Exp cells were co-transformed with pRSFDuet_*nisB*C(co-Ec) and the respective pETDuet construct. The influence of PMBN was studied by addition of 20 µg/ml PMBN when expression was induced. After expression (B.3.1), the crude, cell-free supernatant was subjected to an agar well diffusion assay (*Figure 27 B*).

A

Construct	NisBC	NisA	NisT	His6-tag
	X	-	X	-
	X	X	-	X
	X	X	X	X
	X	X	-	-
	X	X	X	-

B

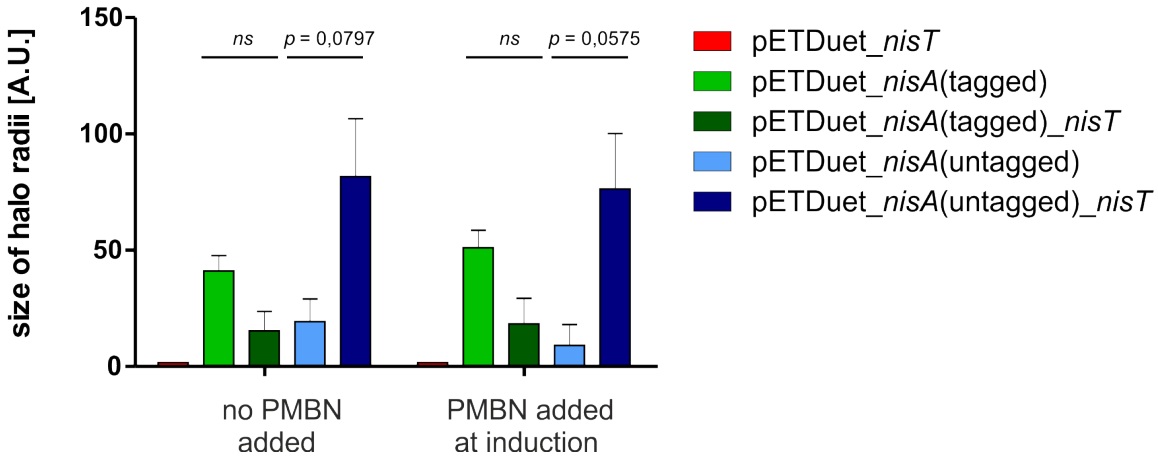

Figure 27. Results of the NisT experiment. (A) Overview of the tested combinations. The colour code represents the respective combination of constructs. Red stands for T7 Exp cotransformed with pRSFDuet_*nisB*C(co-Ec) and pETDuet_without *nisA*_*nisT*(co-Ec). The green/blue combinations contain His6-tagged/untagged *nisA*(co-Ec) on the pETDuet vector. Dark green/blue includes *nisT*(co-Ec), light green/blue is lacking *nisT*. **(B) Comparison of halo sizes** measured with ImageJ after a 24 h growth period. Same conditions for the expression were applied for all combination of constructs. The cell-free supernatants were subjected to an agar well diffusion assay. Two conditions were investigated [1] no polymyxin B nonapeptide (PMBN) was added, [2] PMBN was added at induction. Error bars indicate the SEM.

No antimicrobial activity could be found for pETDuet_*nisT*, demonstrating the necessity of *nisA* for nisin's production and proving that hypothesis [1] is true. Coherently, halos were observed for the four other constructs, which included *nisA*. Comparing the halo sizes of the setup with His6-tagged *nisA* (light green) and the one which additionally included *nisT* (dark green), no significant difference could be found. In the absence of *nisT*

a slight tendency towards larger halos could be observed. Looking at the small halos for His6-tagged *nisA*, there is reason to suspect a negative influence of the His6-tag for nisin's capability to be transported via NisT, supporting hypothesis [2]. The picture differs completely, when the His6-tag is omitted. Here, considerably larger halos could be seen when *nisT* was included (dark blue) compared to its absence (light blue), encouraging the assumption that NisT is capable to transport active nisin A over the membrane of *E. coli* and supporting hypothesis [3]. Addition of PMBN did not show any noteworthy effect on the halo size in all five tested constructs, suggesting that the release of active nisin to the supernatant is not depending on PMBN. Hence, hypothesis [4] can be rejected.

C.2.5 Conclusion

Mature nisin A could successfully be produced, using the expression host *E. coli* T7 Exp. Purification of the crude product was achieved by metal affinity chromatography, gel filtration and hydrophobic interaction chromatography. Whereas densitometry revealed a higher yield of nisin when *nisA*(co-Ec) was used for expression, activity tests showed more antimicrobial activity when *nisA*(wt) was used. HPLC and mass spectrometry both indicated the presence of an inhomogeneous product mix when the codon optimized NisA sequence was employed. The results of the NisT experiment suggest functionality of the transporter in the gram negative bacterium *E. coli* when untagged NisA is used for peptide expression.

D Discussion

Antimicrobial resistance is one of the biggest challenges modern medicine faces and will face in the near future. Only by discovering new classes of antibiotics, doctors will have a chance to successfully treat threatened patients (8). In this context, lantibiotics, which are ribosomally synthesized and posttranslationally modified bacteriocins, represent auspicious candidates for a completely new class of antibiotics in human medicine. Despite the considerable number of 15 PTMs, being reported in various family members, the introduction of specifically tailored chemical modifications would open up a vast new pool of possibilities to enhance the properties of lantibiotics (42,120). Enhancing e.g. the stability of lantibiotics towards intestinal proteases would bring researchers one step closer to application of lantibiotics in medicine. To benefit in full extent from ncAA-technology, nisin and nisin expression systems need to be engineered to ensure high fidelity and efficiency of ncAA incorporation, thereby obtaining a homogenous product.

D.1 Leak expression of truncated side-products strongly compromises the amber suppression efficiency

In the scope of this project, elimination of truncated side-products which strongly biased the observed fluorescence intensity in the absence of the ncAA was a major concern. A first set of data, screening eight selected positions in nisin with and without addition of the model ncAA BocK, showed only little or no FI difference between the two measurements at almost all positions investigated (*Figure 9 and 10*). Other than expected, GFP fluorescence could be observed even when BocK was not present in the reaction mixture, indicating either unspecific work of the tRNA-synthetase or presence of truncated products, which include the C-terminal eGFP part, hence, contributing to a stronger fluorescence. Closer investigation of the expression products by Western blot analysis with an anti-GFP (C-terminus) and anti-His6 (N-terminus) antibody revealed strong product bands, which were only stained by anti-GFP, but not by anti-His6 antibodies (data not shown, details can be found in Miriam Thewes' thesis). These product bands appeared in the size range which would be expected for proteins, which included the C-terminal PLrigid-eGFP part, but lacked the N-terminal part concordant with translation termination

at the TAG codon. These observations support the assumption that not an unspecifically working aaRS was the reason for the limited suppression efficiency, but the presence of N-terminally truncated expression products. In case that aaRS works unspecifically, canonical amino acids would be incorporated into the nascent peptide and the full-length protein would get translated. Accordingly, these products would get stained by both: anti-His6 and anti-GFP antibodies.

Two hypotheses were deduced from the mentioned results: [i] enigmatic RBS sequences (Shine-Dalgarno sequences) and/or [ii] M17/21 in the nisin sequence serve as alternative translation initiators and thus, lead to observation of truncated products. To address both working hypothesis, the experiment was designed as shown in *Figure 11*.

The Shine-Dalgarno (SD) sequence is a short, highly conserved RNA motif (with the mRNA sequence 5'…AGGA GGU…3') which is located in the 5' untranslated region of prokaryotic mRNA and interacts with a 3'-terminal 'anti-SD' sequence of the 16S rRNA of the prokaryotic ribosome to form a stable translation initiation complex (121). Apart from the SD sequence, other mRNA elements can affect formation of the initiation complex. The most important ones among them are: hybridization between the start codon and the $tRNA^{fMet}$ anti-codon, nucleotides adjacent of SD and initiation codon, secondary structure elements of the mRNA and spacing region between SD and initiation codon (2,122). By nature, prokaryotes in contrast to eukaryotes possess mRNAs with several sequential open reading frames (ORF), which are therefore called 'polycistronic' mRNAs (123). This leads to occurrence of a phenomenon which is called 'translational coupling' and is defined as 'the interdependence of translation efficiency of neighboring genes encoded by the same polycistronic mRNA', adding another level of complexity to the, already highly sophisticated, translation mechanism (124).

To reduce the influence of one, or even various, of the mentioned genetic elements and mechanisms acting together to influence the translation initiation, a codon optimization algorithm was used (*Table 2*). Verification of a beneficial effect of the codon optimization upon the ribosome binding strength at undesired positions was done by means of the RBS calculator (Salis lab, Penn State University). This web-based tool predicts the rate of translation initiation rate (TIR) for every start codon in an mRNA transcript, based on a statistical thermodynamic model of bacterial translation initiation which takes into ac-

count the 35 nucleotides before and after the start codon (2). The Gibbs free energy of ribosome binding is related to a protein coding sequence's translation rate, predicting the TIR on a linear proportional scale, provided that all other conditions are equal, from 0.001 to 100.000 A.U.

Entering the wildtype *nisA* sequence yields 21261 A.U. for base the start codon at position 1 corresponding to a comparably very strong TIR (*Figure 28 B*). The desired start codon right in front of the His6-tagged *nisA* is referred to as position 1. Comparing the TIR between the wildtype and codon-optimized NisA sequence reveals that the TIR could be reduced in every single case where a RBS was present in *nisA*(wt) and *nisA*(co-Ec) by codon-optimization (*Figure 28 A and B*). By changing base pairs in the codon optimization process, four RBSs (64, 70, 175, 186) were deleted, while four new ones (79, 152, 172, 203) were created. All of the newly created ones showed weak TIRs (<56 A.U.). The TIR for the desired start codon starting at position 1 was boosted by 40 % in *nisA*(co-Ec).

A

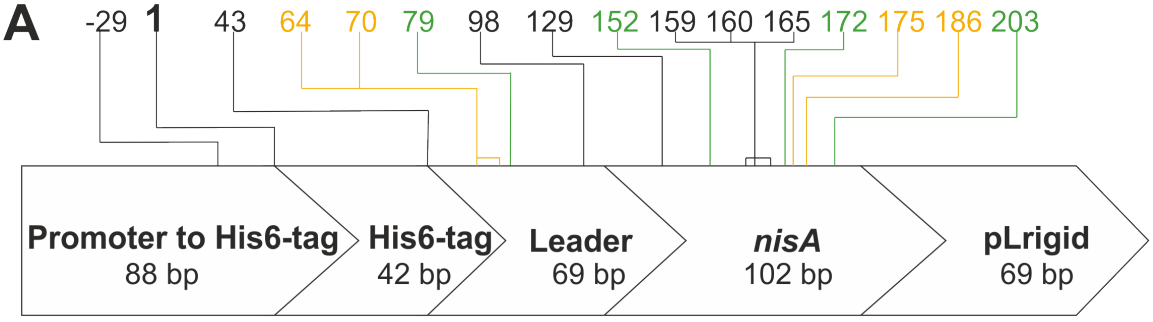

B

Start Position	-29	1	43	64	70	98	129	159	160	165	175	186
nisA (wt)	58,5	21261,9	567,5	20,2	3,7	238,9	18,6		149,9	39,3	39,6	7,8
M17WM21K_*nisA* (wt)	58,5	21261,9	567,5	20,2	3,7	238,9	110,4	30,1		107,2		11,5
TAG17_*nisA* (wt)	58,5	21261,9	567,5	20,2	3,7	238,9	110,4			140,4	73,6	3,4
Start Position	**-29**	**1**	**43**	**79**	**98**	**129**	**152**	**159**	**160**	**165**	**172**	**203**
nisA (co-Ec)	28,9	29798,3	22,8	41,3	22,3	2,0	1,2		4,8	0,6	32,7	1,7
M17WM21K_*nisA* (co-Ec)	28,9	29798,3	22,8	41,3	22,3	2,1	3,0	13,6		3,8		1,2
TAG17_*nisA* (co-Ec)	28,9	29798,3	22,8	41,3	22,3	2,1	1,6			2,1	55,3	2,8

Translation initiation rate [a.u.]	<10	10-25	25-50	50-150	150-300	300-600	>600

Figure 28. Influence of codon optimization upon the RBS strength. (A) The anterior gene elements of the His6-tagged nisA-eGFP fusion protein are shown. Their respective length is given and all RBSs calculated from the RBS calculator (Salis lab, Penn State University) are marked in black (occurring in wt and co-Ec variant), orange (only detectable in wt) or green (only in co-Ec). (B) Three different constructs of the wt and co-Ec variant were selected and their translation initiation rate for each RBS was calculated. Depending on the binding strength, values are highlighted in different colors (red indicates a very low translation initiation rate and green a strong one) (2,125).

Codon optimization of the gene's sequence did not show any reduction effect on the occurrence of biasing side-products in our amber suppression efficiency screening using eGFP fusion proteins (*Figure 16*). Results of the screening with NisA(wt) (*Figure 17 B*) and NisA(co-Ec) both did not show the FI reduction in the absence of BocK we aimed at. Other than expected, overall $FI_{effective}$ values were higher in 6 out of the 8 studied TAG positions when the wildtype gene sequence was used. The higher protein yield which was postulated to be achieved by codon optimization was not experimentally reproducible. A possible explanation for this observation might be a phenomenon described as 'ribosome collisions and queues', which is fueled by the enhanced TIR that was reached through codon optimization (compare *Figure 28 B*) (126,127). A stronger TIR correlates with a faster recruitment of ribosomes at the translation start. That this is not always to be equated with a higher protein expression, was shown by TULLER et al.. They identified an evolutionary conserved profile of translation efficiency along mRNAs, which shows that the first 30-50 codons are on average translated with a low efficiency. Hence, they suggest that 'the slow 'ramp' at the beginning of mRNAs serves as a late stage of translation initiation, forming an optimal and robust means to reduce ribosomal traffic jams, thus minimizing the cost of protein expression' (128). As this was neglected in our optimized sequence, codon optimization, although being a powerful tool to increase protein expression in several other cases, might not have had the desired effect in our setup.

Consequently we turned our attention to hypothesis [ii]. Based on the presumption that M17/M21 represent alternative start codons, translation could reinitiate and N-terminally truncated products would be formed. In 1990, ADHIN et al. proposed a scanning-like movement of the ribosome, which occurs upon premature termination, and leads to translation reinitiation at the closest found start codon (129). In our case, applicability of this model is reinforced by the distribution pattern of the amber suppression reporter assay (*Figure 9*). eGFP fluorescence at the different positions was variably strong observable, even when BocK was absent. This phenomenon was particularly dominant for the TAG positions closer to the N-terminus, and noticeably weaker observable for TAG position 22, 29 and 32. Seeing a constant low fluorescence level for the three C-terminal positions, an explanation could be the absence of N-terminally truncated expression products. Whereas at positions which are closer to the N-terminus (*Figure 29 A*) the ribosome is stalled when it reaches a TAG codon and hence, 'jumps' to the next Met in

proximity to TAG to restart translation ('translational reinitiation'), this phenomenon cannot happen at TAG position 22, 29 and 32 (*Figure 29 B*) as there does not exist an alternative translation start in form of Met at the C-terminus of nisin.

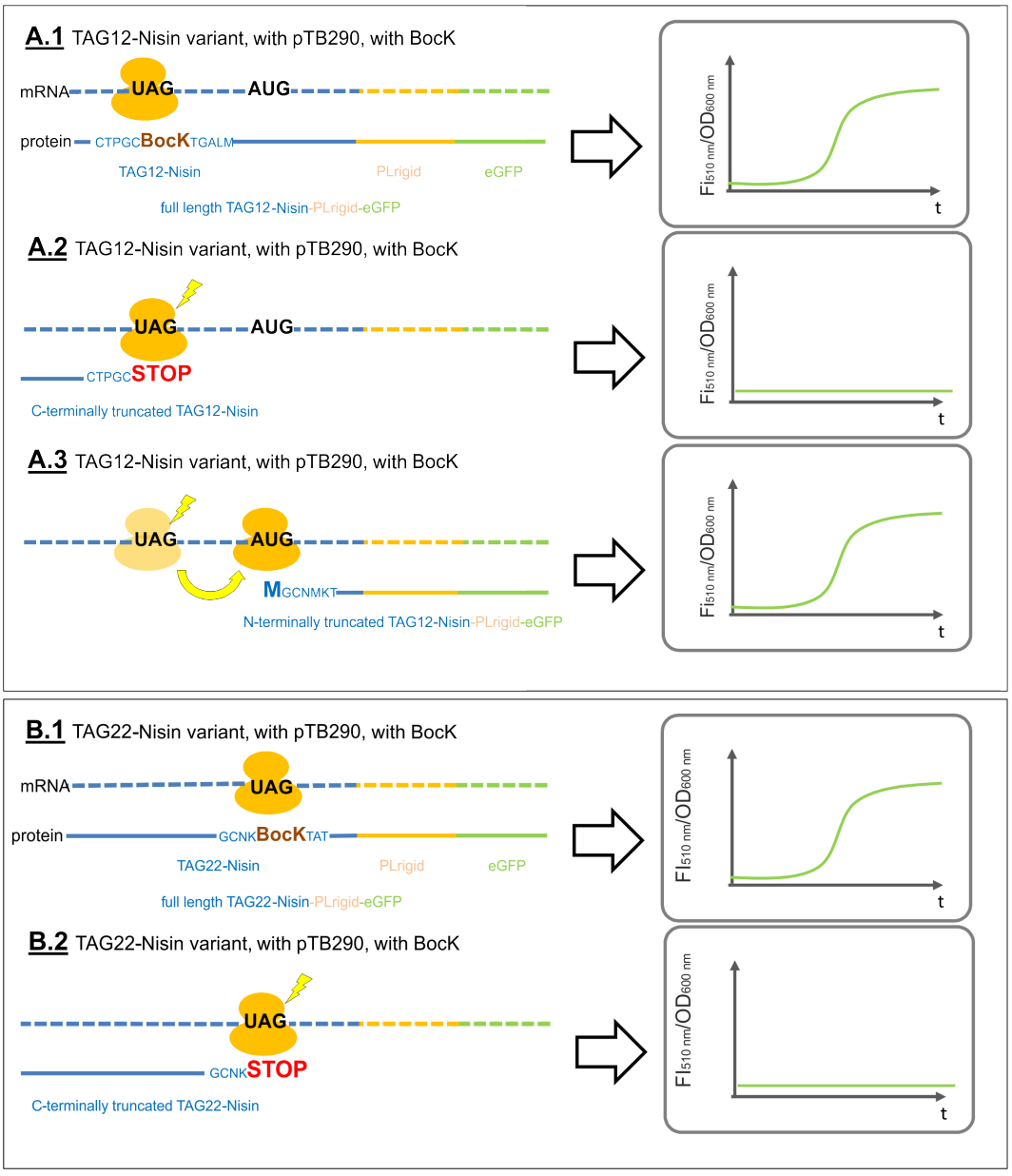

Figure 29. (A) Expected translational events and products for a TAG variant lying 5' of M17/21 (TAG12 is exemplarily shown) when pTB290 and BocK are present. (A.1) Successful incorporation of BocK at the reassigned TAG-codon leads to the full-length nisin-eGFP fusion protein. (A.2) Translation termination at the TAG codon leads to the C-terminally truncated Nisin without eGFP, showing no fluorescence. (A.3) Interruption of translation at the TAG-codon leads to translation reinitiation at M17/21, yielding an N-terminally truncated nisin-eGFP fusion protein. **(B) Expected translational events and products for a TAG variant lying 3' of methionine 17 or 21 (TAG22 is exemplarily shown).** (B.1) Incorporation of BocK at the reassigned TAG leads to the full-length fusion protein. (B.2) Translation termination at the TAG codon leads to the C-terminally truncated Nisin. In this case no translation reinitiation can occur, as no methionine lies C-terminal of the TAG codon.

Gratifyingly, a clear effect in the amber suppression efficiency screening of the M-aaS NisA(wt) and NisA(co-Ec) was visible (*Figure 17 and 17*). Consistent with our hypothesis, the effective FI in the absence of BocK now dropped to a constant basal level and a $SE_{relative}$ of at least 145 % could be reached for all wildtype variants, except for the constructs with TAG 5 and TAG 32 (*Figure 17*). For these two variants, usual reasons which influence the suppression efficiency might play a role (see D.2).

Nonetheless, the questions remained where the background fluorescence in the screening of M-aaS NisA(wt) and NisA(co-Ec) originated from and why it differed from TAG position 5 to 17 for M17WM21K NisA(co-Ec) (*Figure 19 A*). Approximately one third of this background can be explained by fluorescence from the growth medium and the cells themselves (*Figure 19 B.1 to B.3*). The other two thirds can rationally only be explained by two theories: [1] a canonical tRNA recognizes the amber codon as anticodon and introduces its associated amino acid or [2] truncated expression products harboring the eGFP are expressed.

If the tRNA anticodon has two nucleotides, which are identical with the amber stop codon, this tRNA is a near-cognate sense codon (130). These tRNA species can misread an amber codon as their individual sense codon with a frequency in the range of $1{,}1x10^{-4}$ to $7{,}0x10^{-3}$, depending on the adjacent downstream nucleotides (130,131). Accordingly, this ‘readthrough’ could contribute to translation of GFP and a related fluorescence increase, thereby providing one explanation ([1]) for the remaining background fluorescence.

Interestingly, KALSTRUP and BLUNCK observed leak expression through translation reinitiation at non-canonical start codons when ncAAs were incorporated into the 70 aa comprising N-terminal part of the so-called ‘Shaker’ voltage-gated potassium channel in *Xenopus laevis* oocytes. Contrary to nisin, no methionine is present in the first 70 aa of the Shaker channel protein. There are seven (eight for M17WM21K NisA(wt)) non-canonical start codons present in the NisA(wt) sequence (*Figure 30*), which could contribute to a detectable extent to leak expression and thereby explain the remaining two thirds of the background fluorescence. Of course, it is also possible that translation reinitiation at M17/21 contributes to $FI_{effective}$ in the absence of the ncAA for NisA(wt) and NisA(co-Ec).

1 ATGGGCAGCAGCCATCACCATCATCACCACAGCCAGGATCCG**ATG**AGTACAAAAG
55 ATTTTAAC**TTG**GAT**TTG**GTATCTGTTTCG**AAG**AAAGATTCAGGTGCATCACCACGC
112 **ATT**ACAAGT**ATT**TCGCTATGTACACCCGGTTGTAAAACAGGAGCT**CTG**TGGGGTTG
168 TAAC***AAG***AAAACAGCAACTTGTCATTGTAGT**ATT**CACGTAAGCAAA

Figure 30. DNA sequence of nisin with highlighted non-canonical start codons. DNA sequence of His6-tagged (black letters), M17WM21K_*nisA*(wt) (red) with leader (grey). The non-canonical start codons are highlighted bold and underlined in black. The italic *AAG* codon is the lysine codon at position 21, which replaces M21.

To the best of our knowledge, no leak-expression of N-terminally truncated products in *E. coli* which are formed through translation reinitiation at an internal methionine, when ncAAs are incorporated, has been reported so far. Our findings therefore show that careful examination of the protein to be modified with amber SPS upon internal methionines is essential and provide an approach to reduce leak expression.

D.2 Limits of amber suppression

Whilst incorporation of ncAA using amber stop codon reassignment is a useful technology to engineer peptides and proteins *in vivo* and has made outstanding progress in the past, efficient modification is hampered by low suppression efficiencies (67,132). Various reasons have been identified as barriers which can compromise amber suppression: inherent competition of amber-recognizing release factor protein 1 (RF1) and $tRNA^{ncAA}$, local sequence context, and suboptimal design and copy number of suppressor pairs (73,74,133–135).

If both, RF1 and $tRNA^{ncAA}$, are present in the cell, 80 % of translation terminate at the amber codon and only 20 % yield the full-length ncAA-modified protein (132,136). Prokaryotic cells rely on RF1 to terminate translation at UAA (ochre) and UAG (amber), while RF2 recognizes the UAA and UGA (opal) stop codons (73). Though RF1 has long been accepted as essential in *E. coli*, MUKAI et al. firstly succeeded in creating a RF1 deficient, viable *E. coli* strain, hence, turning UAG into an unused sense codon (74,137,138). Following this breakthrough, RF1 deficient *E. coli* strains B-95, where 95 of 273 UAG codons were replaced synonymously, and C321.ΔA, carrying only UAA instead of UAG codons, were designed (139,140). Poor viability, productivity and increased near-cognate suppression of RF1 knockout strains, however, outweigh their advantages largely (134,135). Influences of the mRNA secondary structure is still little

understood and studied until now. Looking at the mRNA context, a few factors which vary the suppression efficiency could be revealed. Showing no distinct dependence on the ncAA structure, a few general design rules for the determination of preferential sites and/or the exploitation of codon degeneracy for the design of flanking codons were identified. Apparently composition of the two codons up- and downstream of the nonsense codon affects amber suppression strongly, with a preference for a low GC- and high A-content, especially at position +4 (133,141). Moreover, it has been studied that the identity of the nucleotide directly downstream of the stop codon (the '4th nucleotide') is of particular importance and supports a suppression instead of a termination event in the hierarchy A>G>C>U (127).

Additionally, amber suppression can be weakened by translation of by-products through e.g. translation reinitiation at non-canonical start codons (compare (134)) and internal methionines. The latter could be proved with our experimental data.

Taken together, all the mentioned factors influence the amber suppression efficiency to a varying extent, depending on the position of TAG within the protein. Therefore, it would be highly interesting to screen every single amino acid position of nisin upon its individual suppression efficiency to reveal if ncAAs are especially efficient incorporable into distinct parts of nisin. Regarding our reduced methionine-deficient TAG position panel, incorporation into the N-terminal (TAG5) and more C-terminal (TAG12-29) part seems to work almost equally well, while variants with TAG8 and 32 did not yield as many expression products (compare *Figure 17 A* and *Figure 18*).

However, given the in vivo nature of the amber suppression methodology, overall yield of recombinant ncAA modified protein has not been reported to exceed 50 % compared to the wildtype protein (135). Considering this, the suppression efficiencies reached in our M-aaS NisA(wt) and NisA(co-Ec) screenings are comparably high.

D.3 Towards an effective methionine deficient nisin variant

Before proceeding with suppression efficiency screenings was rational, identification of a methionine deficient nisin variant, which was comparably active to wildtype nisin, was a main objective that needed to be reached. No such variant was found in literature, despite for several mutagenesis studies conducted with nisin (105). However, a solid set of

data which showed equal activity to wildtype nisin against *L. lactis* and even enhanced activity against selected gram negative bacteria was available for nisin M21K (29,53). For the rational design of a M-aaS nisin variant, bioinformatic tools could be used. Based on the work of DAYHOFF et al., these tools provide information about the probability and even about the effects of amino acid exchanges. The so-called original Dayhoff matrix analyzes the number of accepted point mutations from 1572 closely related sequences, hereby giving a mutation probability. For M17, the four highest scoring substitutions are in order of decreasing probability: leucine, lysine, valine and isoleucine (142). A more recent approach is the Protein Variation Effect Analyzer (PROVEAN). It generates an alignment based score, which provides information about the probable effect on the protein's functionality based on a BLAST search (143). According to the PROVEAN web server tool, the predicted effect of an amino acid substitution at position M17 on the functionality would be deleterious for every single amino acid (144). Nonetheless, functionality prediction is particularly hard for a small, extensively modified and versatile molecule such as nisin (49).

As rational design proved difficult and literature data was rare, substitution of M17 by each of the remaining 19 amino acids was the logical consequence. Relative activity comparison via growth curve analysis (*Figure 14*) and agar well diffusion assay (*Figure 13*) gave the consistent, but unexpected result of variant M17WM21K as best in class. Because of its bulky aromatic indole sidechain tryptophane was expected to disturb nisin's activity. When comparing the results of the two activity assays, one needs to keep in mind that observations might be altered by the nature of the performed activity assays. Diffusion rate, solubility and surface activity play a role in both tests and even one amino acid substitution can influence these parameters, thereby disguising the substitution's influence on the antimicrobial activity. However, consistent results of our nisin M21K activity tests with other studies and demonstration of the confirmable gain of information from comparative agar well diffusion assays by FIELD et al. support the reliability of our findings (53). Identification of nisin variants with enhanced activity and novel properties represents a tough challenge, where only little progress has been made so far. Novel variants with an activity better than the wildtype peptide could possibly be effective against other interesting germs and therefore, might represent urgently needed new opportunities.

To prove the obtained results from the comparative activity assays, absolute determination of activity (MIC) for variant M21K and wildtype (as references), M17FM21K, M17QM21K, M17WM21K (as promising candidates) and M17EM21K (exemplarily bad candidate) would be the next step. This was not achieved within this project, because quantification of variants was a tremendous obstacle. To enable quantification in future experiments, a leader with lysine mutated to tryptophan at position -8 was cloned into pScreen_*nisA* vectors, carrying the respective variant. The K-8W_leader was identified earlier in the group as the best leader to yield fully modified and active nisin, allowing precise quantification through absorbance measurement at 280 nm (145). Furthermore, cleavage of the leader peptide monitored by HPLC and comparison with a synthetically produced leader peptide of known concentration would be a very exact option for future quantification attempts.

Activity of the identified and exactly quantified nisin A variants against antibiotic-resistant pathogens of the WHO's 'global priority list', such as *Enterococcus faecium*, *Staphylococcus aureus* and members of the *Enterobactericeae* family, would be of special interest for future experiments (146).

D.4 Production of nisin in *Escherichia coli*

Expression of the nisin precursor peptide was achieved by KARAKAS-SEN et al., and ZAMBALDO et al. were able to confirm the expression and purification protocol established by SHI et al. (93,147,148). Here, we were able to gain pure modified nisin A from an *E. coli* expression culture, using T7 Exp and a modified protocol of SHI et al.. Contrary to SHI et al. we used T7 Exp instead of BL21(D3) for our experiments. In a comparative experiment for the choice of the expression strain, peptide expression was carried out simultaneously using exactly the same protocol. Due to a larger halo observed around the purified cell-lysate of T7 Exp, these cells were used for subsequent experiments (*Figure 21*). Although expression conditions were identical for both cell strains, cell density was not measured here. To address the hypothesis that T7 Exp is the more efficient host for nisin production than BL21(D3), and higher activity is not only explainable by a stronger growth rate of T7 Exp, a similar experiment should be set up with an additional normalization step on the obtained biomass after expression.

Peptide yields were in the range of 8-63 % (depending on expression scale and quantification method) for nisin A (wt) compared to the reported 24 mg nisin per liter of culture obtained by SHI et al., despite of using the potentially more productive T7 Exp instead of DH10B (compare *Figure 22 and Figure 26*) (93). Indicating the yield in mg per liter of culture, however, is not the best unit to compare yields, since it does not specify which cell density, meaning what biomass, was obtained. Cell density is an important parameter which can easily influence the protein yield and can be increased by optimized growth conditions. Differences between the yields could be explained by modification of the purification protocol. Product loss could be due to omission of the denaturation step, which aims at extraction of peptide from inclusion bodies, and/or because of introduction of a gel filtration step (NAP column), which was necessary for buffer exchange prior to HPLC purification. Further improvement of yields of fully dehydrated nisin could be achieved by overexpression of $tRNA^{Glu}$/GluRS, which is needed for dehydration by NisB, thereby increasing NisB's efficiency (compare A.5.1) (38,148).

Within the Synpeptide project it was planned to test antibiotic candidates using a high-throughput nanoliter-reactor (nl-reactor) assay (149). In principle this assay works by co-incubating one bacterium, which produces an antibiotic variant, and one target bacterium in a nanoliter droplet. Next, this droplet is getting checked for the 'winner' – antibiotic producer or bacterium – by e.g. fluorescence signals, which differ depending on the battle's outcome (150). For this purpose, the ultimate goal for expression of (modified) lantibiotic variants in *E. coli* would be the establishment of a system which fulfills all requirements from end to end. This means: [i] efficient production and, if required, modification, [ii] full post-translational processing and, eventually, [iii] expeditious export from the producer cell. Observation of higher antimicrobial activity in the cell supernatant of *nisA/B/C* and *nisT* harboring cells, compared to the setup without *nisT* (*Figure 27*), leads to the intriguing conclusion that NisT might actually be able to transport nisin from the inside to the outside of the cell. This would be a huge step on the way to realize [iii] expeditious export and would facilitate the use of the nl-reactor assay. Efforts to achieve cell lysis, which is needed to get to the intracellular produced antibiotic, would then be redundant.

On the basis of the found results, further experiments with untagged *nisA*, *nisB/C* and *nisT* should be carried out to corroborate the positive transportation effect of NisT sug-

gested by the results of the pilot experiment. In particular, exact quantification of nisin in the supernatant of *E. coli* and *L. lactis* expression cultures encoding *nisT*, would be highly interesting.

D.5 Prospects for the incorporation of non-canonical amino acids into nisin

The ultimate goal for the incorporation of ncAA into nisin is quality enhancement, which can generally be achieved through engineering of either its pharmacokinetic and/or pharmacodynamic properties. The concept of pharmacokinetics includes bio-physical parameters, such as resistance towards proteolytic degradation, heat stability and solubility at physiological pH, whereas pharmacodynamics describes the component's mode of action, action profile and dose-response relationship (151). Improving these parameters would help to produce the first generation of peptide-based antibiotics for clinical use.

Enhancing a substance's potency is certainly the most tempting approach for drug engineering. Extensive mutagenesis studies have been conducted so far, including hinge region residues (compare C.1.4) and randomisation of serine at position 29 (152). The latter revealed nisin derivate S29G and S29A, which were active against gram positive and negative bacteria (53). However, a major breakthrough is still outstanding. Introducing point mutations into nisin might not be the suitable answer to augment nisin's potency. Instead, we propose to target its mode of action. Here, the following is conceivable: [i] increasing nisin's affinity towards lipid II or [ii] facilitating recruitment of the lipid II:nisin complex components for accelerated pore formation. A nisin derivative with increased affinity to lipid II would be highly desirable, because of a double effect: more effective disruption of cell wall synthesis and enhanced pore formation. But design of such a derivative is also very challenging, as nisin already shows extremely high-affinity binding to lipid II ($2x10^7$ M^{-1}) and as interaction of nisin's first two lanthionine rings with lipid II's pyrophosphates is an intricate arrangement, which is most probably already close to perfect (48,153). Contrary, concept [ii] can be addressed in a more straightforward manner. One pore consists of four subunits, which are characterized by two nisins that bind one lipid II molecule. Based on the composition of a nisin-induced pore, one rational design

approach is to link either two or eight nisin molecules via a flexible linker, in order to facilitate complex formation (compare *Figure 32.2*). A suitable glycine- and/or serine-rich linker, which does not hamper the protein function and shows good solubility in aqueous solutions, could easily be introduced by combining ncAA technology and 'click chemistry' (70,154,155). 'Click chemistry' describes reaction types, which combine small, modular 'building blocks' via a heteroatom link (C-X-C) in a very efficient, stereospecific manner (156). Examples for such reactions are oxime bond forming reactions of ketone-containing ncAAs with alkoxy-amine derivatives (*Figure 31 A*) or cycloadditions of an azide and an activated alkyne (*Figure 31 B*) (157).

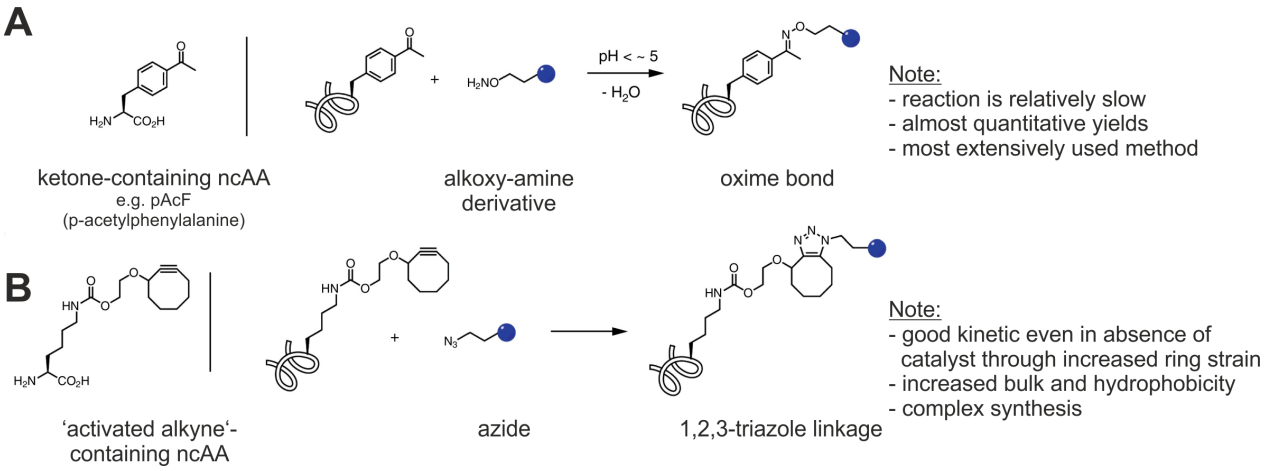

Figure 31. Examples of click chemistry reactions with ncAAs used for site-specific protein conjugation. Figure adapted from KIM et al. (157).

In the case of nisin, not only potency increase is of interest, but an even equally intriguing question is: How can we use its high potency and render it active against gram negative bacteria, too? Clearly, antibiotics against gram negative bacteria are most urgently needed, and nisin's natural target spectrum does not include those (146). Fighting gram negative targets can be facilitated by combining cell-permeabilizing 'warheads' with nisin in a two-component drug, hence, ensuring that nisin can traverse the outer membrane and may bind to lipid II (*Figure 32.3*). In this regard, a promising substance is polymyxin B nonapeptide (PMBN), which is an outer membrane-disorganizing peptide that has already been tested once in combination with nisin, turning naturally resistant targets sensitive to treatment with nisin (53). Other outer membrane permeabilization agents are EDTA, lysine polymers or aminoglycosides (158). A major drawback of nisin, as for most peptide drugs, is it's susceptibility to the action of human intestinal proteases

and a resulting low serum half-life (120,159). This pharmacokinetic property can be improved through site-specific conjugation with polyethylene glycol (PEG), which has already been successfully conducted with human growth hormone and fibroblast growth factor 21 (*Figure 32.1*). Here, minimal loss of biological activity combined with enhanced pharmacokinetic properties could be demonstrated (157).

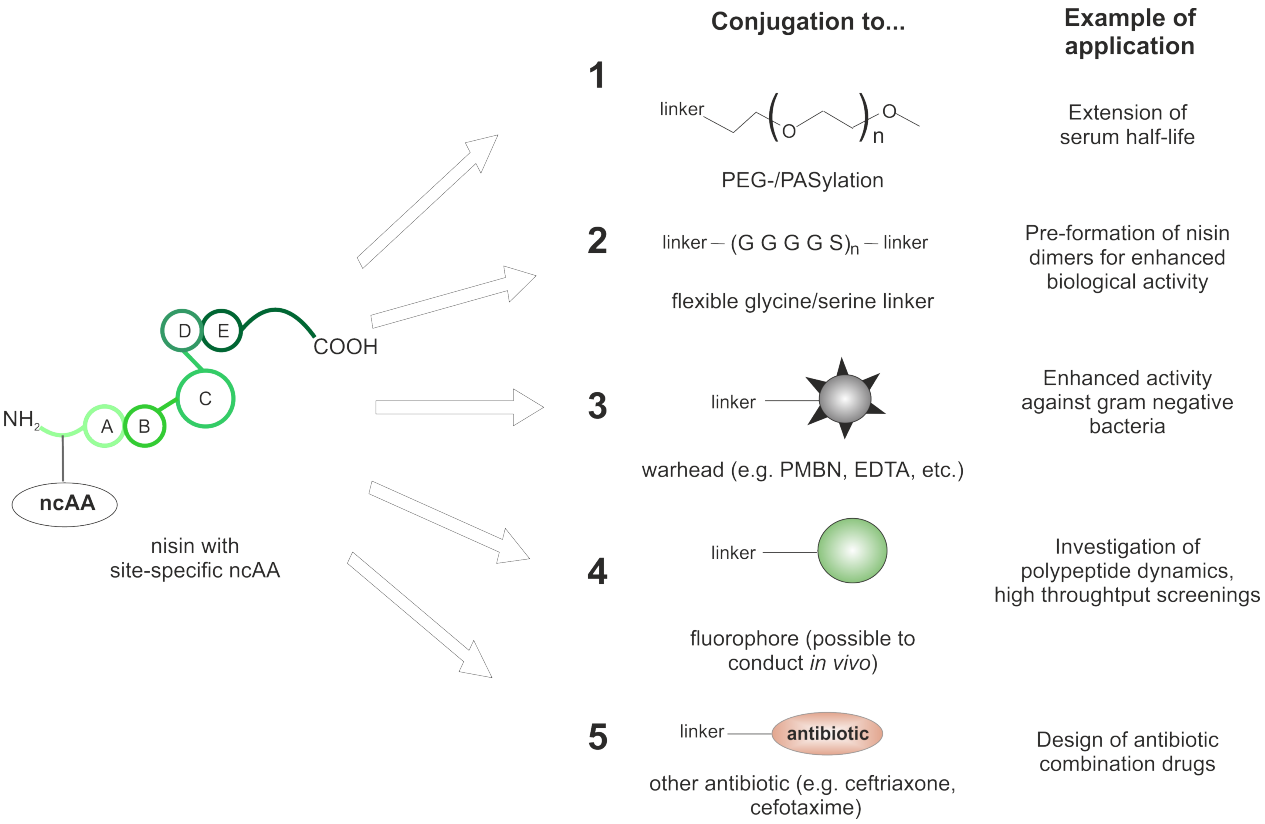

Figure 32. Prospects for the incorporation of ncAAs into nisin. (1) PEG-/PASylation of nisin for plasma half-life extension (160). (2) Coupling of two (or more) nisin molecules via a flexible glycine/serine linker to facilitate and accelerate pore formation. (3) Conjugation to a 'warhead', e.g. PMBN, EDTA, to penetrate the membrane of gram negative bacteria. (4) Conjugation to a fluorophore so study the peptide dynamics and for high throughput screenings. (5) Linkage to other antibiotics to create a combination drug.

In conclusion, the potential applications of ncAA incorporation into nisin are vast and bear a tremendous potential for bioengineering approaches. Overcoming the obstacle of leak expression through internal methionines and establishing *E. coli* as expression host for nisin was therefore only a first modest step into the direction of turning nisin applicable in medicine. Clearly, further research is necessary to figure out if a ncAA can fulfill the desired goals.

E Appendix

E.1 Material

E.1.1 Consumables

All consumables (reaction cups, plastic dishes, pipette tips, falcon tubes, electroporation cuvettes etc.) were purchased from Biozym Biotech (Austria), BD Bioscience (United States), Eppendorf (Germany), Peqlab (Germany), or Sarstedt (Germany).

E.1.2 Chemicals

All required chemicals were obtained from Merck (Germany), Roth (Germany) and Sigma-Aldrich (Germany), unless otherwise stated.

E.1.3 DNA

E.1.3.1 Primer sequences

Primers were ordered at Eurofins (Luxembourg).

Primer name	Function	Primer sequence (5‘-3‘)
AmpR (#180)	Sequencing of pScreen	CTGTCAGACCAAGTTTACT
InsertNdeI_pETDuet (#468)	Insert NdeI to cut out His6-Tag	GATCGACATATGAGCACCAAAGATTTC
M17X_*nisA*_fw	Introduction of NNK mutation at position M17	GGTTGTAAAACTGGTGCTCTTNNKGGTTGTAAT
M17X_*nisA*_rev	Introduction of NNK mutation at position M17	AGAGCACCAGTTTTACAACCTGG
M17H_*nisA*_fw	M17H mutation *nisA*(co-LI)	GGTTGTAAAACTGGTGCTCTTCATGGTTGTA
M17W_*nisA*_fw	M17W mutation *nisA*(co-LI)	GGTTGTAAAACTGGTGCTCTTTGGGGTTGTA

M17Y_*nisA*_fw	M17Y mutation *nisA*(co-LI)	GGTT-GTAAAACTGGTGCTCTTTATGGTT-GTA
M17C_*nisA*_fw	M17C mutation *nisA*(co-LI)	GGTTGTAAAACTGGTGCTCTTT-GTGGTTGTA
M17E_*nisA*_fw	M17E mutation *nisA*(co-LI)	GGTTGTAAAACTGGTGCTCTT-GAAGGTTGTA
M17T_*nisA*_fw	M17T mutation *nisA*(co-LI)	GGTT-GTAAAACTGGTGCTCTTACAGGTT-GTA
M17I_*nisA*_fw	M17I mutation *nisA*(co-LI)	GGTT-GTAAAACTGGTGCTCTTATTGGTT-GTA
M21K_nisA(wt)_fw	Introduce M21K mutation in *nisA*(wt)	AGCTCTGATGGGTTGTAACAA-GAAAACAGC
M21K_nisA(wt)_rev	Introduce M21K mutation	GTTACAACCCATCAGAGCT
nisA(co-Ec)_TAA_Xho1_rev	Introduce stop codon and XhoI site at the end of *nisA*(co-Ec)	GTGGTGCTCGAGTTATTT-GCTAACATGAATGCT
nisA(co-Ec)_fw	Fw primer for introduction of stop and XhoI into *nisA*(co-Ec)	GATCGACATATGGGTAGC
NisT(co-ec)_rev	Amplify NisT oligonucleo-tide	CGATCAAGCTTTCATTCATC
NisT(co-ec)_fw	Amplify NisT oligonucleo-tide	GATCGCCATGGATGAAGTG
NisT(co-ec)_1_fw	Sequencing of pETDuet	GAGCGAGAATAACATTAGC
pET21a_His6_PLrigid_*nisA*_*egfp*_seq1	Sequencing of pET21a	ATTCGCCACAACATTGAA
pET21a_His6_PLrigid_*nisA*_*egfp*_seq2	Sequencing of pET21a	TTTATTTTTCTAAATACA
pET21a_His6_PLrigid_*nisA*_*egfp*_seq3	Sequencing of pET21a	AGACAGATCGCTGAGATA

pET21a_His6_PLrigid_ *nisA*_*egfp*_seq4	Sequencing of pET21a	GTATTACCGCCTTTGAGT
pET21a_His6_PLrigid_ *nisA*_*egfp*_seq5	Sequencing of pET21a	CGTATCGGTGATTCATTC
pET21a_His6_PLrigid_ *nisA*_*egfp*_seq6	Sequencing of pET21a	TGAGATATTTATGCCAGC
pNZ_fw (#61)	Sequencing of pScreen	CATGCAGGAATTGACGATTT
pNZ_rev (#62)	Sequencing of pScreen	TATCAATCAAAGCAACACGTGC
pNZ_Primer 1 (#152)	Sequencing of pScreen	CATAATCGTTAAAACAGGCG
pNZ_Primer 2 (#153)	Sequencing of pScreen	GCTCGCGTTTTTAGAAGGAT
pNZ_Primer 3 (#154)	Sequencing of pScreen	TGAATAAATAAAAGCCCCCCTG
pNZ_Primer 4.2 (#179)	Sequencing of pScreen	CACGTGTTGCTTTGATTGATAG
pNZ_Primer 5 (#156)	Sequencing of pScreen	TTCAAGTAGTCGGGGATGTC
pNZ_Primer 6 (#204)	Sequencing of pScreen	CATGCAGGAATTGACGATTT
PS1 (#28)	Fw primer for Overlap Extension PCR	AGGGCGGCGGATTTGTCC
PS2 (#29)	Rev primer for Overlap Extension PCR	GCGGCAACCGAGCGTTC
TAG5_*nisA*(co-Ec)_fw	Introduce mutation TAG5	TCCGCGTATTACCAG-CATTTAGCTGTGTAC
TAG5_*nisA*(co-Ec)_rev	Introduce mutation TAG5	AATGCTGGTAATACGCGGACTTG
TAG8_*nisA*(co-Ec)_fw	Introduce mutation TAG8	TACCAGCATT-AGCCTGTGTTAGCCGGGTTG
TAG8_*nisA*(co-Ec)_rev	Introduce mutation TAG8	ACACAGGCTAATGCTGGTAATAC
TAG12_*nisA*(co-Ec)_fw	Introduce mutation TAG12	CCTGTGTACACCGGGTTGTTAGAC-CGGTGC
TAG12_*nisA*(co-Ec)_rev	Introduce mutation TAG12	ACAACCCGGTGTACACAGGCTAA
TAG13_*nisA*(co-Ec)_fw	Introduce mutation TAG13	GTGTACACCGGGTTGTAAA-TAGGGTGCACT
TAG13_*nisA*(co-Ec)_rev	Introduce mutation TAG13	TTTACAACCCGGTGTACACAGGC

TAG17_*nisA*(co-Ec)_fw	Introduce mutation TAG17	TTGTAAAACCGGTGCACTG-TAGGGTTGTAA
TAG17_*nisA*(co-Ec)_rev	Introduce mutation TAG17	CAGTGCACCGGTTTTACAACCCG
TAG22_*nisA*(co-Ec)_fw	Introduce mutation TAG22	ACTGATGGGTTGTAATATGTAGAC-CGCAAC
TAG22_*nisA*(co-Ec)_rev	Introduce mutation TAG22	CATATTACAACCCATCAGTGCAC
TAG29_*nisA*(co-Ec)_fw	Introduce mutation TAG29	AACCGCAACCTGTCATTGCTAGAT-TCATGT
TAG29_*nisA*(co-Ec)_rev	Introduce mutation TAG29	GCAATGACAGGTTGCGGTTTTCA
TAG32_*nisA*(co-Ec)_fw	Introduce mutation TAG32	CTGTCATTGCAGCATTCATTAGAG-CAAAGG
TAG32_*nisA*(co-Ec)_rev	Introduce mutation TAG32	ATGAATGCTGCAATGACAGGTTG
M17WM21K_TAG22_ *nisA*(co-Ec)_fw	Introduce mutation TAG22	ACTGTGGGGTTGTAATAAGTAGAC-CGCAAC
M17WM21K_TAG22_ *nisA*(co-Ec)_rev	Introduce mutation TAG22	CTTATTACAACCCCACAGTGCAC
M17WM21K_TAG29_ *nisA*(co-Ec)_rev	Introduce mutation TAG29	GCAATGACAGGTTGCGGTTTTCT
M17WM21K_*nisA*(wt)_ fw	Introduce M17WM21K mutation into *nisA*(wt)	GAGCTCTGTGGGGTTGTAACAA-GAAAACAG
M17WM21K_*nisA*(wt)_ rev	Introduce M17WM21K mutation into *nisA*(wt)	GTTGCTGTTTTCTT-GTTACAACCCCACAGA
TAG22_*nisA*(wt)_fw_M17WM21K	Introduce mutation TAG22 into M17WM21K_*nisA*(wt)	CTGTGGGGTTGTAACAAGTAGA-CAGCAACT
TAG22_*nisA*(wt)_rev_M17WM21K	Introduce mutation TAG22 into M17WM21K_*nisA*(wt)	CTTGTTACAACCCCACAGAGCTC
TAG29_*nisA*(wt)_fw_M17WM21K	Introduce mutation TAG29 into M17WM21K_*nisA*(wt)	ACAGCAACTTGTCATTGTTAGAT-TCACGTA
TAG29_*nisA*(wt)_rev_M17WM21K	Introduce mutation TAG29 into M17WM21K_*nisA*(wt)	ACAATGACAAGTTGCTGTTTTCT

TAG32_*nisA*(wt)_fw_M17WM21K	Introduce mutation TAG32 into M17WM21K_*nisA*(wt)	TGTCATTGTAGTATTCACTAGAG-CAAAGGC
TAG32_*nisA*(wt)_rev_M17WM21K	Introduce mutation TAG32	GTGAATACTACAATGACAAGTTG

E.1.3.2 Oligonucleotide sequences

Oligonucleotides were ordered at Eurofins (Luxembourg), GeneArt Gene Synthesis (Germany) or at Ella Biotech (Germany).

Oligonucleotide name	**Oligonucleotide sequence (5‘-3‘)**
M17WM21K_*nisA*(co-Ec)_fw	GTACCGGTGCACTGTGGGGTTGTAATAAGAAAACCGCAAC-CTGTCATTGC
M17WM21K_*nisA*(co-Ec)_rev	GATCATGCGGCCGCCTTTGCTAACATGAATGCTG-CAATGACAGGTTGCGG
M21K_*nisA*(co-LI)_fw	GTCGGTGCTAGCCCACGTATTACTTCAATTTCACTTT-GTACTCCAGGTTGTAAAACTGGTGCTCTTATGGGTTGTAAT
M21K_*nisA*(co-LI)_rev	GCCGTTCAAAGAAAGCTTATCATTTTGAAACATGAATT-GAACAATGACAAGTAGCAGTTTTCTTATTACAACCCATAAGAG-CAC
M17WM21K_*nisA*(co)_fw	GTACCGGTGCACTGTGGGGTTGTAATAAGAAAACCGCAAC-CTGTCATTGC
M17WM21K_*nisA*(co)_rev	GATCATGCGGCCGCCTTTGCTAACATGAATGCTG-CAATGACAGGTTGCGG
nisA(co-Ec)	GATCGACATATGGGTAGCAGCCATCAC-CATCATCATCATAGCCAAGATCCGATGAGCACCAAAGAT-TTCAATCTGGATCTGGTTAGCGTGAGCAAAAAAGATAGCGGTG-CAAGTCCGCGTATTACCAGCATTAGCCTGTGTACACCGGGTT-GTAAAACCGGTGCACTGATGGGTTGTAATATGAAAACCGCAAC-CTGTCATTGCAGCATTCATGTTAGCAAAGGCGGCCGCGATCG
nisT(co-Ec)	GATCGCCATGGATGAAGTGAAAGAGTTTACCAGCAAACAG-TTTTTTAACACCCTGCTGACCCTGCCGAGCACACTGAAACTGAT-TTTTCAACTGGAAAAACGC-TATGCCATCTATCTGATTGTTCTGAATGCAATTACCGCATTT-GTTCCGCTGGCAAGCCTGTTTATCTATCAGGATCTGATTAA-TAGCGTGTTAGGTAGCGGTCGTCATCTGATCAACATTATCATCAT CTATTTTATCGTGCAGGTCATTACCACCGTTCTGGGTCAGCTG-

	GAAAGCTATGTTAGCGGTAAATTTGATATGCGTCTGAGC- TATAGCATTAACATGCGCCTGATGCGTACCACCAGTAGCCTG- GAACTGAGCGATTATGAACAGGCAGATATGTATAACATCATCGA- GAAAGTTACCCAGGACAGCACCTATAAAC- CGTTTCAGCTGTTTAATGCCATTATTGTTGTGCTGAG- CAGCTTTATTAGCCTGCTGAGTAGCCTGTTTTTTATCGGCAC- CTGGAATATTGGTGTT- GCAATTCTGCTGCTGATTGTGCCGGTTCTGAGCCTGGTTCTGTTT CTGCGTGTTGGCCAGCTGGAATTTCTGATTCAGTGGCAGCGTG- CAAGCAGCGAACGTGAAACCTGGTATATTGTTTATCTGCTGAC- GCACGATTTCAGCTTCAAAGAAATTAAGCTGAACAACATCAG- CAACTATTTCATCCACAAATTCGGCAAACTGAA- GAAGGGCTTTATTAACCAGGATCTGGCAATTGCAC- GCAAAAAAACCTATTTCAACATCTTCCTGGACTTTATCCTGAAC- CTGATTAACATCCTGACCATCTTTGCAATGAT- TCTGAGCGTTCGTGCCGGTAAACTGCTGATCGG- TAATCTGGTTAGCCTGATTCAGGCAATTAGCAAAATTAACAC- CTATAGCCAGACCATGATCCAGAACATCTACATTATCTATAACAC- CTCGCTGTTTATGGAACAACTGTTCGAGTTTCTGAAACGTGAAA- GCGTTGTGCATAAAAAGATCGAAGATACCGAAATCTGCAACCAG- CATATTGGCACCGTTAAAGTTATTAACCTGAGC- TATGTTTACCCGAACAGCAATGCATTT- GCCCTGAAAAACATTAATCTGAGCTTTGAAAAAGGTGAGCTGAC- CGCAATTGTTGGTAAAAATGGTAGTGGTAAAA- GCACCCTGGTGAAAATTATCAGCGGTCTG- TATCAGCCGACAATGGGTATTATTCAGTATGATAAAATGCGCAG- CAGCCTGATGCCGGAAGAATTTTATCAGAAAAA- TATCTCCGTGCTGTTCCAGGACTTTGTGAAATATGAACTGAC- CATTCGCGAAAATATTGGTCTGAGCGATCTGAGCAGCCAGTGG- GAAGATGAAAAAATCATTAAAGTGCTGGATAACCTGGGCCTT- GATTTTCTGAAAACCAATAATCAGTACGTCCTGGATACCCAG- TTAGGCAATTGGTTTCAA- GAAGGTCATCAGCTGAGCGGTGGCCAGTGGCAGAAAATTGCAC- TGGCACGTACATTTTTCAAAAAGGCCAGCATTTATATCCTG- GATGAACCGAGCGCAGCACTGGACCCGGTTGCAGAAAAA- GAAATCTTTGATTATTTTGTGGCCCTGAGCGAGAATAACATTAG- CATTTTTATCAGCCATAGCCTGAATGCAGCACGTAAA- GCAAACAAAATTGTGGTGATGAAAGATGGCCAGGTTGAA- GATGTGGGTAGCCATGATGTTCTGCTGCGTCGTTGTCAG- TATTATCAAGAACTGTATTATAGCGAGCAGTACGAGGATAAC- GATGAATGAAAGCTTGATCG

E.1.3.3 Plasmids

Plasmid	Characteristic	Reference
pScreen_final_*ccdB*	*mCherry*, *ccdB box*, Amp^R, Ery^R	Wagner lab

pIL3BTC	*nisBTC*, Ery^R	van Heel et al. (2013) (104)
pNZ_*nisP*(8K)	*nisP*, Cam^R	Kuipers lab
pSEVA_silent	*ccdB*, Kana^R	Standard European Vector Architecture (SEVA)
pET21a_*nisA*(wt)	*nisA*(wt), Amp^R	David Peterhoff (Wagner lab)
pETDuet	dual T7 expression cassette, Amp^R	Merck (Merck)
pRSFDuet	dual T7 expression cassette, Kana^R	Merck (Merck)
pTB290	*pylRS*(Y384F) (co-Ec), Cam^R	Dr. Tobias Baumann (Budisa lab, TU Berlin)

E.1.4 Enzymes, proteins and other

Name	Supplier
100bp Standard	New England Biolabs (Cat. No.: N3231)
1kb Standard	New England Biolabs (Cat. No.: N3232)
Agarose	Bio&Sell (Cat. No.: BS20.46.500)
BglII	New England Biolabs (Cat. No.: R0144S)
Calf Intestinal Alkaline Phosphatase	New England Biolabs (Cat. No.: M0290L)
Coomassie Brilliant Blue R-250	AppliChem (Cat. No.: A1092)
10x CutSmart Buffer	New England Biolabs (Cat. No.: B7204S)
dNTPs	New England Biolabs (Cat. No.: NO447)
Gel Loading Dye, Purple (6X)	New England Biolabs (Cat. No.: B7024S)
GeneJET Plasmid MiniPrep Kit	Thermo Scientific (Cat. No.: K0503)
GoTaq Green Master Mix	Promega (Cat. No.: M7121)
HindIII-HF	New England Biolabs (Cat. No.: R0104S)
His GraviTrap Talon	GE Healthcare (Cat. No.: 29-0005-94)
Low Molecular Weight Standard	New England Biolabs (Cat. No.: N0474S)

M17 broth	Sigma-Aldrich (Cat. No.: 56156)
Illustra NAP-10 columns	GE Healthcare (Cat. No.: 170854-01)
NheI-HF	New England Biolabs (Cat. No.: R3131S)
Nisin from *L. lactis*	Sigma-Aldrich (Cat. No.: N5764)
Nisin A	Cayman Chemicals (Cat. No.: 16532) (german distributor: Biomol GmbH)
Nisin ZP	Handary (Code: 0304)
Precision Plus Protein Dual Xtra Standards	Bio Rad (Cat. No.: 161-0377)
Protease Inhibitor Cocktail cOmplete™ ULTRA Tablets, Mini, *EASYpack*	Sigma-Aldrich/Roche (Cat. No.: 000000005892970001)
5x Phusion HF Buffer	New England Biolabs (Cat. No.: B0518S)
Phusion HF DNA Polymerase	New England Biolabs (Cat. No.: 0530L)
QIAGEN Plasmid Plus Midi Kit	QIAGEN (Cat. No.: 12945)
QIAquick Gel Extraction Kit	QIAGEN (Cat. No.: 28704)
Quick Ligation Kit	New England Biolabs (Cat. No.: M2200L)
SpeI	New England Biolabs (Cat. No.: R3133S)
T4 DNA Ligase	New England Biolabs (Cat. No.: M0202L)
T4 DNA Ligase Buffer	New England Biolabs (Cat. No.: B0202S)

E.1.5 Instruments

Name	Manufacturer
AlphaImager HP System	ProteinSimple
BioShake iQ thermomixer	Quantifoil Instruments GmbH
Centrifuge 5810R	eppendorf

Centrifuge 5417R	eppendorf
MicroPulser^{TM} Electroporator	Bio-Rad
Incubator	Heraeus Instruments
Incubation shaker Multitron Standard	InforsHT
Nano Drop ND-1000	Peqlab
PCR-thermocycler T100 gradient	Bio-Rad
PCR-thermocycler MyCycler	Bio-Rad
Rotixa 50 RS	Hettich Zentrifugen
SmartSpec Plus spectrophotometer	Bio-Rad
Infinite 200 microplate reader	Tecan

E.2 Plasmid maps

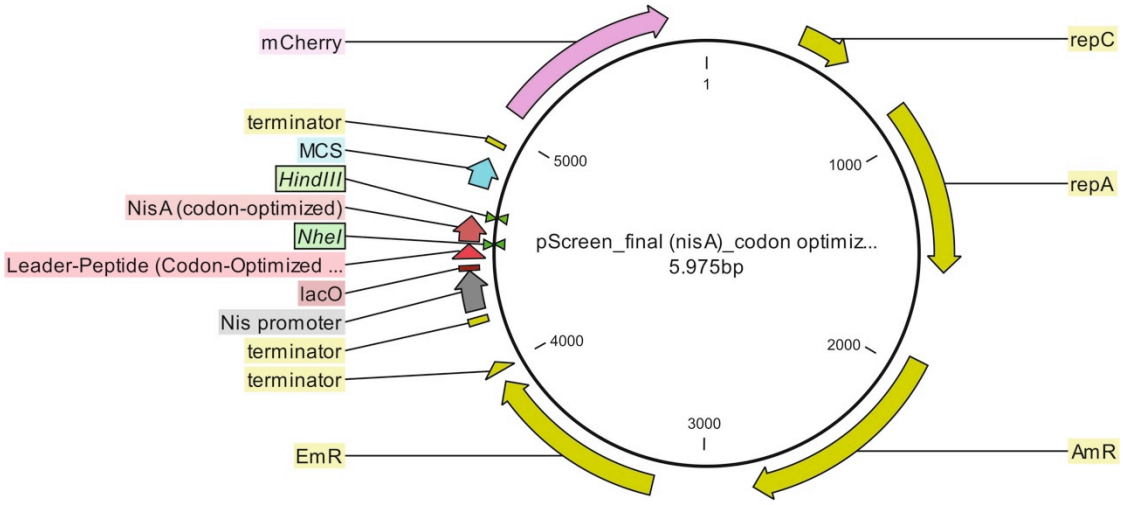

Plasmid map 1. pScreen_ *nisA*

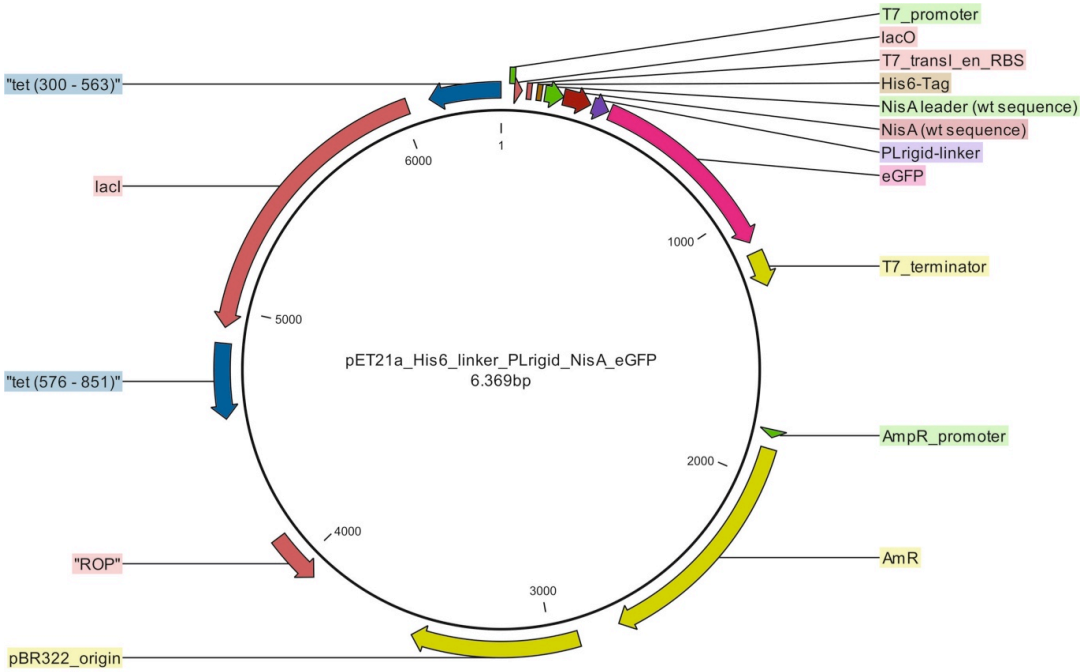

Plasmid map 2. pET_*nisA_egfp*

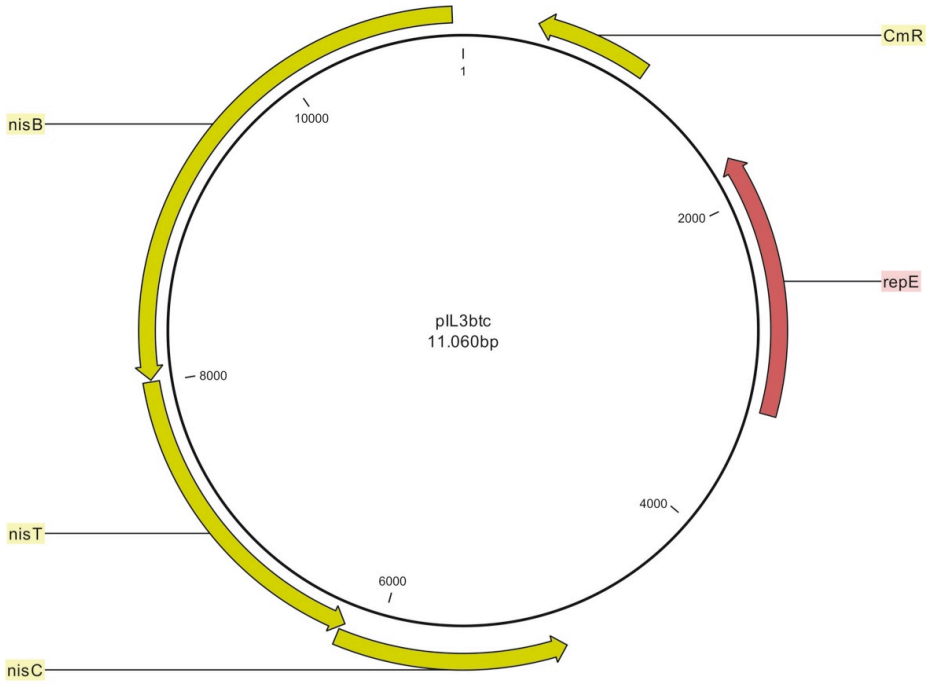

Plasmid map 3. pIL3BTC

Plasmid map 3. pET_*nisA*(here: wt)

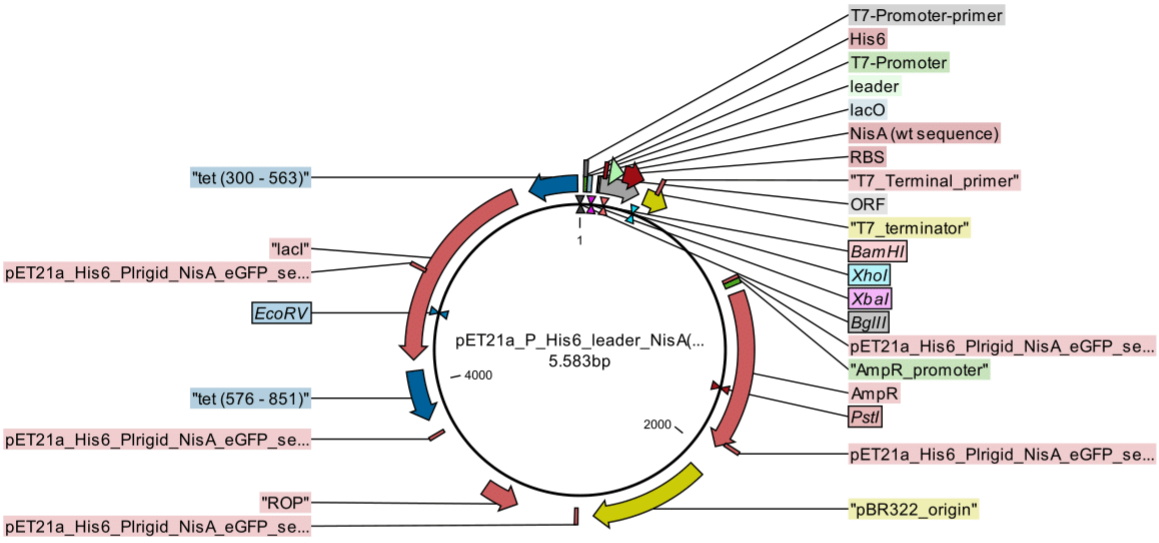

Plasmid map 4. pRSF_*nisBC*(co-Ec)

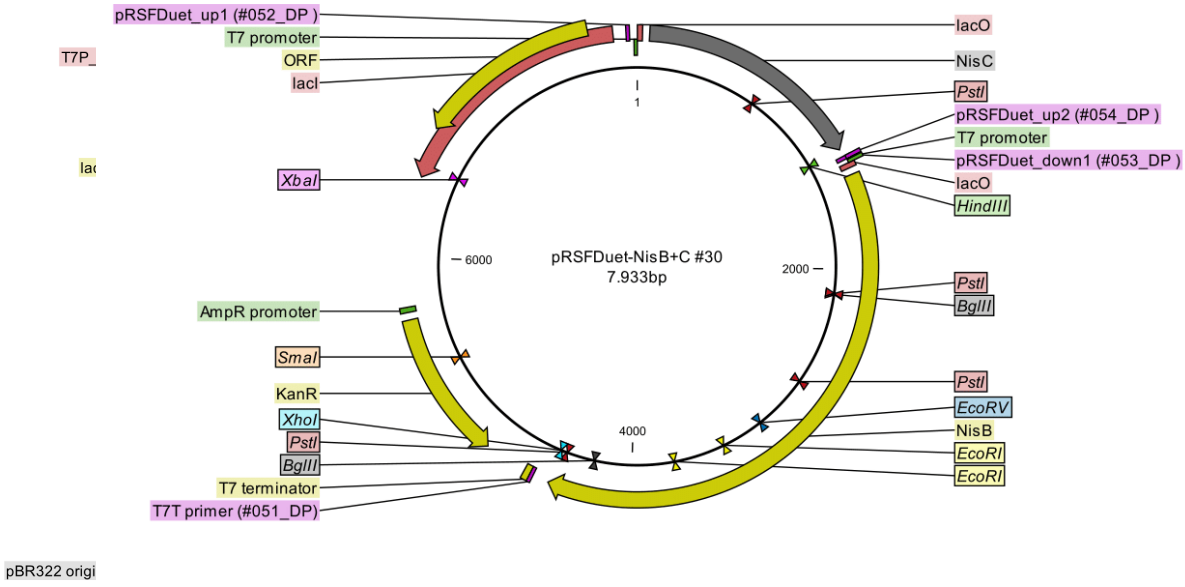

Plasmid map 5. pETDuet_His6_*nisAT*(co-Ec)

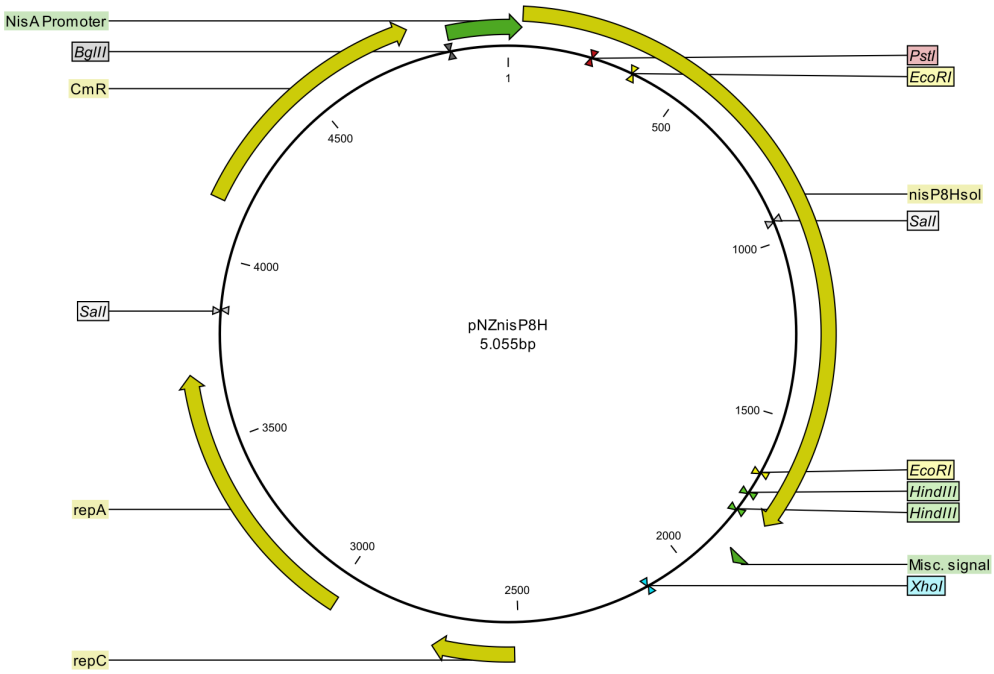

Plasmid map 6. pNZ_*nisP*

Plasmid map 7. pIL253

E.3 Supplementary data

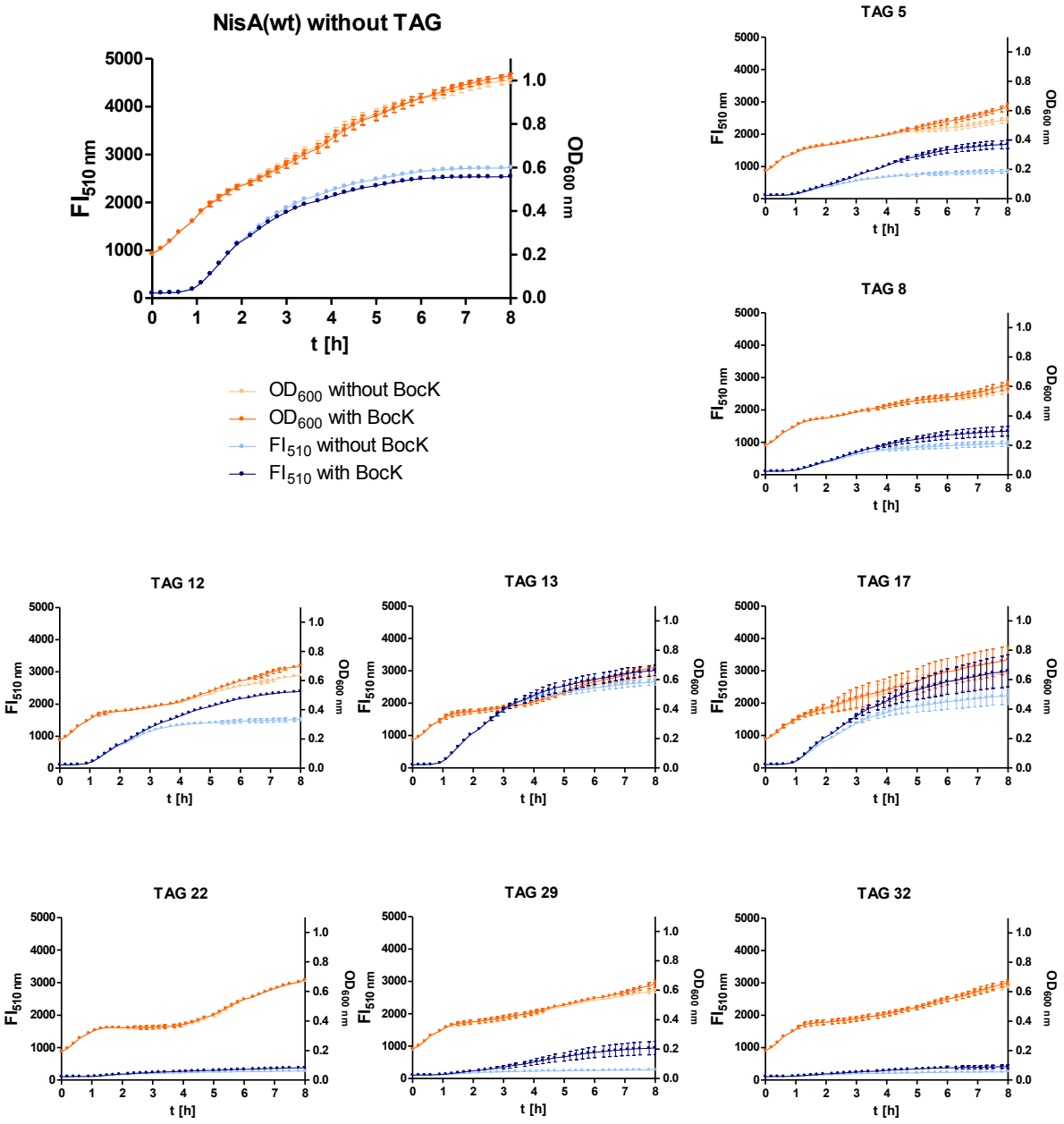

Supplementary Figure S1. OD and FI curves of NisA(wt). T7 Exp cells were transformed with pTB290 (orthogonal suppressor pair) and pET_*nisA*(wt)_*egfp*, which harbored an amber stop codon (TAG) at a selected position (as indicated above the diagrams). NisA(wt) without TAG served as control. Cultures were diluted to OD 0,2 after their growth rate was synchronized and expression was induced with IPTG and arabinose. BocK was added simultaneously. Addition of water served as negative control (-BocK). Bacterial growth and fluorescence from eGFP was monitored for 8 h with the Tecan Infinite Pro 200. Error bars indicate the SEM of three independent experiments.

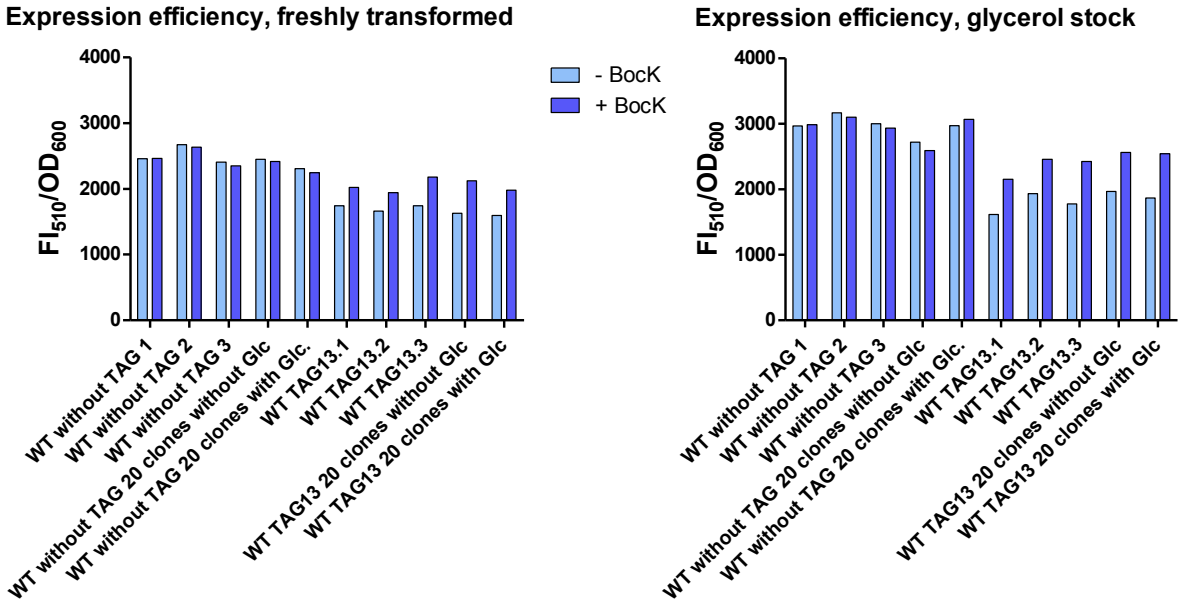

Supplementary Figure S2. Control experiment for amber suppression efficiency screening. T7 Exp cells were transformed with pTB290 (orthogonal suppressor pair) and pET_*nisA*(wt)_*egfp*. Cultures were diluted to OD 0,2 after their growth rate was synchronized and expression was induced with IPTG and arabinose. BocK was added simultaneously. Addition of water served as negative control (-BocK). Growth and fluorescence was monitored for 8 h with the Tecan Infinite Pro 200. Here, the FI values 6 h post induction are divided by the respective OD. The left diagram shows the results when bacterial clones were used to inoculate overnight cultures straight after transformation, while overnight cultures for the right diagram were inoculated from glycerol stocks. The first three groups are independent experiments (1, 2, 3, each performed in technical triplicates) with pET_*nisA*(wt)_*egfp* with NisA(wt) containing no TAG codon. Here, overnight cultures were inoculated from a single bacterial colony. Group number four and five are single experiments (performed in technical triplicates) with the same construct but with overnight cultures inoculated from 20 bacterial colonies. Once (group 4) no glucose was added to the medium of the overnight culture and once (group 5) this was done. Groups 6-12 show the same settings as groups 1-6, but with NisA(wt) harboring a TAG codon at position 13.

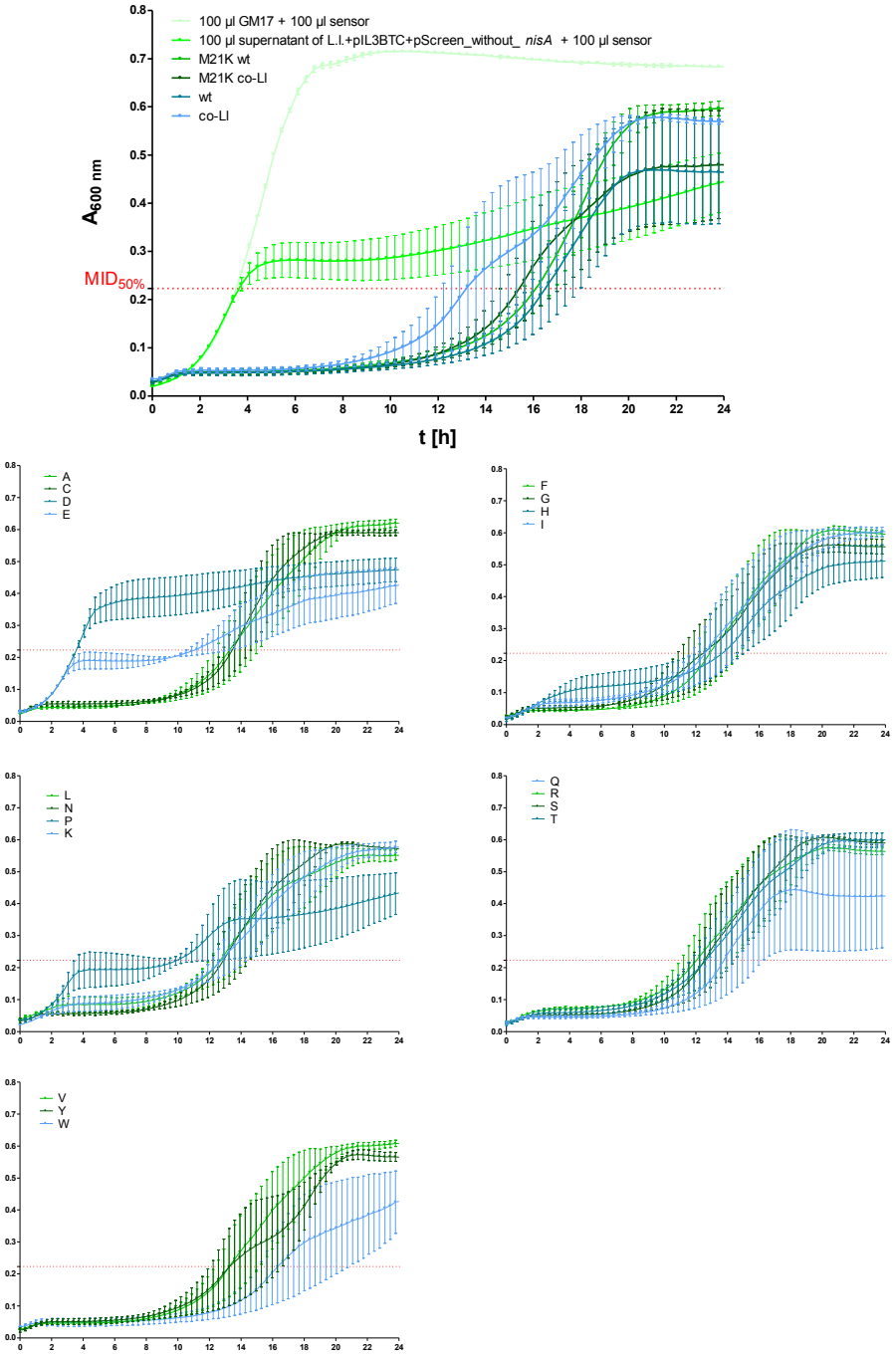

Supplementary Figure S3. Growth curves of the sensor *L. lactis* [pIL,pNZ] under the influence of cell-free supernatants of M17XM21K NisA(co-LI) expression cultures. The OD which corresponds to 50 % of the maximal OD of *L. lactis* [pIL,pNZ], supplemented with the cell-free supernatant of *L. lactis* (containing pIL3BTC and pScreen_without*nisA*), was determined and is indicated by the red dashed line. In the diagram on top all controls are shown. Each experiment was performed by mixing equal volumes (100 µl) of the sensor culture, diluted to OD 0,1, and cell-free supernatants of *L. lactis* (pIL3BTC and pScreen harboring the respective NisA variant) and subsequent measurement of the OD at 600 nm with the Tecan Infinite 200 Pro. The one letter code for abbreviation of amino acids shows by which M17 was replaced in pScreen_M17XM21K_*nisA*(co-LI) (five smaller diagrams). Error bars indicate SEM of three independent experiments.

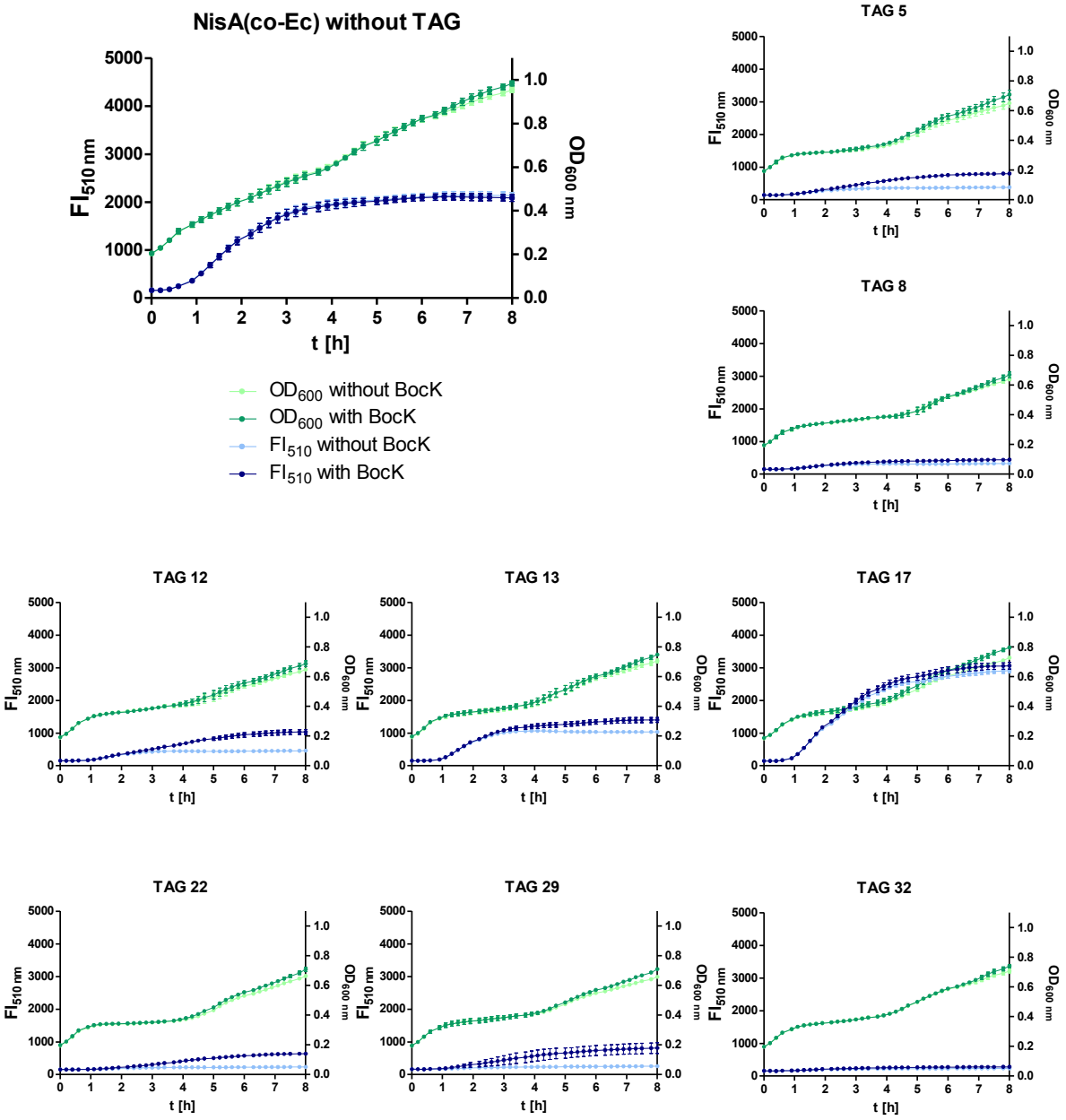

Supplementary Figure S3. OD and FI curves of NisA(co-Ec). Same experimental and evaluation conditions as for *Supplementary Figure S1* applied.

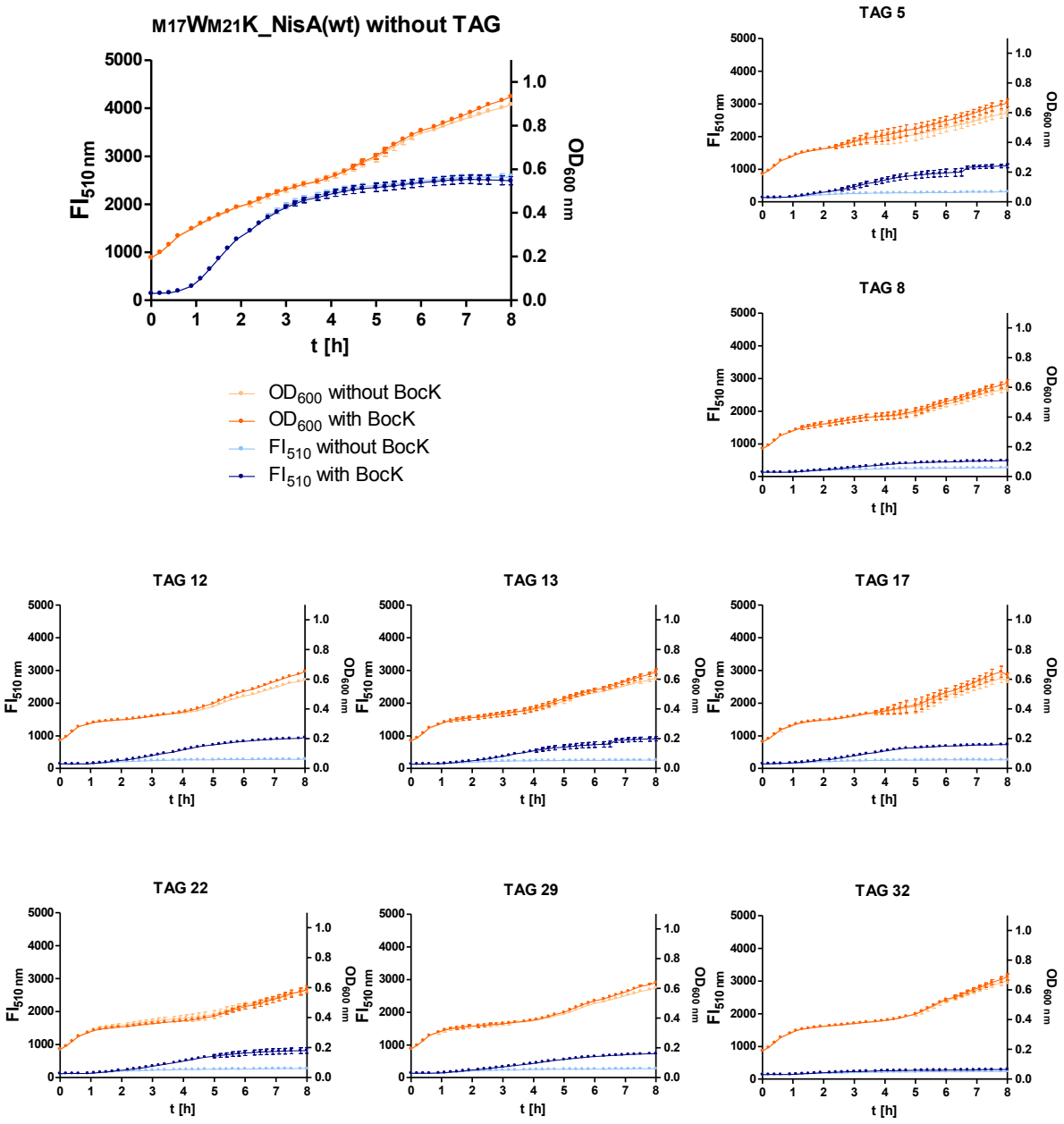

Supplementary Figure S4. OD and FI curves of M17WM21K NisA(wt). Same experimental and evaluation conditions as for *Supplementary Figure S1* applied.

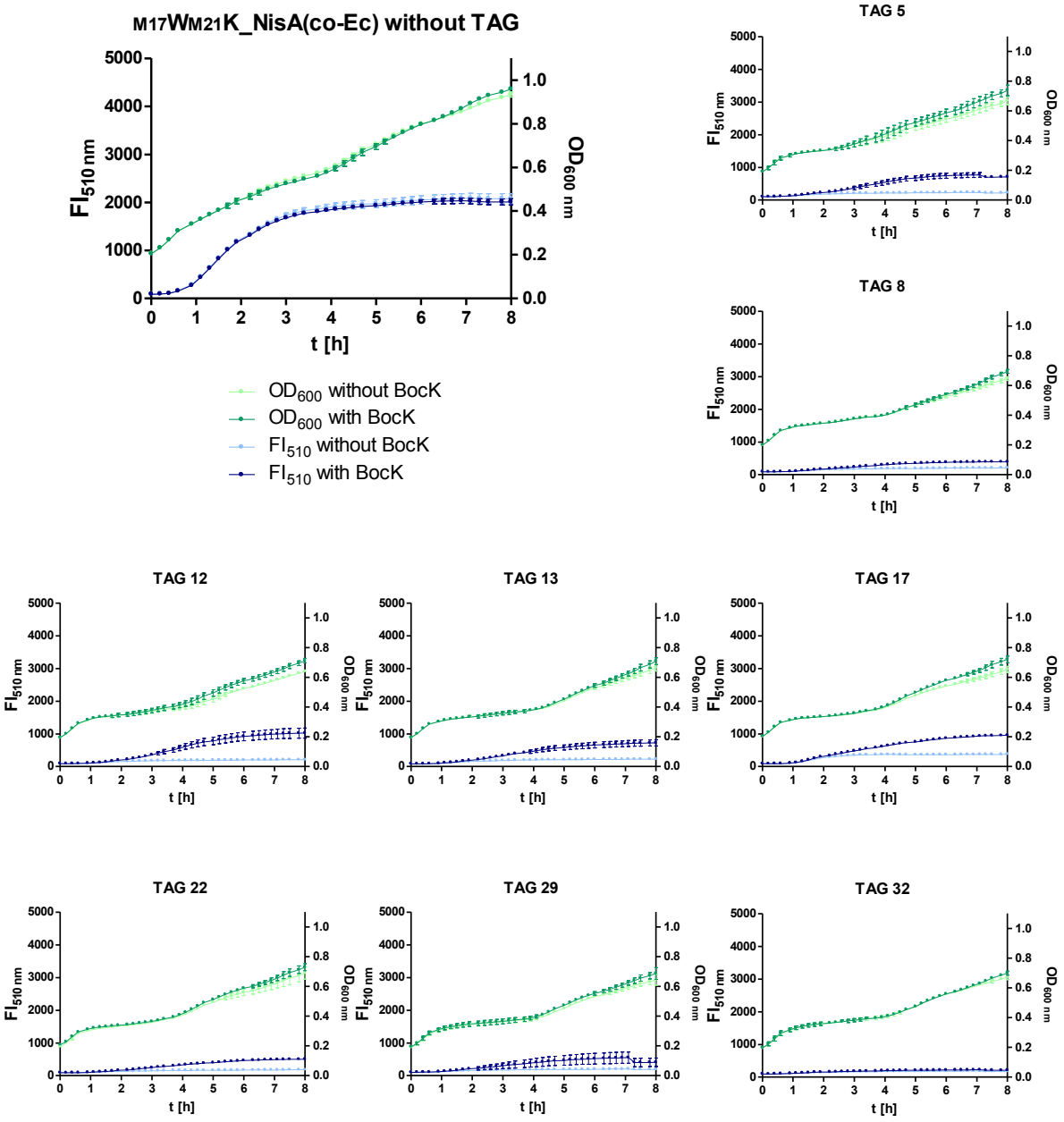

Supplementary Figure S5. OD and FI curves of M17WM21K NisA(wt). Same experimental and evaluation conditions as for *Supplementary Figure S1* applied.

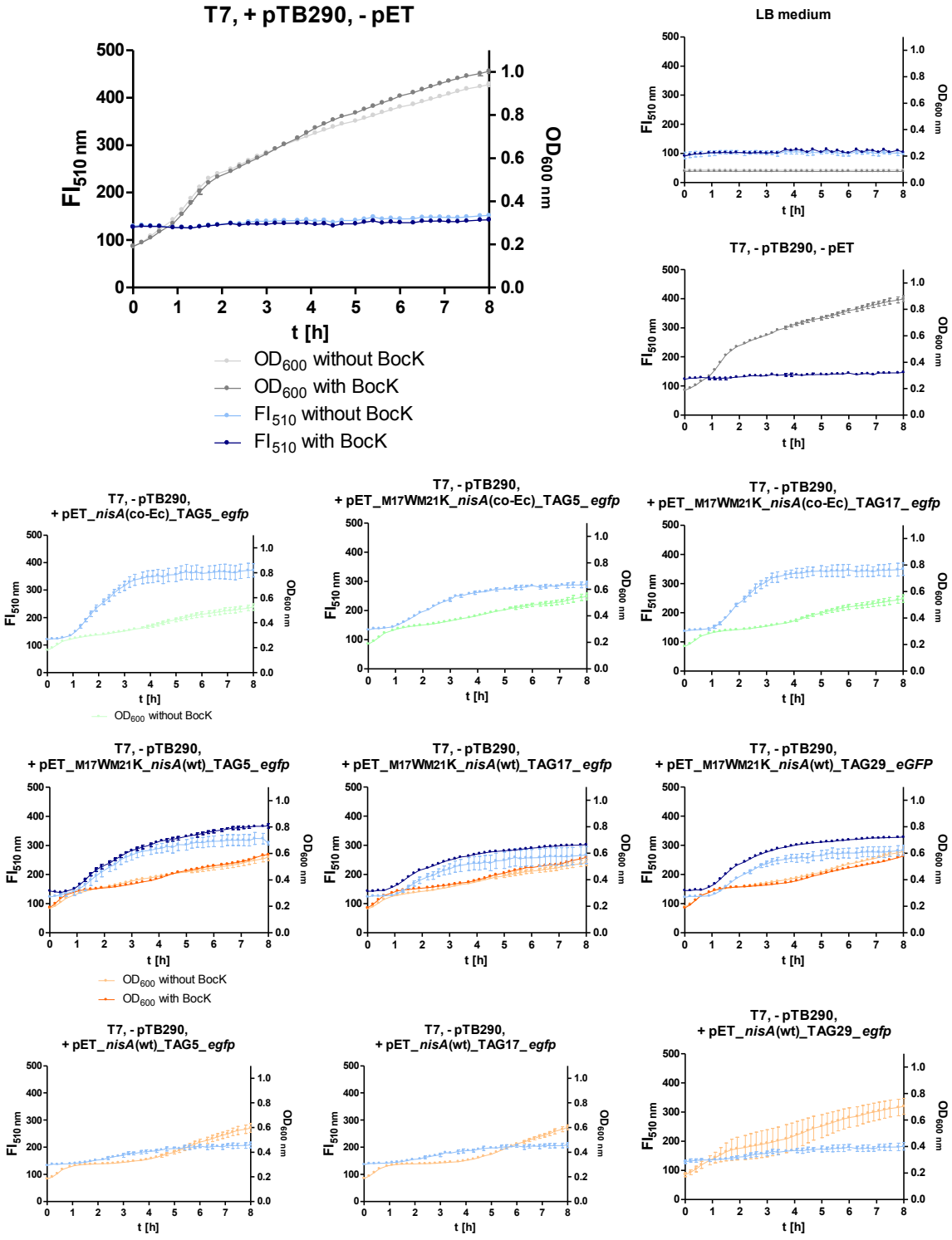

Supplementary Figure S6. Control experiments for the amber suppression efficiency screening. Tested plasmid combinations are indicated above the diagrams. Other than that, same experimental and evaluation conditions as for *Supplementary Figure S1* applied.

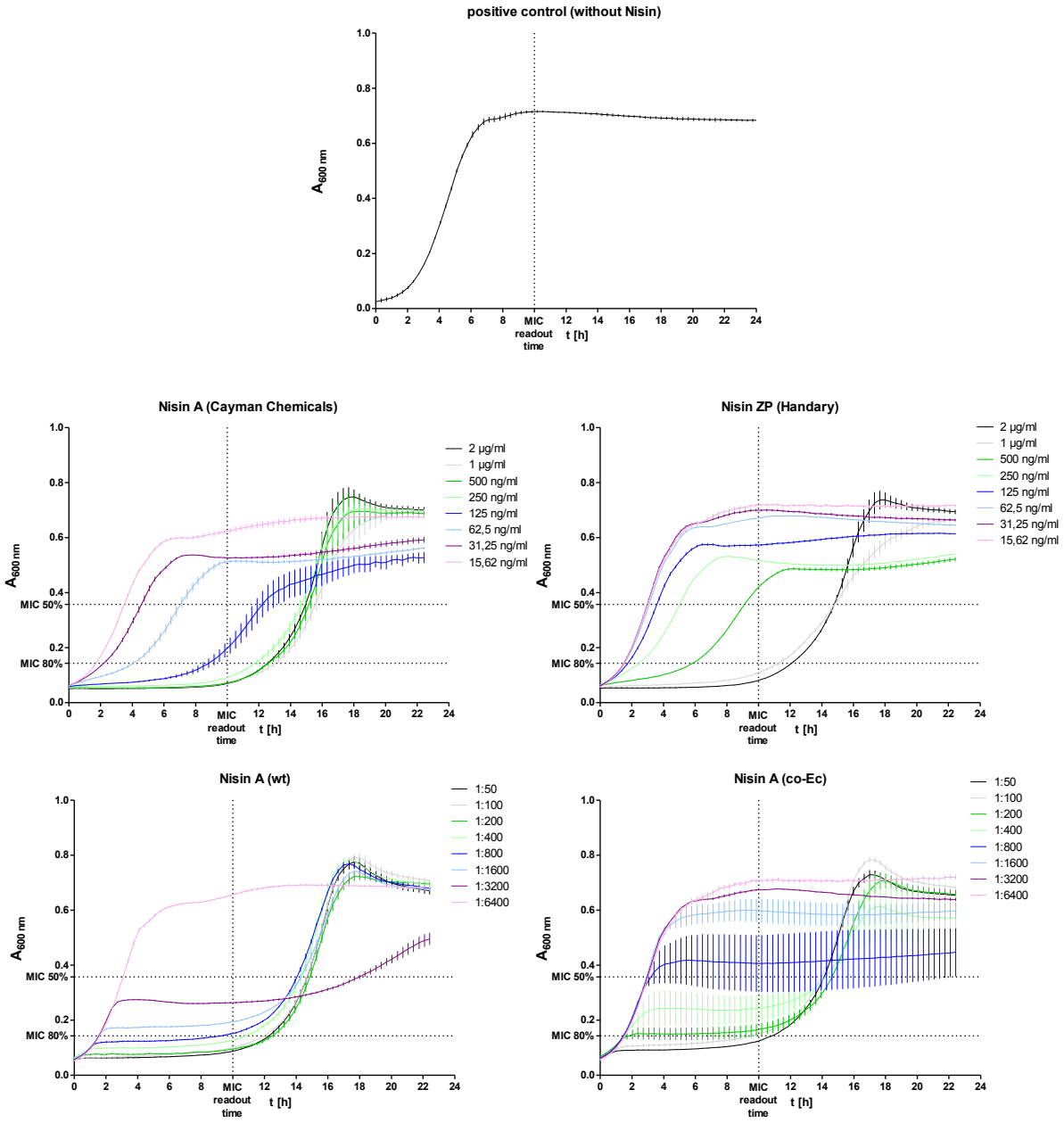

Supplementary Figure S7. Growth curves for the MIC/MID assay to determine the nisin concentration. Each experiment was performed by mixing equal volumes (100 µl) of the sensor culture (*L. lactis* [pIL,pNZ]) diluted to OD 0,1 and samples to be tested. Subsequent OD measurement was done with the Tecan Infinite 200 Pro. A positive control (growth control) with the sensor strain *L. lactis* [pIL,pNZ] supplemented with plain GM17 medium was made to determine the ideal MID readout time. As bacteria had maintained a steady growth rate for ca. 3 h, the readout time was set to 10 h (as indicated on the x-axis). The two diagrams in the middle show the growth curves of the MIC assay, where a dilution series of the two commercial nisin variants (Nisin A from Cayman Chemicals and Nisin ZP from Handary) was tested. The two diagrams on the bottom show growth curves of the MID assay, where a dilution series of HPLC purified samples of nisin A expressed in *E. coli* (once with the wt and once with the co-Ec sequence) was tested. Error bars indicate the SEM.

E.4 Abbreviations

Amino acids were abbreviated with the one letter code according to IUPAC criteria.

A	Adenine, alanine	F	Farad
aa	amino acid	F	phenylalanine
aaRS	aminoacyl-tRNA-synthetase	FAO	Food and Agriculture Organization of the United Nations
$Amp^{(R)}$	ampicillin (resistance)	FI	fluorescence intensity
A.U.	arbirtary unit	fMet	*N*-formylmethionine
b	bases	fw	forward
BLAST	Basic Local Alignment Search Tool	G	guanine
BocK	N-Boc L-lysine	g	gramm, g-force
bp	base pair	*glnS*	glutamate tRNA ligase gene
C	cytosine	Glu, E	glutamate
$Cam^{(R)}$	chloramphenicol (resistance)	(e)GFP	(enhanced) green fluorescent protein
Cat. No.	catalog number	*(e)gfp*	(enhanced) green fluorescent protein gene
ccdB	control of cell death B gene	h	hour
CIP	Calf Intestinal Alkaline Phosphatase	HF	high-fidelity
co-Ec	codon optimized DNA sequence for *E. coli*	His6-tag	protein tag with the amino acid sequence $(H)_6$
co-Ll	codon optimized DNA sequence for *L. lactis*	HNSCC	head and neck squamous cell carcinoma
DNA	deoxyribonucleic acid	IPTG	isopropyl β-D-1-thiogalactopyranoside
dNTP	deoxynucleotide triphosphate	K	lysine
dsDNA	double stranded DNA	$Kana^{(R)}$	kanamycin (resistance)
E. coli	*Escherichia coli*	ko	knockout
EDTA	ethylenediaminetetraacetic acid	l	liter
Ery	erythromycin	LB	Lysogeny broth

lacI	gene of the inhibitor protein (lacI) of the lac operon	pBR322/p15a/ RSF ori	pBR322/p15a/RSF origin of replication
lacO	regulatory DNA-binding site for lacI	PBS	phosphate buffered saline
leader	23 amino acid long nisin leader peptide (compare A.5.1)	PEG	polyethylene glycol
L. lactis	*Lactococcus lactis* NZ9000	PLrigid	rigid α-helical linker with the sequence $(EAAAR)_4$ (compare (100))
L. lactis [pIL, pNZ]	*L. lactis* harboring pIL253 and pNZ_*nisP*	PROVEAN	Protein Variation Effect Analyzer
m	meter	PTM	post-translational modification
M	molar, methionine	PylRS(Y384F)	pyrrolysyl-tRNA-synthetase with an Y384F mutation
MCS	multiple cloning site	RT-PCR	reverse transcription polymerase chain reaction
M-aaS	methionine amino acid substitution	RBS	ribosome binding-site
MIC/MID	minimal inhibitory concentration/dilution assay	rev	reverse
min	minute	rpm	rounds per minute
mRNA	messenger RNA	rRNA	ribosomal RNA
N	asparagine	S	mass unit (non-linear Svedberg centrifugation coefficient)
ncAA	non-canonical amino acid	sec	second
nisA/B/C/T/P	nisin A/B/C/T/P gene	SD	standard deviation, Shine-Dalgarno sequence
nisA/B/C/T/P	nisin A/B/C/T/P protein	SDS-PAGE	sodium dodecyl sulfate polyacrylamide gel electrophoresis
nisA	prepeptide of nisin A (prenisin A)	SEM	standard error of the mean
nisB	lantibiotic dehydratase	*Staph. aureus*	*Staphylococcus aureus*
nisC	nisin cyclase	T	thymine, threonine
nisP	nisin leader peptidase	T7	promoter sequence for T7 RNA polymerase
nisT	ATP binding casette transporter	T7 Exp	T7 Express I^q cells
OM	outer membrane	TAG	amber stop codon

TCA	trichloroacetic acid	w/v	weigth per volume
TIR	translation initiation rate	w/w	weigth per weigth
$tRNA^{(Pyl)}$	(pyrrolysyl-) transfer RNA	WHO	World Health Organization
Trp promoter	tryptophan promoter	wt	wildtype DNA sequence
trunc. prod.	truncated products	Ω	Ohm
U	unit, uracile	[+BocK]	in the presence of BocK
V	volt	[-BocK]	in the absence of BocK
v/v	volume per volume		

E.5 List of figures

E.6 List of tables

E.7 Literature

1. Thermo Fisher Scientific. GeneOptimizer [Internet]. [cited 2018 Jan 11]. Available from: https://www.thermofisher.com/de/de/home/life-science/cloning/gene-synthesis/geneart-gene-synthesis/geneoptimizer.html

2. Salis HM. The ribosome binding site calculator. Methods Enzymol. 2011;498:19–42.

3. Heckenberg SGB, Brouwer MC, Van de Beek D. Bacterial meningitis. 1st ed. Vol. 121, Handbook of Clinical Neurology. Elsevier B.V.; 2014. 1361–1375 p.

4. Godemeier C. Penicillin. Dtsch Arztebl. 2006;103(September):2286.

5. Nobel Media AB. “Sir Alexander Fleming - Biographical.” 2014. p. [cited 2018 Jan 11]. http://www.nobelprize.org/nobel_prizes/medicine/la.

6. Ventola CL. The antibiotic resistance crisis: part 1: causes and threats. P T. 2015 Apr;40(4):277–83.

7. Arkadiusz Gladki (Author), Yiqun Wu (Author), Roger L. Chang (Author), Victor Kuete (Author), Markus Reise (Author) MP (Author). The application of antibacterial drug. Scientific Research Publishing, Inc., USA; 2016. 309 p.

8. WHO. Antibacterial Agents in Clinical Development - An analysis of the antibacterial clinical development pipeline, including tuberculosis. Who. Geneva; 2017.

9. Glenn T. WHO’s first global report on antibiotic resistance reveals serious, worldwide threat to public health [Internet]. WHO. 2014 [cited 2017 Feb 22]. p. www.who.int. Available from: http://www.who.int/mediacentre/news/releases/2014/amr-report/en/

10. Cassini A, Högberg LD, Plachouras D, Quattrocchi A, Hoxha A, Simonsen GS, et al. Attributable deaths and disability-adjusted life-years caused by infections with antibiotic-resistant bacteria in the EU and the European Economic Area in 2015: a population-level modelling analysis. Lancet Infect Dis. 2019;19(1):56–66.

11. ECDC. The bacterial challenge : time to react. Vol. 6 July 201, Reproduction. 2009. 42 p.

12. WHO. Antimicrobial resistance: global report on surveillance 2014. Geneva; 2014.

13. WHO. WHO_Europe _ Antimicrobial resistance - Data and statistics [Internet]. [cited 2017 Feb 22]. Available from: http://www.euro.who.int/en/health-topics/disease-prevention/antimicrobial-resistance/data-and-statistics

14. Rappuoli R, Bloom DE, Black S. Deploy vaccines to fight superbugs. Nature. 2017 Dec 14;552(7684):165–7.

15. Synpeptide Project. Synpeptide [Internet]. 2017 [cited 2017 Feb 22]. Available from: http://synpeptide.eu/

16. Hancock REW, Chapple DS. MINIREVIEW Peptide Antibiotics. Antimicrob Agents Chemother. 1999;43(6):1317–23.

17. da Costa JP, Cova M, Ferreira R, Vitorino R. Antimicrobial peptides: an alternative for innovative medicines? Appl Microbiol Biotechnol. 2015;99(5):2023–40.

18. Henninot A, Collins JC, Nuss JM. The Current State of Peptide Drug Discovery: Back to the Future? J Med Chem. 2017;acs.jmedchem.7b00318.

19. Reiners J, Abts A, Clemens R, Smits SHJ, Schmitt L. Stoichiometry and structure of a lantibiotic maturation complex. Sci Rep. 2017;7(January):42163.

20. Knerr PJ, van der Donk WA. Discovery, Biosynthesis, and Engineering of Lantipeptides. Annu Rev Biochem. 2012 Jul 7;81(1):479–505.

21. Piper C, Cotter PD, Ross RP, Hill C. Discovery of Medically Significant Lantibiotics. Curr Drug Discov Technol. 2009;6(0):1–18.

22. Khosa S, AlKhatib Z, Smits SHJ. NSR from Streptococcus agalactiae confers resistance against nisin and is encoded by a conserved nsr operon. Biol Chem. 2013;394(11):1543–9.

23. Alvarez-Sieiro P, Montalbán-López M, Mu D, Kuipers OP. Bacteriocins of lactic acid bacteria: extending the family. Appl Microbiol Biotechnol. 2016;100(7):2939–51.

24. Cotter PD, Ross RP, Hill C. Bacteriocins - a viable alternative to antibiotics? Nat Rev Microbiol. 2013;11(2):95–105.

25. Rogers LA, Whittier EO. Limiting factors in the lactic fermentation. J Bacteriol. 1928;16(4):211–29.

26. Abts A, Mavaro A, Stindt J, Bakkes PJ, Metzger S, Driessen AJM, et al. Easy and rapid purification of highly active nisin. Int J Pept. 2011;2011.

27. Breukink E, De Kruijff B. The lantibiotic nisin, a special case or not? Biochim Biophys Acta - Biomembr. 1999;1462(1–2):223–34.

28. Abbas HT, Kylä-Nikkilä K, Ra R, Saris PEJ. Nisin induction without nisin secretion. Microbiology. 2006;152(5):1489–96.

29. Yuan J, Zhang Z-Z, Chen X-Z, Yang W, Huan L-D. Site-directed mutagenesis of the hinge region of nisinZ and properties of nisinZ mutants. Appl Microbiol Biotechnol. 2004 Jun 1;64(6):806–15.

30. S M, ER T, BB B, JD H. Docking and molecular dynamics simulations of the ternary complex nisin2:lipid II. Nat Publ Gr. 2016;(August 2015):1–11.

31. Shin JM, Gwak JW, Kamarajan P, Fenno JC, Rickard AH, Kapila YL. Biomedical applications of nisin. J Appl Microbiol. 2016;120(6):1449–65.

32. O'Sullivan JN, O'Connor PM, Rea MC, O'Sullivan O, Walsh CJ, Healy B, et al. Nisin J, a novel natural nisin variant, is produced by *Staphylococcus capitis* sourced from the human skin microbiota. J Bacteriol. 2019;(November).

33. Wiedemann I, Breukink E, van Kraaij C, Kuipers OP, Bierbaum G, de Kruijff B, et al. Specific Binding of Nisin to the Peptidoglycan Precursor Lipid II Combines Pore Formation and Inhibition of Cell Wall Biosynthesis for Potent Antibiotic Activity. J Biol Chem. 2001 Jan 19;276(3):1772–9.

34. Gharsallaoui A, Oulahal N, Joly C, Degraeve P. Nisin as a Food Preservative: Part 1: Physicochemical Properties, Antimicrobial Activity, and Main Uses. Crit Rev Food Sci Nutr. 2016;56(8):1262–74.

35. Harmsen RAG, Ghalit N, Kemmink J, Breukink E, Liskamp RMJ, Rijkers DTS. A conformationally constrained fused tricyclic nisin AB-ring system mimic toward an improved pyrophosphate binder of lipid II. Tetrahedron. 2014;70(42):7691–9.

36. Jones E, Salin V, Williams G. NISIN and the Market for Commercial Bacteriocins. Reports. 2005.

37. Khosa S, Frieg B, Mulnaes D, Kleinschrodt D, Hoeppner A, Gohlke H, et al. Structural basis of lantibiotic recognition by the nisin resistance protein from Streptococcus agalactiae. Sci Rep. 2016;6(August 2015):18679.

38. Ortega M a, Hao Y, Zhang Q, Walker MC, van der Donk W a, Nair SK. Structure and mechanism of the tRNA-dependent lantibiotic dehydratase NisB. Nature. 2014;517(7535):509–12.

39. Dischinger J. Novel lantibiotics from microbial genomes. 2012.

40. Chatterjee C, Paul M, Xie L, van der Donk WA. Biosynthesis and mode of action of lantibiotics. Chem Rev. 2005;105(2):633–83.

41. Li B. Structure and Mechanism of the Lantibiotic Cyclase Involved in Nisin Biosynthesis. Science (80-). 2006 Mar 10;311(5766):1464–7.

42. Oman TJ, van der Donk WA. Follow the leader: the use of leader peptides to guide natural product biosynthesis. Nat Chem Biol. 2010 Jan 1;6(1):9–18.

43. Garg N, Salazar-Ocampo LMA, van der Donk WA. In vitro activity of the nisin dehydratase NisB. Proc Natl Acad Sc.i USA. 2013;110(18):7258–63.

44. Plat A, Kluskens LD, Kuipers A, Rink R, Moll GN. Requirements of the engineered leader peptide of nisin for inducing modification, export, and cleavage. Appl Environ Microbiol. 2011;77(2):604–11.

45. Oman TJ, van der Donk WA. Follow the leader: the use of leader peptides to guide natural product biosynthesis. Nat Chem Biol. 2010 Jan 1;6(1):9–18.

46. Field D, Cotter PD, Hill C, Ross RP. Bioengineering lantibiotics for therapeutic success. Front Microbiol. 2015;6(NOV):1–8.

47. de Kruijff B, van Dam V, Breukink E. Lipid II: A central component in bacterial cell wall synthesis and a target for antibiotics. Prostaglandins Leukot Essent Fat Acids. 2008;79(3–5):117–21.

48. Breukink E, de Kruijff B. Lipid II as a target for antibiotics. Nat Rev Drug Discov. 2006;5(4):321–32.

49. Pag U, Sahl H-G. Multiple Activities in Lantibiotics - Models for the Design of Novel Antibiotics. Curr Pharm Des. 2002;8(9):815–33.

50. Peschel A, Sahl HG. The co-evolution of host cationic antimicrobial peptides and microbial resistance. Nat Rev Microbiol. 2006;4(7):529–36.

51. Rink R, Wierenga J, Kuipers A, Kluskens LD, Driessen AJM, Kuipers OP, et al. Dissection and modulation of the four distinct activities of nisin by mutagenesis of rings A and B and by C-terminal truncation. Appl Environ Microbiol. 2007;73(18):5809–16.

52. George S, Hamblin MR, Kishen A. Uptake pathways of anionic and cationic photosensitizers into bacteria. Photochem Photobiol Sci. 2009;8(6):788.

53. Field D, Begley M, O'Connor PM, Daly KM, Hugenholtz F, Cotter PD, et al. Bioengineered Nisin A Derivatives with Enhanced Activity against Both Gram Positive and Gram Negative Pathogens. PLoS One. 2012;7(10).

54. Fernández L, Delgado S, Herrero H, Maldonado A, Rodríguez JM. The Bacteriocin Nisin, an Effective Agent for the Treatment of Staphylococcal Mastitis During Lactation. J Hum Lact. 2008;24(3):311–6.

55. Field D, O'Connor R, Cotter PD, Ross RP, Hill C. In vitro activities of nisin and nisin derivatives alone and in combination with antibiotics against Staphylococcus biofilms. Front Microbiol. 2016;7(APR):1–11.

56. Kim SG, Becattini S, Moody TU, Shliaha P V., Littmann ER, Seok R, et al. Microbiota-derived lantibiotic restores resistance against vancomycin-resistant Enterococcus. Nature. 2019;572(7771):665–9.

57. Koopmans T, Wood TM, 'T Hart P, Kleijn LHJ, Hendrickx APA, Willems RJL, et al. Semisynthetic Lipopeptides Derived from Nisin Display Antibacterial Activity and Lipid II Binding on Par with That of the Parent Compound. J Am Chem Soc. 2015;137(29):9382–9.

58. Heunis TDJ, Smith C, Dicks LMT. Evaluation of a nisin-eluting nanofiber scaffold to treat staphylococcus aureus-induced skin infections in mice. Antimicrob Agents Chemother. 2013;57(8):3928–35.

59. O'Neill J. Tackling drug-resistant infections globally: final report and recommendations. Rev Antimicrob Resist. 2016;(May):84.

60. Field D, O'Connor R, Cotter PD, Ross RP, Hill C. In vitro activities of nisin and nisin derivatives alone and in combination with antibiotics against Staphylococcus biofilms. Front Microbiol. 2016;7(APR).

61. Brumfitt W, Salton MRJ, Hamilton-Miller JMT. Nisin, alone and combined with peptidoglycan-modulating antibiotics: activity against methicillin-resistant Staphylococcus aureus and vancomycin-resistant enterococci. J Antimicrob Chemother. 2002;50(5):731–4.

62. Giacometti A, Cirioni O, Barchiesi F, Scalise G. In-vitro activity and killing effect of polycationic peptides on methicillin-resistant Staphylococcus aureus and interactions with clinically used antibiotics. Diagn Microbiol Infect Dis. 2000;38(2):115–8.

63. Tomasz A. Antibacterial efficacy of nisin against multidrug-resistant Gram- positive pathogens. J Antimicrob

Chemother. 1998;41(3):341–7.

64. Kamarajan P, Hayami T, Matte B, Liu Y, Danciu T, Ramamoorthy A, et al. Nisin ZP, a bacteriocin and food preservative, inhibits head and neck cancer tumorigenesis and prolongs survival. PLoS One. 2015;10(7):1–20.

65. Joo NE, Ritchie K, Kamarajan P, Miao D, Kapila YL. Nisin, an apoptogenic bacteriocin and food preservative, attenuates HNSCC tumorigenesis via CHAC1. Cancer Med. 2012;1(3):295–305.

66. Baumann T, Nickling JH, Bartholomae M, Buivydas A, Oscar P, Budisa N, et al. Prospects of in vivo incorporation of noncanonical amino acids for the chemical diversification of antimicrobial peptides. 2017;8(February):1–9.

67. Summerer, D.; Schmidt MJ. Erweiterung des genetischen Codes. Nachrichten aus der Chemie. 2013;61:303–7.

68. Noren CJ, Anthony-Cahill SJ, Griffith MC, Schultz PG. A general method for site-specific incorporation of unnatural amino acids into proteins. Science. 1989 Apr 14;244(4901):182–8.

69. Wang L, Brock a, Herberich B, Schultz PG. Expanding the genetic code of Escherichia coli. Science. 2001;292(5516):498–500.

70. Sakin V, Hanne J, Dunder J, Anders-Össwein M, Laketa V, Nikić I, et al. A Versatile Tool for Live-Cell Imaging and Super-Resolution Nanoscopy Studies of HIV-1 Env Distribution and Mobility. Cell Chem Biol. 2017;1–11.

71. Yuan Z, Wang N, Kang G, Niu W, Li Q, Guo J. Controlling Multicycle Replication of Live-Attenuated HIV-1 Using an Unnatural Genetic Switch. ACS Synth Biol. 2017;6(4):721–31.

72. Kuriakose J, Hernandez-Gordillo V, Nepal M, Brezden A, Pozzi V, Seleem MN, et al. Targeting intracellular pathogenic bacteria with unnatural proline-rich peptides: Coupling antibacterial activity with macrophage penetration. Angew Chemie - Int Ed. 2013;52(37):9664–7.

73. Wals K, Ovaa H. Unnatural amino acid incorporation in E. coli: current and future applications in the design of therapeutic proteins. Front Chem. 2014;2(April):1–12.

74. Johnson DBF, Xu J, Shen Z, Takimoto JK, Schultz MD, Schmitz RJ, et al. RF1 knockout allows ribosomal incorporation of unnatural amino acids at multiple sites. Nat Chem Biol. 2011;7(11):779–86.

75. Wang L, Xie J, Schultz PG. Expanding the Genetic Code. Annu Rev Biophys Biomol Struct. 2006;35(1):225–49.

76. Liu CC, Schultz PG. Adding New Chemistries to the Genetic Code. Annu Rev Biochem. 2010;79(1):413–44.

77. Young TS, Schultz PG. Beyond the canonical 20 amino acids: Expanding the genetic lexicon. J Biol Chem. 2010;285(15):11039–44.

78. Wan W, Tharp JM, Liu WR. Pyrrolysyl-tRNA synthetase: An ordinary enzyme but an outstanding genetic code expansion tool. Biochim Biophys Acta - Proteins Proteomics. 2014 Jun;1844(6):1059–70.

79. Flügel V, Vrabel M, Schneider S. Structural basis for the site-specific incorporation of lysine derivatives into proteins. PLoS One. 2014;9(4):1–7.

80. Exner MP. Incorporation of novel noncanonical amino acids in model proteins using rational and evolved variants of Methanosarcina mazei pyrrolysyl-tRNA synthetase. 2016.

81. Zhou L, Shao J, Li Q, Van Heel AJ, De Vries MP, Broos J, et al. Incorporation of tryptophan analogues into the lantibiotic nisin. Amino Acids. 2016;48(5):1309–18.

82. Bartholomae M, Baumann T, Nickling JH, Peterhoff D, Wagner R, Budisa N, et al. Expanding the genetic code of Lactococcus lactis and Escherichia coli to incorporate non-canonical amino acids for production of modified lantibiotics. Front Microbiol. 2018;9(APR):1–11.

83. Grant SGN, Jessee J, Bloom FR, Hanahan D. Differential plasmid rescue from transgenic mouse DNAs into Escherichia coli methylation-restriction mutants. Proc Natl Acad Sci U S A. 1990;87(12):4645–9.

84. Bernard P, Couturier M. Cell killing by the F plasmid CcdB protein involves poisoning of DNA-topoisomerase II complexes. J Mol Biol. 1992;226(3):735–45.

85. Casadaban MJ, Cohen SN. Analysis of gene control signals by DNA fusion and cloning in Escherichia coli. J Mol Biol. 1980;138(2):179–207.

86. T7 Express Iq strain specification [Internet]. 2010 [cited 2010 Sep 28]. Available from: www.neb.com/nebcomm/products/productC2833.asp

87. Kuipers OP, De Ruyter PGGA, Kleerebezem M, De Vos WM. Quorum sensing-controlled gene expression in lactic acid bacteria. J Biotechnol. 1998;64(1):15–21.

88. Inoue H, Nojima H, Okayama H. High efficiency transformation of Escherichia coli with plasmids. Gene. 1990;96(1):23–8.

89. Holo H, Nes IF. High-frequency transformation, by electroporation, of Lactococcus lactis subsp. cremoris grown with glycine in osmotically stabilized media. Appl Environ Microbiol. 1989;55(12):3119–23.

90. Protocol Q. QIAquick ® Gel Extraction Kit. 2015;(July):6–7.

91. NEB. Optimizing restriction endonuclease reactions [Internet]. [cited 2018 Jan 11]. Available from: https://www.neb.com/protocols/2012/12/07/optimizing-restriction-endonuclease-reactions

92. Ho SN, Hunt HD, Horton RM, Pullen JK, Pease LR. Site-directed mutagenesis by overlap extension using the polymerase chain reaction. Gene. 1989;77(1):51–9.

93. Shi Y, Yang X, Garg N, van der Donk WA. Production of Lantipeptides in *Escherichia coli*. J Am Chem Soc. 2011;133(8):2338–41.

94. Schägger H, von Jagow G. Tricine-sodium dodecyl sulfate-polyacrylamide gel electrophoresis for the separation of proteins in the range from 1 to 100 kDa. Anal Biochem. 1987;166(2):368–79.

95. Dechert U. Anleitung PAGE. In: Gentechnische Methoden - Eine Sammlung von Arbeitsanleitungen für das molekularbiologische Labor. 5th ed. Heidelberg: Jansohn, Monika Rothhämel, Sophie; 2012. p. 660.

96. Switzer RC, Merril CR, Shifrin S. A highly sensitive silver stain for detecting proteins and peptides in polyacrylamide gels. Anal Biochem. 1979;98(1):231–7.

97. Shapiro SS, Wilk MB. An Analysis of Variance Test for Normality (Complete Samples). Biometrika. 1965;52(3/4):591.

98. Fischer M. Optimierungen zur Expression von Nisin als Grundlage für den späteren Einbau nicht- kanonischer Aminosäuren in Escherichia coli. Universität Regensburg; 2014.

99. Merck. pET-21a-d (+) [Internet]. 1998 [cited 2017 Dec 19]. p. 1–2. Available from: http://www.merckmillipore.com/DE/de/product/pET-21a+-DNA-Novagen,EMD_BIO-69740#anchor_VMAP

100. Yan W, Imanishi M, Futaki S, Sugiura Y. α-helical linker of an artificial 6-zinc finger peptide contributes to selective DNA binding to a discontinuous recognition sequence. Biochemistry. 2007;46(29):8517–24.

101. NEB. Protein Expression with T7 Express Strains. 2016;6–7.

102. Sharp PM, Li WH. The codon Adaptation Index--a measure of directional synonymous codon usage bias, and its potential applications. Nucleic Acids Res. 1987 Feb 11;15(3):1281–95.

103. Raab D, Graf M, Notka F, Schödl T, Wagner R. The GeneOptimizer Algorithm: Using a sliding window approach to cope with the vast sequence space in multiparameter DNA sequence optimization. Syst Synth Biol. 2010;4(3):215–25.

104. Van Heel AJ, Mu D, Montalbán-López M, Hendriks D, Kuipers OP. Designing and producing modified, new-to-nature peptides with antimicrobial activity by use of a combination of various lantibiotic modification enzymes. ACS Synth Biol. 2013;2(7):397–404.

105. Maffioli S, Monciardini P, Sosio M, Donadio S. New Lantibiotics from Engineered Strains. In: Genilloud O,

Vicente F, editors. Drug Discovery from Natural Products. 1st ed. Cambridge: The Royal Society of Chemistry; 2012.

106. O'Sullivan DJ, Klaenhammer TR. High- and low-copy-number Lactococcus shuttle cloning vectors with features for clone screening. Gene. 1993;137(2):227–31.

107. Bonev B, Hooper J, Parisot J. Principles of assessing bacterial susceptibility to antibiotics using the agar diffusion method. J Antimicrob Chemother. 2008;61(6):1295–301.

108. Zhou L, van Heel AJ, Kuipers OP. The length of a lantibiotic hinge region has profound influence on antimicrobial activity and host specificity. Front Microbiol. 2015 Jan 29;6:11.

109. Caroline A Schneider WSR& KWE. NIH Image to ImageJ: 25 years of image analysis. Nat Methods. 2012;9(Historical Commentary):671–675.

110. Xie L, Chatterjee C, Balsara R, Okeley NM, Van der Donk WA. Heterologous expression and purification of SpaB involved in subtilin biosynthesis. Biochem Biophys Res Commun. 2002;295(4):952–7.

111. Merck. pRSFDuet-1 Vector [Internet]. 2000 [cited 2018 Dec 19]. Available from: http://www.merckmillipore.com/DE/de/product/pRSFDuet-1-DNA-Novagen,EMD_BIO-71341?ReferrerURL=https%3A%2F%2Fwww.google.de%2F&bd=1#anchor_VMAP

112. Kuipers, Bas J. H. GH. Prediction of Molar Extinction Coefficients of Proteins and Peptides Using UV Absorption of the Constituent Amino Acids at 214 nm To Enable Quantitative Reverse Phase High-Performance Liquid Chromatography −Mass Spectrometry Analysis. J Agric Food Chem. 2007;55:5445–51.

113. Anthis NJ, Clore GM. Sequence-specific determination of protein and peptide concentrations by absorbance at 205 nm. Protein Sci. 2013;22(6):851–8.

114. Grotefend S, Kaminski L, Wroblewitz S, Deeb S El, Kühn N, Reichl S, et al. Protein quantitation using various modes of high performance liquid chromatography. J Pharm Biomed Anal. 2012;71:127–38.

115. Vos WM, Mulders JWM, Siezen RJ, Hugenholtz J, Kuipers OP. Properties of Nisin-Z and Distribution of Its Gene, Nisz, in Lactococcus-Lactis. Appl Environ Microbiol. 1993;59(1):213–8.

116. Oman TJ, Van Der Donk WA. Insights into the mode of action of the two-peptide lantibiotic haloduracin. ACS Chem Biol. 2009;4(10):865–74.

117. Ofek I, Cohen S, Rahmani R, Kabha K, Tamarkin D, Herzig Y, et al. Antibacterial synergism of polymyxin B nonapeptide and hydrophobic antibiotics in experimental gram-negative infections in mice. Antimicrob Agents Chemother. 1994;38(2):374–7.

118. Sys- M. Binding of Polymyxin B Nonapeptide to Gram-Negative Bacteria. 1985;27(4):548–54.

119. Schroeder G, Brandenburg K, Seydel U. Polymyxin B induces transient permeability fluctuations in asymmetric planar lipopolysaccharide/phospholipid bilayers. Biochemistry. 1992;31(3):631–8.

120. Blaskovich MAT. Unusual Amino Acids in Medicinal Chemistry. J Med Chem. 2016;acs.jmedchem.6b00319.

121. Shine J, Dalgarno L. The 3'-Terminal Sequence of Escherichia coli 16S Ribosomal RNA: Complementarity to Nonsense Triplets and Ribosome Binding Sites. Proc Natl Acad Sci. 1974;71(4):1342–6.

122. Simonetti A, Marzi S, Jenner L, Myasnikov A, Romby P, Yusupova G, et al. A structural view of translation initiation in bacteria. Cell Mol Life Sci. 2009;66(3):423–36.

123. Kozak M. Initiation of translation in prokaryotes and eukaryotes. Gene. 1999;234(2):187–208.

124. Levin-Karp A, Barenholz U, Bareia T, Dayagi M, Zelcbuch L, Antonovsky N, et al. Quantifying translational coupling in E. coli synthetic operons using RBS modulation and fluorescent reporters. ACS Synth Biol. 2013;2(6):327–36.

125. Salis HM, Mirsky EA, Voigt CA. Automated design of synthetic ribosome binding sites to control protein expression. Nat Biotechnol. 2009;27(10):946–50.

126. Mitarai N, Sneppen K, Pedersen S. Ribosome Collisions and Translation Efficiency: Optimization by Codon Usage and mRNA Destabilization. J Mol Biol. 2008;382(1):236–45.

127. Chemla Y, Ozer E, Algov I, Alfonta L. Context effects of genetic code expansion by stop codon suppression. Curr Opin Chem Biol. 2018;46(Box 1):146–55.

128. Tuller T, Carmi A, Vestsigian K, Navon S, Dorfan Y, Zaborske J, et al. An evolutionarily conserved mechanism for controlling the efficiency of protein translation. Cell. 2010;141(2):344–54.

129. Adhin MR, van Duin J. Scanning model for translational reinitiation in eubacteria. J Mol Biol. 1990;213(4):811–8.

130. Wei Y, Wang J, Xia X. Coevolution between Stop Codon Usage and Release Factors in Bacterial Species. Mol Biol Evol. 2016;33(9):2357–67.

131. Dabrowski M, Bukowy-Bieryllo Z, Zietkiewicz E. Translational readthrough potential of natural termination codons in eucaryotes – The impact of RNA sequence. RNA Biol. 2015;12(9):950–8.

132. Chin JW. Reprogramming the genetic code. EMBO J. 2011;30(12):2312–24.

133. Pott M, Schmidt MJ, Summerer D. Evolved sequence contexts for highly efficient amber suppression with noncanonical amino acids. ACS Chem Biol. 2014;9(12):2815–22.

134. Kalstrup T, Blunck R. Reinitiation at non-canonical start codons leads to leak expression when incorporating unnatural amino acids. Sci Rep. 2015;5(1):11866.

135. Smolskaya S, Zhang ZJ, Alfonta L. Enhanced Yield of Recombinant Proteins with Site-Specifically Incorporated Unnatural Amino Acids Using a Cell-Free Expression System. PLoS One. 2013;8(7):1–10.

136. Wang K, Neumann H, Peak-Chew SY, Chin JW. Evolved orthogonal ribosomes enhance the efficiency of synthetic genetic code expansion. Nat Biotechnol. 2007;25(7):770–7.

137. Gerdes S, Scholle MD, Campbell JW, Balázsi G, Ravasz E, Daugherty MD, et al. Experimental determination and system level analysis of essential genes in Escherichia coli MG1655. J Bacteriol. 2003;185(19):5673–84.

138. Mukai T, Hayashi A, Iraha F, Sato A, Ohtake K, Yokoyama S, et al. Codon reassignment in the Escherichia coli genetic code. Nucleic Acids Res. 2010;38(22):8188–95.

139. Mukai T, Hoshi H, Ohtake K, Takahashi M, Yamaguchi A, Hayashi A, et al. Highly reproductive Escherichia coli cells with no specific assignment to the UAG codon. Sci Rep. 2015;5:9699.

140. Lajoie MJ, Rovner AJ, Goodman DB, Aerni H-R, Haimovich AD, Kuznetsov G, et al. Genomically Recoded Organisms Expand Biological Functions. Science (80-). 2013;342(6156):357–60.

141. Fluck MM, Salser W, Epstein RH. The influence of the reading context upon the suppression of nonsense codons. MGG Mol Gen Genet. 1977;151(2):137–49.

142. Dayhoff MO, Schwartz RM, Orcutt BC. A model of evolutionary change in proteins. Vol. 5 suppl. 3, Atlas of protein sequence and structure. 1978. p. 345–51.

143. Choi Y, Sims GE, Murphy S, Miller JR, Chan AP. Predicting the Functional Effect of Amino Acid Substitutions and Indels. PLoS One. 2012;7(10).

144. Choi Y, Chan AP. PROVEAN web server: a tool to predict the functional effect of amino acid substitutions and indels. Bioinformatics. 2015 Aug 15;31(16):2745–7.

145. Pfaller A. Identification of a Nisin Leader-tag for Purification and Quantification of Lanthipeptides. Regensburg; 2016.

146. Tacconelli E, Magrini N. Global Priority List Of Antibiotic-Resistant Bacteria To Guide Research, Discovery, And Development Of New Antibiotics. Geneva; 2017.

147. Karakas-Sen A, Narbad a. Heterologous expression and purification of NisA, the precursor peptide of lantibiotic nisin from *Lactococcus lactis*. Acta Biol Hung. 2012;63(2):301–10.

148. Zambaldo C, Luo X, Mehta AP, Schultz PG. Recombinant Macrocyclic Lanthipeptides Incorporating Non-Canonical Amino Acids. J Am Chem Soc. 2017;139(34):11646–9.

149. ETH Zürich. SYNPEPTIDE Report Summary. Bruxelles; 2015.

150. Schmitt S, Montalbán-López M, Peterhoff D, Deng J, Wagner R, Held M, et al. Analysis of modular bioengineered antimicrobial lanthipeptides at nanoliter scale. Nat Chem Biol. 2019;

151. Lüllmann H, Mohr K, Hein L, editors. Pharmakologie und Toxikologie. Stuttgart: Georg Thieme Verlag; 2010.

152. Field D, Cotter PD, Ross RP, Hill C. Bioengineering of the model lantibiotic nisin. Bioengineered. 2015;6(4):187–92.

153. Breukink E, Wiedemann I, Van Kraaij C, Kuipers OP, Sahl HG, de Kruijff B. Use of the Cell Wall Precursor Lipid II by a Pore-Form Peptide Antibiotic. Science (80-). 1999;286(December):2361–4.

154. Reddy Chichili VP, Kumar V, Sivaraman J. Linkers in the structural biology of protein-protein interactions. Protein Sci. 2013;22(2):153–67.

155. Manuscript A. Fusion Protein Linkers: Property, Design and Functionality. NIH Public Access. 2014;65(10):1357–69.

156. Kolb HC, Finn MG, Sharpless KB. Click Chemistry: Diverse Chemical Function from a Few Good Reactions. Angew Chemie - Int Ed. 2001;40(11):2004–21.

157. Kim CH, Axup JY, Schultz PG. Protein conjugation with genetically encoded unnatural amino acids. Curr Opin Chem Biol. 2013;17(3):412–9.

158. Vaara M. Agents that increase the permeability of the outer membrane. Microbiol Rev. 1992;56(3):395–411.

159. Otvos L, Wade JD. Current challenges in peptide-based drug discovery. Front Chem. 2014;2(August):8–11.

160. Schlapschy M, Binder U, Börger C, Theobald I, Wachinger K, Kisling S, et al. PASylation: A biological alternative to PEGylation for extending the plasma half-life of pharmaceutically active proteins. Protein Eng Des Sel. 2013;26(8):489–501.

Selbstständigkeitserklärung

Ich erkläre hiermit, dass ich die vorliegende Arbeit ohne unzulässige Hilfe Dritter und ohne Benutzung anderer als der angegebenen Hilfsmittel angefertigt habe. Die aus anderen Quellen direkt oder indirekt übernommenen Daten und Konzepte sind unter Angabe der Quelle gekennzeichnet. Insbesondere habe ich nicht die entgeltliche Hilfe von Vermittlungs- bzw. Beratungsdiensten (Promotionsberater oder andere Personen) in Anspruch genommen. Niemand hat von mir unmittelbar oder mittelbar geldwerte Leistungen für Arbeit erhalten, die im Zusammenhang mit dem Inhalt der vorgelegten Dissertation stehen. Die Arbeit wurde bisher weder im In- noch im Ausland in gleicher oder ähnlicher Form einer anderen Prüfungsbehörde vorgelegt.

Regensburg, den

_____

Malin Zaddach

Danksagung

Damit ich diese Doktorarbeit verfassen konnte, haben mir eine ganze Reihe an lieben Menschen geholfen. Bei ihnen möchte ich mich an dieser Stelle bedanken.

Ein riesiges Dankeschön an Ralf für die ausdauernde Unterstützung und ganz besonders für die richtigen Worte in den unterschiedlichen Phasen meiner Doktorarbeit. Tausend Dank für die Zeit, die du dir jede Woche für unsere kleinen Synpeptide-Besprechungen, und wann immer ich ein Anliegen hatte, genommen hast. Danke für die Unterstützung bei der Bewerbung für das Stipendium und für meine Stelle als Assistenzärztin. Danke, dass ich meine Arbeit in deiner Gruppe anfertigen durfte und dein Vertrauen zur Verwendung aller Materialien und Geräte bekommen habe.

Ein großes Dankeschön an Herrn Professor Bernd Salzberger für die Übernahme des Zweitgutachtens.

Ich danke der Fakultät für Medizin der Universität Regensburg für die Unterstützung in Form des Promotionsstipendiums.

Vielen herzlichen Dank an David für die zahlreichen Inputs bei unseren Besprechungen und zu meiner Ausarbeitung, sowie für die Hilfestellungen bei praktischen Dingen. Danke für dein Vertrauen mit der HPLC – die Arbeit daran war für mich immer ein experimentelles Highlight!

Ganz besonders möchte ich mich außerdem bei den besten Laborkollegen der Welt, Anja und Jogi, für die tolle Zeit im 80er Labor bedanken. Ohne euch wäre die Arbeit nicht mal auch nur ein Zehntel so lustig gewesen! Danke für die aufmunternden Worte, danke für die zusätzliche Musikbildung, das Tanzen (wie ein Pferd) und die Hilfe sowohl bei praktischen als auch bei den theoretischen Dingen.

Ein Danke geht auch an Miri, Anh, Meli, Alex, Christina, Richie, Ali, Ivan, Tom, Robert Heyd und Patrick Neubert dafür, dass sie meine Laborzeit einmalig gemacht haben und mir bei den verschiedensten Dingen geholfen haben. Vielen Dank auch dir, Benedikt, für deine Hilfestellungen und deine herzliche Art!

Ohne die Unterstützung meiner Eltern während meines gesamten Studiums (und natürlich auch schon weit davor) wäre diese Arbeit sicher nicht entstanden. Dafür möchte ich Ihnen ganz herzlich danken! Danke dir, Jonas, dass du an einem Tiefpunkt da warst und mir geholfen hast einen Weg zum Weitermachen zu finden.

Von ganzem Herzen danke ich dir, Richard, dafür, dass du mir immer zur Seite stehst! Ich danke dir für das unermüdliche Ermutigen, Korrekturlesen und Zuhören – nicht nur während der Doktorarbeit, sondern während meines gesamten Studiums.